DELAMINATION SUPPRESSION IN GRAPHITE/EPOXY COMPOSITES VIA EFFICIENT USE OF FILM ADHESIVE LAYERS

by

Narendra Venugopal Bhat

B.Tech., Indian Institute of Technology, Bombay, India

(1987)

Submitted to the Department of Aeronautics and Astronautics

in partial fulfillment of

the requirements for the degree of

Master of Science

in Aeronautics and Astronautics

at the

Massachusetts Institute of Technology

February 1990

Signature of Author _____

Department of Aeronautics and Astronautics

September 18, 1989

Certified by _____

Professor Paul A. Lagace

Thesis Supervisor

Accepted by _____

Professor Harold Y. Wachman

Chairman, Departmental Graduate Committee

DELAMINATION SUPPRESSION IN GRAPHITE/EPOXY COMPOSITES VIA EFFICIENT USE OF FILM ADHESIVE LAYERS

by

Narendra Venugopal Bhat

Submitted to the Department of Aeronautics and Astronautics on September 18, 1989 in partial fulfillment of the requirements for the Degree of Master of Science.

ABSTRACT

Delamination suppresion by the efficient placement of film adhesive interlayers in $[\pm 15_7/0_7]_s$ AS4/3501-6 graphite/epoxy laminates was investigated. Efficiency was achieved by placing film adhesive in the form of strips at the free edge at delamination critical interfaces only. Five types of laminates were tested; the first type were control specimens without film adhesive, the second type had a full-width ply of film adhesive, and the remaining three types had strips of film adhesive 3 mm, 6 mm and 9 mm wide, at the free edges of the laminate. All film adhesive was placed at the +15°/-15° interface. For all the specimens with film adhesive, the delamination initiation load was about 50% higher than for the control specimens. The width of the film adhesive strips, up to manufacturable sizes, did not affect the suppression of delamination. The specimens with film adhesive also failed at stresses which were about 40% higher than the control specimens. Again, no significant difference was observed between the fracture stresses of specimens with different widths of film adhesive. An analysis was developed to predict the interlaminar stresses at the dropoff and showed that these interlaminar stresses at the dropoff are negligibly small as compared to the interlaminar stresses at the free edge of the specimen. Specimens with film adhesive plies at the +15°/-15° interface and delamination implants of width 3 mm, 6 mm, and 9 mm at the free edge at the +15°/FA interface were tested to examine the effect of film adhesive on growth of delamination Specimens with 6 mm and 9 mm wide delamination implants showed delamination behavior similar to the control specimens, indicating that the film adhesive was not capable of suppressing the growth of delamination. The behavior of specimens with 3 mm wide delamination implantes, however, conformed to that of the specimens with film adhesive. This indicates the possibility of the existence of a critical delamination size necessary for growth to occur.

Thesis Supervisor: Paul A. Lagace

Title: Associate Professor, Department of Aeronautics and Astronautics, Massachusetts Institute of Technology.

ACKNOWLEDGEMENTS

This thesis is a document into which went the experience and knowledge of the people who worked with me. I hence, thank all my friends and colleagues whose company has made these last two years an enjoyable and educational experience for me.

I would in particular like to thank my advisor, Paul, who has not only taught me a lot about research, but has also been understanding of any problems that I have had, and encouraged me in my low moments.

A fellow graduate student and friend Kevin Saeger, needs special mention here, for I sincerely believe that I would not have completed in this short time my analytical model without having asked him the million and odd questions, to which I was always provided an answer.

Thanks are the due to Al Supple who was always ready with solutions to my problems in the lab and my UROP's Randy Notestine, Mark Viz, Jeff Kim, and Michael Sadlowski, who helped to speedily expedite my experimental work.

This year has also brought for me one of the tragic moments in life which one hopes will never happen, and yet, it always seems to catch up sooner or later. It is still difficult form me to accept that my father is no more, yet all I can do now is to cherish his love and affection for me, and try to keep his hopes and aspirations alive. I shall remain indebted to my family consisting of my mother, brother, and grandmother, who inspite of their great sorrow, persuaded me to continue my studies, and have been an inexhaustible source of solace and encouragement. I only hope that I will in some way be able to make the times ahead better ones for them.

This work was performed in the Technology Laboratory for Advanced Composites (TELAC) of the Department of Aeronautics and Astronautics at the Massachusetts Institute of Technology. This work was sponsored by Boeing Military Airplane under Boeing Purchase Order 644740.

In loving memory of my father

TABLE OF CONTENTS

CHAPTER PAGE

LIST OF FIGURES

LIST OF TABLES

NOMENCLATURE

{a}	vector of constants in the solution for F and G in the region A
{b}	vector of constants in the solution for F and G in the region B
e_i	constants involving h_i defined in equation 4.24
E_L	longitudinal modulus
F_i	Arbitrary function used to define the in-plane stress σ_{22} and interlaminar stresses σ_{2z} and σ_{zz} at the ith interface
{F}	vector made up of the elements F_i
g_i	constants involving $h_i$and L_i defined in equation 4.25
G	strain energy release rate
G_i	Arbitrary function used to define the in-plane stress σ_{12} and the interlaminar stress σ_{1z}
{G}	vector made up of the elements G_i
h_i	thickness of the ith ply
Hg	mercury
$[I_1]$	modification of the unity matrix used to satisfy σ_{22} boundary conditions
$[I_2]$	used to relate the stresses σ_{22} to the functions F
L_i	constants used in defining the elements of matrices [αij], [βij], and [ηij] as in equations 4.17 through 4.23

M	constants used in the definition of the matrix [Ω] and defined in equations 4.66a through 4.66i
S_{pqkl}	an element of the compliance tensor
S^*_{pqkl}	modified compliance tensor in accordance with equation 4.3b
S_{2z}	interlaminar shear strength for σ_{2z}
S_{1z}	interlaminar shear strength for σ_{1z}
Z^t	tensile interlaminar normal strength
$[\alpha ij]$	a coefficient matrix in equation 4.15
β	real part of eigenvalue λ
$[\beta ij]$	a coefficient matrix in equation 4.15
Γ	matrices used in the matching of boundary conditions between regions A and B
δ	variational
δ_{ij}	kronecker delta
$[\eta ij]$	a coefficient matrix in equation 4.15
θ	lamination angle
λ	eigenvalues
Π_c	Complimentary energy
σ_{11A}	far-field stress in region A
$\{\phi\}$	eigenvectors
$\{\phi^F\}$	eigenvectors associated with the function F

$\{\Phi^F\}$	matrix consisting of the eigenvectors $\{\phi^F\}$
$\{\phi^G\}$	eigenvectors associated with the function G
$\{\Phi^G\}$	matrix consisting of the eigenvectors $\{\phi^G\}$
$\{\psi\}$	Lagrange multiplier
ω	imaginary part of eigenvalue λ

Subscripts and Superscripts

a	indicates region A
b	indicates region B
i	indicates the ith ply
d	indicates the dropped ply
F	indicates associated with function F
G	indicates associated with function G
L	indicates values obtained from Classical Laminated Theory

CHAPTER 1

INTRODUCTION

Composites, once known as the materials of the future, are today being applied in a wide spectrum of applications. The aerospace industry, which initially started out applying these materials to military airplanes, is currently using them increasingly for secondary structures of commercial aircraft like the Boeing 757, 767, the McDonnell Douglas MD-80, and the Airbus. The experience gained in these aircrafts have led the designers to increasingly employ these materials in the primary structures of some aircrafts like the Northrop F-20 lightweight fighter, and the Boeing Vertol V-22 Osprey tilt-rotor. Special mention must also be made of the FAA-certified Beechcraft Starship I corporate jet, utilizing all-composite fuselage and wings. These make use of the strength and weightsaving abilities of composites to improve their performance capabilities. There are on the other hand, aircraft like the Grumman/DARPA X-29, the Sikorsky/NASA X-wing helicopter and the Voyager (which circled the world nonstop), which would have not been possible without the advantages offered by composite materials.

The high strength-to-weight and stiffness to weight ratios of composite materials offer considerable returns in terms of improved performance in aircraft. These materials offer designers an immense amount of freedom to tailor the properties as per the loadings on the structure being designed, thus optimizing the strength and weight of the airplane.

The realization of this potential has led to an ever increasing body of users and applications for composite materials. This has resulted in the development of a data base which makes possible the construction of more

reliable, cost and performance efficient structures. Increased usage has also fueled research leading to a better insight into the mechanics and behavior of composite materials.

Composites exhibit a range of damage modes which are unique, most of which are still not completely understood. Fiber breakage, fiber pullout, matrix cracking, fiber/matrix debonding, ply delamination, angle ply splitting, buckling at the fiber, ply and laminate levels, are but a few of the damage modes. Additionally, there exist interactions between these failure modes, making it increasingly difficult for the designer to understand the capabilities and limitations of the designed structure. This is one of the primary factors restricting the widespread use of composites.

Delamination is a failure mode characteristic of laminated composites, and not observed in conventional metals. Delamination refers to the failure of the interply matrix layer in a laminate due to the presence of out-of-plane stresses (interlaminar stresses), which arise at the stress-free edges of a laminate or in any gradient stress field. Delamination by itself does not cause failure, but leads to significant loss in stiffness and strength of certain laminates.

In real-world structures that employ composites the various components need to be adequately tailored to the given strength requirements. The required changes in strength and stiffness of these components can be achieved in two ways : by altering the orientation of individual lamina (or by changing the stacking sequence), and by varying the total number of plies (i.e. the thickness). This change in laminate thickness can be affected by terminating or inserting internal plies. This process of ply termination is called 'ply dropoff'. For example, ply dropoffs are used in the wing skins of aircraft to reduce the stiffness from root to tip. They are also useful in

enhancing the ability to contour components, as is required in currently designed composite rotor hubs, which being hingeless and bearingless to reduce the weight, the drag and the number of parts, involve tapering of the laminate by dropping some plies in the flexure region of the hub. However a ply dropoff causes a thickness discontinuity in the structure, which in turn gives rise to a gradient stress field and hence, possible delamination initiation. It has observed been observed [1] that straight-edged test specimens from certain graphite/epoxy laminates failed at stresses which were less than half of those predicted by in-plane theory, a discrepancy attributed to delamination. Delamination is not restricted to test specimens in laboratories but has been observed in structures like the Lockheed L-1011 vertical tail [2] and in helicopter rotor hubs [3].

The problem of delamination demands that it be necessary to calculate interlaminar stresses and predict the occurrence of delamination. This generally forms a stumbling block in the efficient design of composites as designers try to circumvent the problem by confining themselves to conservative designs with few standard laminates. This leads to an undermining of the vast advantages of structural tailoring offered by composites.

The aerospace industry has over the last two decades tried to better understand and predict delamination. Research is seen targeted at methods to delay or completely suppress delamination. The out-of-plane behavior of the laminates would then be no longer dominant and laminate behavior would be governed by in-plane phenomena in which composites exhibit the greatest stiffness and strength. This would allow the designer to tap into the full potential of composites.

Previous investigations have shown that delamination can be successfully suppressed or delayed by inserting interlaminar shear layers at all the ply interfaces of any laminate. The current study adopts the same basic technique, but looks to examine use of these interlaminar shear layers in a more efficient manner, in terms of the amount of material and its location. Tests are to be conducted on laminates with adhesive layers only on the interfaces most prone to delamination. Furthermore, these adhesive layers will be restricted to a small zone near the free edge where the free edge interlaminar stresses show steep stress gradients. Restricting the shear layers to zones close to the free edge essentially means that they are 'dropped off' some distance from the free edge. Such dropoff regions, as mentioned earlier, could lead to stress gradients, resulting in interlaminar stresses and in consequence to delamination, depending on the laminates and the plies dropped off. In the event the dropoff is close to the free edge, there also belies the possibility of interaction between the free edge and dropoff interlaminar stresses. Hence, the stress gradients near the region of the ply dropoff and its possible ramifications will also be investigated.

The previous work done in this area is summarized in chapter two. Included are discussions on free edge delamination, and some methods of delamination control. Various methods for calculating the interlaminar stress states at the free edge and at ply dropoffs and the ability to predict delamination initiation are evaluated. The experimental program is considered in chapter three. An overview of the test program is followed by the description of the manufacturing procedures and the test methods employed. The method of analysis for interlaminar stresses at ply dropoffs is presented in chapter four. The results of the test program are included in chapter five. The analytical and experimental results are discussed in chapter six. Finally, a summary of

the work done and recommendations for further work are suggested in chapter seven. The FORTRAN source codes for the software developed is included in appendix A.

CHAPTER 2

SUMMARY OF PREVIOUS WORK

2.1 Interlaminar Stresses and Delamination

Over the past two decades of research in the area of delamination, considerable information has been compiled regarding the causes and characteristics of delamination. Delamination is caused by the interlaminar stresses arising in a boundary layer near the stress-free edges of a laminate or at any location with in-plane stress gradients [4]. These interlaminar stresses arise due to the 'compliance mismatch' between adjacent plies of a laminate. A unidirectional composite material is orthotropic in nature. When several plies with varying orientation are stacked, each ply possesses different elastic properties along the laminate axes, and hence there results a compliance mismatch between the individual plies of the laminate.

A composite laminate loaded in unidirectional tension is illustrated in Figure 2.1. The Classical Laminated Plate theory imposes a through-the-thickness continuity which leads to differing stresses in plies with different fiber orientation. Thus, at the free edge the Classical Laminated Plate theory satisfies the stress-free boundary conditions only in the integral sense. In reality, however, as the stresses at the free edge for each individual ply go to zero, other out-of-plane stresses (σ_{2z}, σ_{zz} and σ_{1z}) arise in a small region near the free edge to maintain equilibrium. Thus, there is a boundary layer region near the free edge with significant interlaminar stresses. Outside this boundary layer region, the stresses die away and the Classical Laminated Plate theory assumptions and solution are recovered.

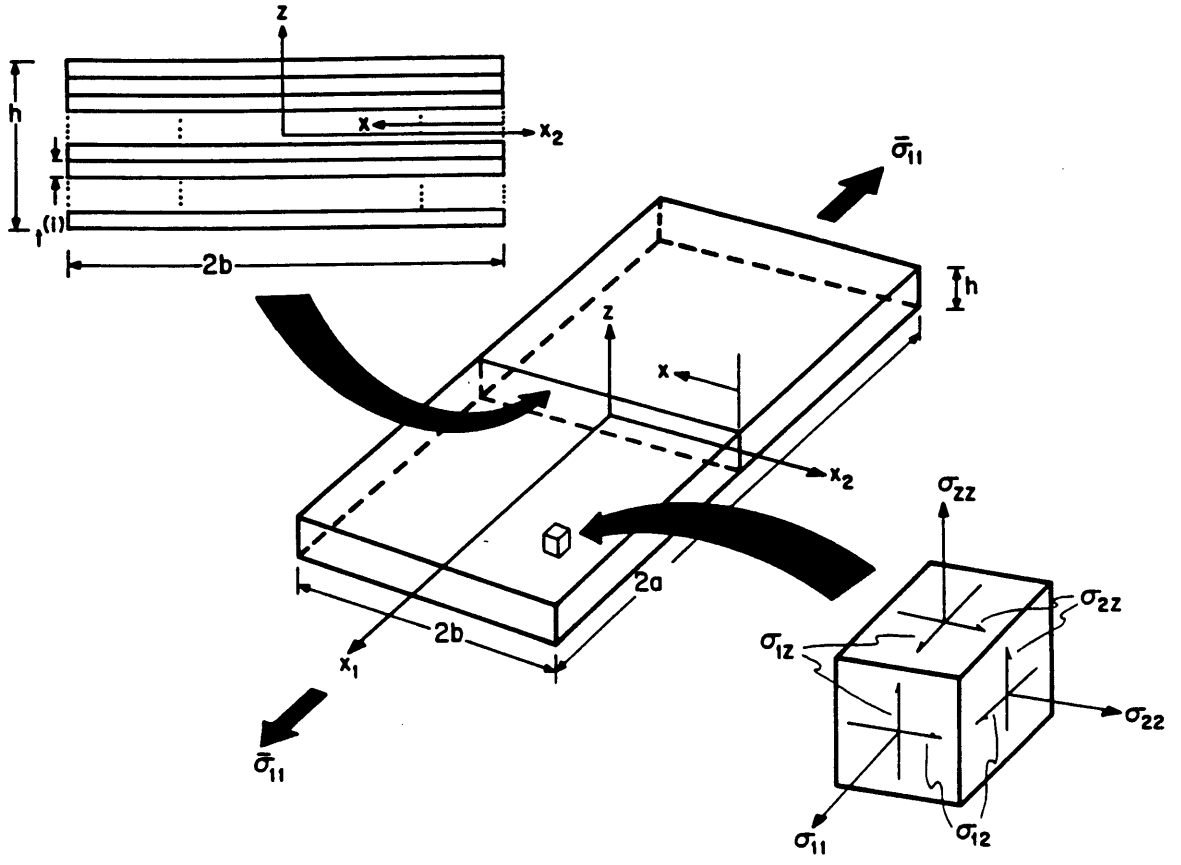

Figure 2.1 Geometry of a composite laminate under uniaxial tension.

One of the early works in the evaluation of the stress state at the free edge was by Pipes and Pagano [4]. They used a finite difference technique and observed for the case of a $[+45/-45]_S$ laminate that the stresses σ_{2z}, σ_{zz} and σ_{1z} were appreciable in the boundary layer. They also observed that σ_{1z} may be singular at the free edge. The global-local variational model by Pagano and Soni [5] and most other solutions like that by Wang and Crossman [6], Rybicki [7], and Stanton, et al. [8] use the finite element method. There also exist other methods like the perturbation solution by Hsu and Herakovich [9]. The results obtained by these methods show reasonable mutual agreement in certain cases, but in the case of the $[\pm 45]_S$ laminate examined by Whitcomb, Raju and Goree [10], the results can be considerably different.

Elasticity solutions to the interlaminar stress problem have been attempted by Wang and Choi [11,12]. They utilized complex stress potentials to calculate the free edge stress field in a $[\pm\theta]_S$ laminate as the sum of infinite eigenfunctions. They were examining the possibility of the existence of a stress singularity at the free-edge and they did find the existence of a weak singularity in each case examined.

The Force Balance Method, developed by Kassapoglou and Lagace [13], couples the three-dimensional equations of elasticity with a set of integral ply equilibrium equations and then assumes nonsingular exponential solutions which satisfy the stress-free boundary conditions at the free edge and approach the Classical Laminated Plate theory solution at the center of the laminate. The solution is obtained by the principle of minimum complementary energy. The Reduced Eigenfunction Stress Technique (REST), developed by Saegar and Lagace [14], is a further development of the Force Balance Method. In this technique, the solutions for the stresses are not assumed *apriori*, as done by

Kassapoglou and Lagace [13], but eigenfunctions are obtained as a result of using the variational principle on the complementary energy.

The end purpose of the calculations of the interlaminar stresses is to better predict delamination initiation. Two basic approaches have been utilized for the predictions.

The first approach falls within the domain of the "fracture mechanics" approach and models the delamination as a crack. The strain energy released by the growth of the crack is compared to some experimentally determined critical strain energy release rate. O'Brien [15] uses a value of the critical strain energy release rate measured from one laminate to predict delamination initiation in other kinds of laminates. This method showed partial success in predicting delamination initiation loads.

O'Brien [16] developed a simple equation for the strain energy release rate, associated with local delaminations growing from matrix ply cracks. The equation was used to predict delamination onset strains in a laminate where delaminations grew from 90° matrix ply cracks. A simple technique developed to calculate the local strain concentrations in the primary load-bearing plies near local delaminations was used to successfully predict certain laminate failure strains.

Another example of the use of this approach is that by Wang, Crossman and Law [17], where an analytical model based on the energy principle is used to predict free edge delamination for graphite/epoxy specimens under uniaxial tension. Predictions include the initiation, growth, and growth stability of the delamination. A finite element procedure in conjunction with the crack-closure technique [18] was used to evaluate the strain energy. The strain energy was expressed in terms of the laminate stiffness, applied stress, and a nondimensional function. This method was used to predict the critical

stresses for delamination initiation, stable growth, and unstable growth. The analytically obtained critical stresses for delamination onset are compared to the experimental results for the quasi-isotropic laminate, $[\pm 45_n/0_n/90_n]_s$ with effective ply thicknesses, n, of one, two and three. The experimental results show good correlation with the analytical results.

The second approach to predicting the delamination initiation uses the averaged interlaminar stresses in a failure criterion. Kim and Soni [19] used only the averaged σ_{zz} to predict delamination in several laminates while Brewer and Lagace [20] developed a Quadratic Delamination Criterion which accounts for the interlaminar shear stresses as well as the normal stresses. While Kim and Soni [19] used an averaging distance equal to the ply thickness, Brewer and Lagace [20] used an averaging distance of the order of a ply thickness which is constant for any given material. The Quadratic Delamination Criterion was, in general, seen to predict initiation better than the strain energy release approach [20].

The methods discussed here suggest several ways to predict interlaminar stresses and delamination initiation. They thus prove to be a useful tool in providing insight into the mechanism of delamination and hence in suggesting ways in which to suppress or delay it.

2.2 Delamination Suppression

In the earlier section, it was shown that the interlaminar stresses at the free edge were responsible for delamination initiation at the free edge. Therefore, there is a need to suppress delamination, and in general all the solutions attempted, can be classified under two general approaches. The first approach involves the strengthening of the interfaces of the laminate and the

second involves the altering of the interlaminar stress state at the free edge of the laminate.

Mignery, Tan and Sun [21] used through-the-thickness stitching to carry the out-of-plane loads and succeeded in arresting delamination growth near the stitch line, but did not always achieve higher ultimate stresses. Kim [22] wrapped fiberglass/epoxy strips around the free edges of delamination-prone laminates and achieved increases in ultimate failure stresses over standard laminates. The mechanism of operation in both these cases mentioned is to produce some sort of compressive stress at the free edge as well as providing an alternate load path for the tensile interlaminar normal stress caused by the compliance mismatches. These techniques are not, in general, completely valid in suppressing delamination as it is shown that the interlaminar shear stress, σ_{1z}, is also significantly important in initiating delamination [23, 24, 25].

Lagace, Weems and Brewer [26] explored the possibility of using cocured film adhesive interlayers to suppress delamination. Film adhesive interlayers were placed at all dissimilar ply interfaces and cocured. This research showed that the delamination was effectively prevented in $[\pm 15_n]_s$, $[0_n/\pm 15_n]_s$, and $[\pm 15_n/0_n]_s$ laminates, and increased the measured fracture stresses of these laminates to those predicted by in-plane failure criterion. The authors attributed this to a reduction in the compliance mismatches between the various plies of the laminate and consequently to a reduction in the interlaminar shear stress, σ_{1z}, at the free edge of the laminate. Since the stress, σ_{1z}, was seen to be the major contributor to the delamination initiation at the free edge, a reduction in this stress resulted in the delay of the delamination initiation load. In cases where the initiation load was delayed

beyond the in-plane failure load of the specimen, the specimen failed at the predicted in-plane failure load.

Chan, Rogers and Akers [27] and Chan [28] also worked on delamination suppression by studying the effectiveness of film adhesive interlayers in certain graphite/epoxy laminates. They showed that either complete sheets or 6.35 mm edge strips of FM1000 film adhesive placed at the 0/90 interface of $[\pm 35/0/90]_S$ laminates delayed delamination initiation until final failure. The authors also performed tests with specimens which had film adhesive strips placed in the interior of the laminates. These specimens were seen to only temporarily delay growth of the delamination. In all cases, however, increases in ultimate strength were realized, but were not correlated to the in-plane predictions. Their analysis attributed the delay in delamination growth to the mode I (viz. G_I/G_{total}) portion of the strain energy release rate being reduced by the presence of the interlayers. The studies by Chan et al. thus showed the success of the strips of film adhesive in delaying or suppressing delamination. They, however, did not relate the width of the strips to the boundary layer region, but instead arbitrarily chose a width of 6.35 mm for the widths. The film adhesive, when used in the form of strips, have to be terminated within the interior of the laminate i.e., they have to be dropped off.

Vizzini [29] examined the possiblilty of edge alterations as a technique to suppress delamination at the free edge. One of the plies involved in a delamination critical interface was terminated before the free edge and substituted by either an isotropic filler material or by a ply with a different orientation. This would result in an internal edge and hence cause interlaminar stresses at the internal edge due to the discontinuity. The idea behind the approach is to choose such a filler material that the interlaminar

stresses at the free edge would be reduced enough so as to not cause delamination and also have interlaminar stresses of about the same magnitude at the internal edge. The internal edge would, however, have to be far enough from the free edge to prevent interaction of the interlaminar stresses at the two edges. The replacement with a ply of differing orientation provided better redistribution of interlaminar stresses than isotropic filler material. The disadvantage of this method, however, would be that, with increasing effective ply thickness, the internal edge would have to be pushed deeper within the laminate to prevent interaction of the internal and free edge interlaminar stresses.

Chan and Ochoa [30] experimented with the termination of a critical ply a small distance away from the free edge as a technique to suppress delamination. The termination of the 90° ply, in the laminates $[30/-30_2/30/90]_s$ and $[\pm 35/0/90]_s$, a small distance from the free edge has been shown to increase the delamination strength. Both static and fatigue tests indicated the absence of delamination and the final failure was seen to be in-plane. The loads or the number of cycles to failure attained were significantly higher than in the case without ply termination. No comparison has been made by the authors, however, with the in-plane failure load. Examination of interlaminar normal and shear stresses indicates the maximum of both to occur at the station before the dropoff in the thick region. The authors compare the through-the-thickness interlaminar stresses near the free edge for the baseline and tapered laminate and show that the stresses are lower for the latter case. This comparison of through-the-thickness stresses, however, should have been made at the dropoff, because this is shown by the authors to be the location of the highest interlaminar stresses. The authors showed experimentally that, for the two laminates considered, the delamination does not occur at the

dropoff. However, considering the high nature of the stresses at the region before the dropoff, there is the possibility that delamination may occur at that location for some other layup.

The current approach uses film adhesive interlayers to suppress delamination in graphite/epoxy laminates, as some of the previous methods mentioned here. The drive here, however, is to place the film adhesive in a selective and efficient manner. Previous work on the use of film adhesive does not take into consideration the efficiency of film adhesive placement in delamination suppression. In this context, it is to be mentioned that American Cyanamid has introduced a special prepreg with interleaving [31]. The use of this material would lead to the presence of the interleaved material at all locations within the laminate, which implies inefficient usage in terms of increase in weight of the laminate. The present approach aims at improving the efficiency of the use of the film adhesive, with an attempt at placing the film adhesive at critical locations where delamination is likely to initiate.

CHAPTER 3

EXPERIMENTAL PROCEDURE

3.1 Overview of the Experimental Program

The experimental program involves the manufacture and testing of AS4/3501-6 graphite/epoxy coupons with implanted film adhesive layers or strips cocured at a specific interface. In the previous work done by Weems [38], plies of film adhesive, FM300M, were placed at all interfaces between dissimilar plies of the laminate. This was shown to successfully delay or suppress delamination depending on the thickness of the film adhesive used in the laminate. The current study looks into the efficient use of film adhesive, which requires an investigation into two types of "efficiencies", the first involves the "critical interfaces" at which the film adhesive needs to be placed and second the possibility of using film adhesive strips instead of entire plies of film adhesive to curtail the delamination initiation.

3.1.1 Efficiencies in Film Adhesive Placement

In the current program of investigation, the film adhesive is not placed at all dissimilar interfaces, but instead a "critical " interface is identified, based on its propensity to delaminate, and the film adhesive is placed at this interface alone. The identification of the critical interface is done by the use of a software package called the Interlaminar Stress Analysis Package based on the Force Balance Method developed by Kassapoglou and Lagace [13]. This package determines the state of the interlaminar stress at any desired

interface in any laminate. An average stress criterion called the Quadratic Delamination Criterion (QDC), developed by Brewer and Lagace [20], utilizes these interlaminar stresses to predict a load at which the delamination is likely to initiate in the given laminate. Therefore, given any laminate, the interlaminar stresses are determined at every interface of the laminate and used in the Quadratic Delamination Criterion to determine the values of in-plane loads at which the various interfaces delaminate. The "critical" interface is then chosen as the one which delaminates for the lowest value of the applied in-plane load. The in-plane load at which this interface delaminates is referred to as the "delamination initiation load". Delamination is predicted to occur at the critical interface only if the delamination initiation load obtained is lower than the in-plane failure load for the laminate.

In studies to date, film adhesive has been used throughout the laminate. However, interlaminar stresses are only appreciable in a region close to the free edge known as the boundary layer. The definition of the boundary layer size is rather arbitrary and the definition used by Kassapoglou [33] is that, for a general laminate which has a nonzero σ_{zz} stress, the boundary layer is the distance over which 99% of the σ_{zz} is counterbalanced. Since it is seen that the boundary layer region is the only region with any significant interlaminar behavior, the current study will examine the possibility of restricting the film adhesive layer to this region. The specimens manufactured would thus have film adhesive in fractions or multiples of the boundary layer size and would be placed such that one edge of the strip coincided with the free edge of the specimen.

Previous work by Brewer and Lagace [20] and by Lagace et al. [24] have shown that the $[\pm 15_n/0_n]_s$ laminates exhibit significant out-of-plane behavior. In his work, Weems [32] used $[\pm 15/0]_s$, amongst other, laminates because this

laminate failed by delamination at stresses much below the predicted in-plane failure load. The critical interface for these laminates is the +15°/-15° interface. The boundary layers as calculated for these laminates, however, are extremely small as is shown in Table 3.1. The material used for these calculations and the specimen manufacture is, Hercules AS4/3501-6 graphite/epoxy. The film adhesive FM300 Interleaf is manufactured by American Cyanamid. The properties of these materials are tabulated in Table 3.2.

The practical limitations to the manufacture and handling of such a small width of strips requires that, for investigating purposes, the effective ply thickness be increased in order to bring the boundary layer to the regime where the strips of that size could be manufactured. It has been shown by Lagace et al. [24] that the boundary layer size increases linearly with the effective ply thickness. In Table 3.1, the sizes of the boundary layer for laminates of the type $[+15_n/FA/-15_n/0_n]_s$ are shown. The 'FA' indicates film adhesive FM300 Interleaf (0.203 mm thick). These values were obtained using the previously mentioned analysis.

Based on the values of the boundary layers shown in Table 3.1, it is seen that the specimen $[+15_7/FA/-15_7/0_7]_s$ is most suitable for the current purpose as the boundary layer size of this specimen is about 9 mm which would enable the manufacture of specimens with film adhesive strips up to the size of 3 mm, which is about a third of the boundary layer size. This laminate was chosen for all further testing purposes in this program.

The standard TELAC coupon used for tensile testing is shown in Figure 3.1 along with the placement of film adhesive. The coupon is 50 mm wide and 350 mm long, with fiberglass loading tabs, of size 75 mm by 50 mm, attached to the ends of the specimen. Thus, the test section of the specimen is 200 mm. The

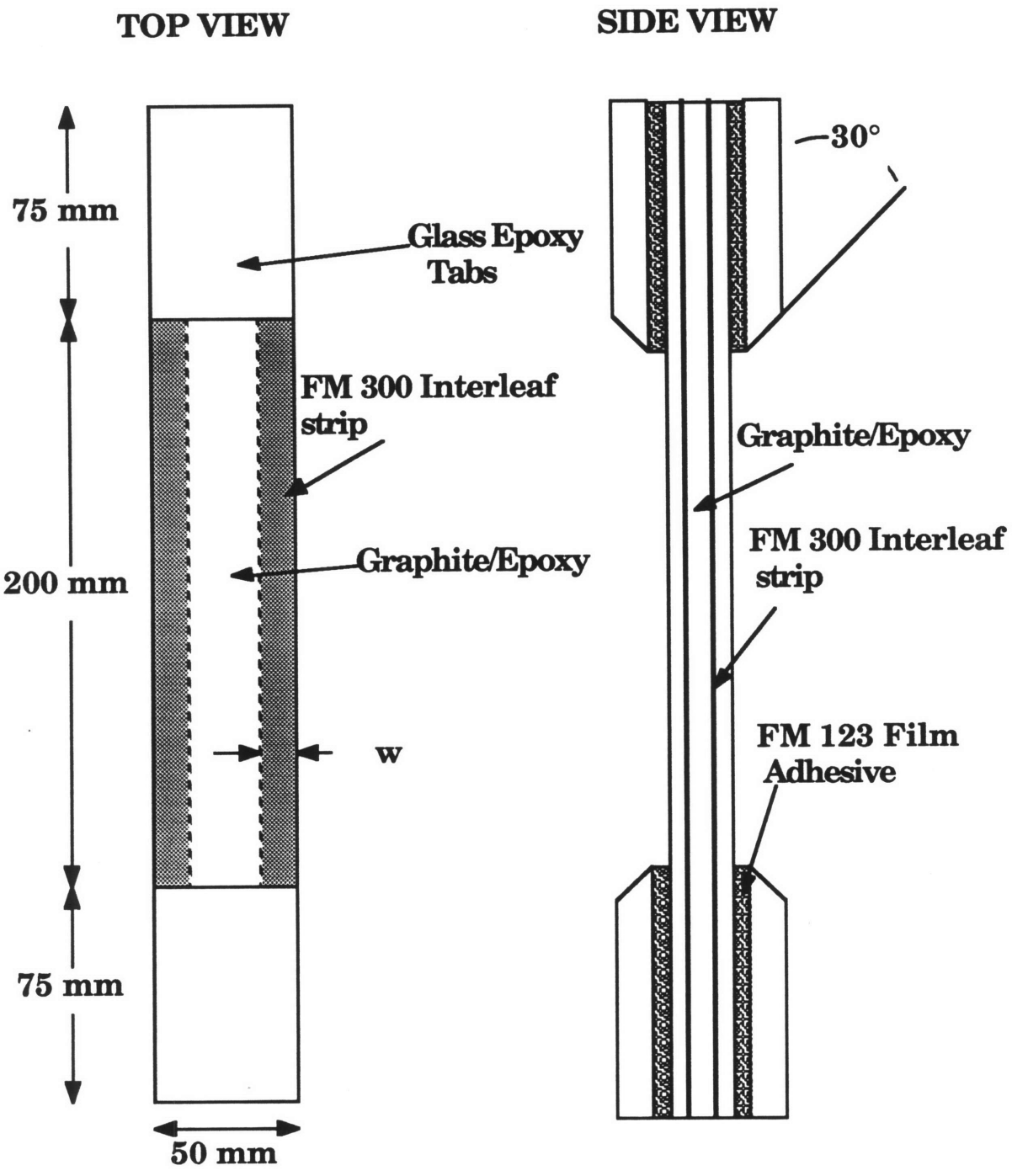

Figure 3.1 Characteristics of the TELAC tensile coupon with film adhesive strips.

Table 3.1 Boundary Layer Sizes for AS4/3501/6 $[+15_n/FA^a/-15_n/0_n]_s$ laminates

Normalized Effective ply thickness, n	Boundary layer size (mm)
1	1.9
2	3.1
4	5.2
6	7.4
7	8.5

[a] FA denotes 0.203 mm thick FM300 Interleaf

Table 3.2 Basic Material Properties of AS4/3501-6 Graphite/Epoxy and FM 300 Interleaf Film Adhesive.

Property	AS4/3501-6 [a] Graphite/Epoxy	FM 300 Interleaf [b] Film Adhesive
E_{11}	138.0 GPa	5.17 GPa
E_{22}	9.4 GPa	5.17 GPa
E_{zz}	9.4 GPa	5.17 GPa
G_{12}	6.0 GPa	1.83 GPa
G_{1z}	6.0 GPa	1.83 GPa
G_{2z}	4.8 GPa	1.83 GPa
ν_{12}	0.30	0.388
ν_{1z}	0.30	0.388
ν_{2z}	0.57	0.388
t_{ply}	0.134 mm	c

[a] As reported by Weems [32]

[b] From data reported by Weems [32] for FM 300M. Manufacturer reported the properties of FM 300M and FM 300 Interleaf to be similar.

[c] Film Adhesive was supplied in three different thicknesses: 0.041 mm, 0.051 mm and 0.102 mm

film adhesive strip is made of 0.203 mm thick (0.008") FM 300 Interleaf. The individual ply thickness of the AS4/3501-6 after cure is expected to be 0.134 mm. The present $[\pm 15_7/0_7]_s$ test specimen has 42 plies and hence the nominal thickness is expected to be about 5.6 mm, with variations at the edges due to the presence of the film adhesive strip.

This part of the testing program involves the manufacture of five sets of specimens. The first set consists of the "control set" which are $[\pm 15_7/0_7]_s$ specimens with no film adhesive implants in them. This set is a reference for all other sets with film adhesive implants in them. The second set of specimens have an entire film adhesive ply at the +15°/-15° interface. The other three sets have film adhesive only in the regions near the free edge, the sizes of these strips being fractions of the boundary layer size viz. strips with one-third the boundary layer size, two-thirds the boundary layer size and strips equal to the boundary layer size. The testing program as carried out is outlined in Table 3.3.

3.1.2 Growth Suppression via Film Adhesive Interlayers

The investigation by Weems [32] and the study outlined in section 3.1.1 provide an insight into the capabilities of the film adhesive with regard to suppressing or delaying delamination. This study, however, is further extended to examine the mechanism of operation of the film adhesive, in particular, to examine whether the film adhesive is capable of delaying delamination initiation alone or in curtailing the growth of the delamination as well. This constitutes the latter half of the experimental program. Specimens with full plies of film adhesive at the critical interfaces and delaminations implanted in them at the free edge are used for this purpose. Delamination implants are achieved by placing 0.08 mm thick, teflon-coated

Table 3.3 Test Matrix of specimens with film adhesive strips and plies at the +15°/-15° interface in the $[\pm 15_7/0_7]_s$ laminate

Width of film adhesive (mm)	Number of specimens
---	4
50 [a]	4
9	4
6	4
3	4

[a] full ply of film adhesive

glass fabric (Guaranteed Nonporous Teflon) strips at the edge of the specimens at the critical interfaces during the layup of the laminate. Varying the width of the teflon strip results in varying the size of the delamination "initiated" at the specimen edge. These specimens when tested should provide information on the effect of film adhesive on the growth of the delamination, given that delamination initiation has already occurred due to the teflon implant.

The experimental program for this study involves the manufacture of specimens with entire plies of film adhesive at the +15°/-15° interface, with teflon strips of various widths placed at the specimen edge. The teflon strips were placed at the +15°/FA interface. Three sets of specimens were manufactured, one with teflon strips of one-third the size of the boundary layer, the second with strips of two-third the size of the boundary layer and the third with strips the size of the boundary layer itself. The testing program is delineated in Table 3.4.

3.2 Specimen Manufacture

Most of the manufacturing procedures utilized were those previously tried and tested in the laboratory, many of which are listed in the TELAC Manufacturing Course Notes [34]. There were, however, certain variations which were mandated by the specific requirements of the specimens and they are mentioned in this section.

3.2.1 Layup Procedure

The standard TELAC manufacturing procedure involves the layup of 305 mm by 350 mm laminates which are cured and cut into five coupons of size 50 mm by 350 mm. This manufacturing procedure was, however, found to

Table 3.4 Test Matrix for $[+15_7/FA^a/-15_7/0_7]_s$ laminates with teflon strips implanted at the +15°/FA interface.

Width of teflon strip (mm)	Number of specimens
9	4
6	4
3	4

[a] full ply of film adhesive

be unsuitable in the present case due to the presence of the film adhesive implants. The specimen cross-section before cure, is illustrated in Figure 3.2, where a laminate with four specimens was attempted. It was intended that the laminate would be cured and later cut into four standard specimens with the film adhesive of required width at the edges. However, the curing process, and the flow stage of the curing process in particular, seemed to have caused movement of the film adhesive strips, thus making it impossible to cut specimens with any desired width of film adhesive implant within it.

The solution for this problem was that the laminate cure was given up for an individual coupon cure and a more suitable film adhesive was utilized. In this new approach, each coupon was layed up and cured individually. In his work, Weems [32] used the FM300M film adhesive due to its cocure compatibility with the 3501-6 resin system. In the current program of manufacture however, this film adhesive was replaced by a relatively new material called FM300 Interleaf, which showed less flow during the cure stages and was meant specifically for purposes of interleaving. The mechanical properties of the FM300 Interleaf is the same as that of the FM300M film adhesive. The specimen manufacture with the above prescribed alterations is described in detail in the next section.

The AS4/3501-6 graphite/epoxy was received as a 310 mm wide roll of preimpregnated unidirectional tape ("prepreg") and stored in a sealed bag in a freezer maintained at or below -18°C. The FM300 Interleaf film adhesive was in several thicknesses: 0.041 mm, 0.051 mm and 0.102 mm (0.0016", 0.002"and 0.004") on rolls 915 mm wide and, like the graphite/epoxy, was sealed and stored in the freezer In each case, either five, four, or two sheets of these, respectively, were laid down to form sheets which were 0.203 mm thick. A warm-up period of about an hour was essential for the film adhesive because

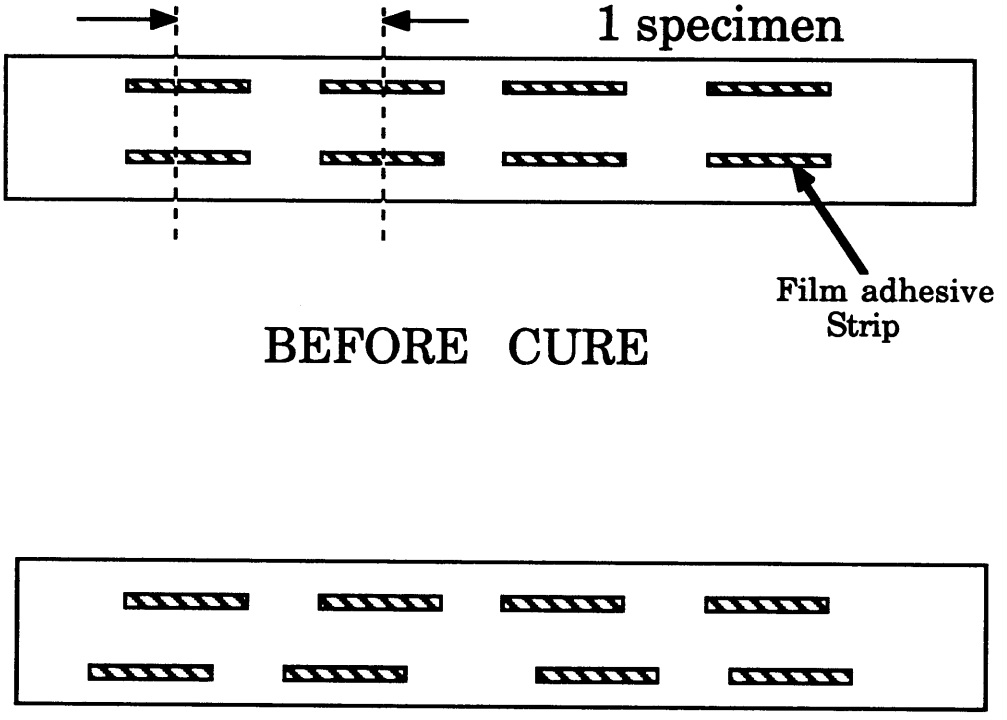

Figure 3.2 Illustration of the laminate cross-section indicating relative movement of the previously utilized FM300M film adhesive during full laminate cure.

the film adhesive was found to be extremely brittle and very difficult to handle at very low temperature.

The graphite/epoxy prepreg was cut using razor knives around machined aluminum templates covered with nonporous teflon. The templates were designed so that 305 mm by 350 mm graphite/epoxy plies could be made with any desired fiber orientation. The cutting was accomplished without having any cut fibers in the center of the plies. Seven plies of a particular angle were put together to form a sublaminate. The resulting sublaminates were $(+15°)_7$, $(-15°)_7$, $(0)_7$, $(+15°)_7$, $(-15°)_7$ and $(0)_7$. These sublaminates were then cut to form coupon sublaminates 70 mm wide and 350 mm long. The cured coupons were originally 70 mm wide so that the edge regions could be cut off to yield the final coupon width of 50 mm. The film adhesive was cut into strips (5+w) mm wide, where "w" is the desired final width of the strip, and placed at a distance of 5 mm from the edge of the specimen. It was originally found that due to some edge distortion of the specimen, distortion of the film adhesive strip occurred, thus causing misalignment of the film adhesive strips within the specimen. The solution was to avoid placement of the film adhesive up to the edge of the 70 mm specimen. Thus, when the additional 10 mm waste was taken off from either side of the 70 mm specimen, the required 50 mm coupon with a strip of film adhesive of width w mm at its free edge was left behind. The film adhesive was cut into widths of 8 mm (w equal to 3 mm), 11 mm (w equal to 6 mm) and 14 mm (w equal to 9 mm). Four strips of any given width were required for a particular specimen.

The layup procedure to build the laminates from the graphite/epoxy sublaminates and the film adhesive strip is similar to that of building the sublaminates and is done by hand using a jig consisting of two short metal walls mounted at right angles to each other on a flat plate. The bottom

sublaminate of a coupon is placed, backing paper down, on double stick tape so that two sides abut the metal walls. Each subsequent sublaminate is set in proper sequence firmly into the corner formed by the walls and then smoothed down on top. In order to achieve an accurate placement of the film adhesive, at the +15°/-15° sublaminate interface, two rulers were taped down on the jig, as shown in Figure 3.3. The sublaminates fit snugly, lengthwise, between the two rulers. A metal square was then set down with one arm set flush to the lower lip of the metal jig. This positioning enabled the other arm of the square to form a straight edge along the length of the sublaminate. By sliding the bottom arm of the square, the vertical arm which now formed a straight edge parallel to the laminate length could be moved anywhere on the laminate and its position read from the rulers attached to the jig. The film adhesive strips were placed against the straight edge formed by the vertical arm of the square at the appropriate widthwise location.

Compaction, which involves leaving the specimen under atmospheric pressure for about three hours by drawing vacuum on the specimens, is normally recommended for specimens which are forty plies or thicker in size. This helps to remove any voids formed during the layup operation. Compaction was attempted in the manufacture of the present specimens, but was discontinued in the final procedure because the specimens which were compacted showed some distortion of the edges and this caused movement of the film adhesive strips from their precise layup positions.

The specimens with teflon implants were manufactured in a similar fashion. The only difference being the fact that these specimens had a full width FM300 Interleaf layer placed at the +15°/-15° interface and the teflon strips were placed at the +15°/FA interface. The jig used for film adhesive strip placement was also used for the placement of the teflon strips.

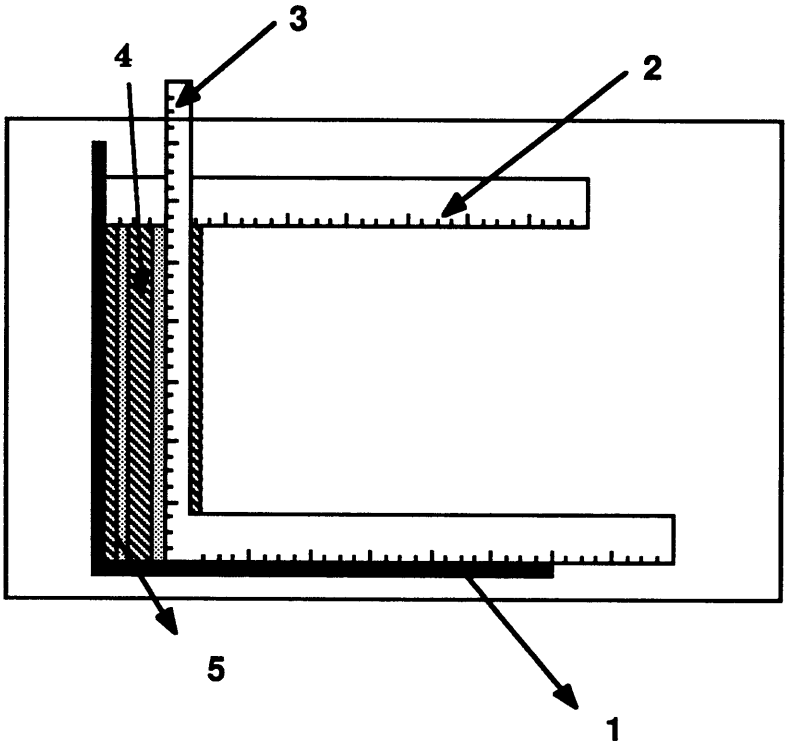

1. Metal jig with ruler attached to base

2. Ruler to locate film adhesive position

3. Metal square

4. Laminate coupon

5. Film adhesive strip

Figure 3.3 Illustration of film adhesive placement during layup of the laminate coupon.

TCGF-EHV, which is a teflon coated glass fabric of an electrical grade with a thickness of 0.08 mm (0.003") was used to make the teflon strips used for delamination implants.

3.2.2 Cure Procedure

The curing of the specimens involved the setting up of the cure assembly on the caul plate. The assembly involved the use of coverplates, cork dams and a variety of other cure materials. A cross-sectional view of the complete cure assembly is shown in Figure 3.4.

The cure plate itself is a flat aluminum plate 6.3 mm thick, with two 12.7 mm diameter holes drilled and appropriate plumbing installed to allow a vacuum to be drawn over the plate during a cure. The laminates are placed on the cure plate and enclosed in dams which are made with several layers of corprene rubber (cork). The cork dams were used in place of aluminum "T-dams" used during a standard cure because specimens cured with cork dams showed less edge distortion. The dams prevent the laminate from moving during the cure. In order to ensure that the laminate did not stick to the cork dams during the cure, the dams were lined with strips of nonporous teflon which were stuck on with double stick tape. Thus, with the laminates placed within these dams and covered with the cover plate, the pressure would be spread out evenly on the laminates, keeping the laminate thickness as even as possible.

The cure cycle used for all laminates, as shown in Figure 3.5, is a slight variation of the standard cure cycle for 3501-6 resin composites. The cycle consists of a one-hour flow stage at 116°C and a two-hour set stage at 177°C , all with a 760 mm Hg vacuum drawn inside the cure assembly and 0.59 mm MPa external (gage) pressure applied 40 minutes into the one-hour flow stage . The

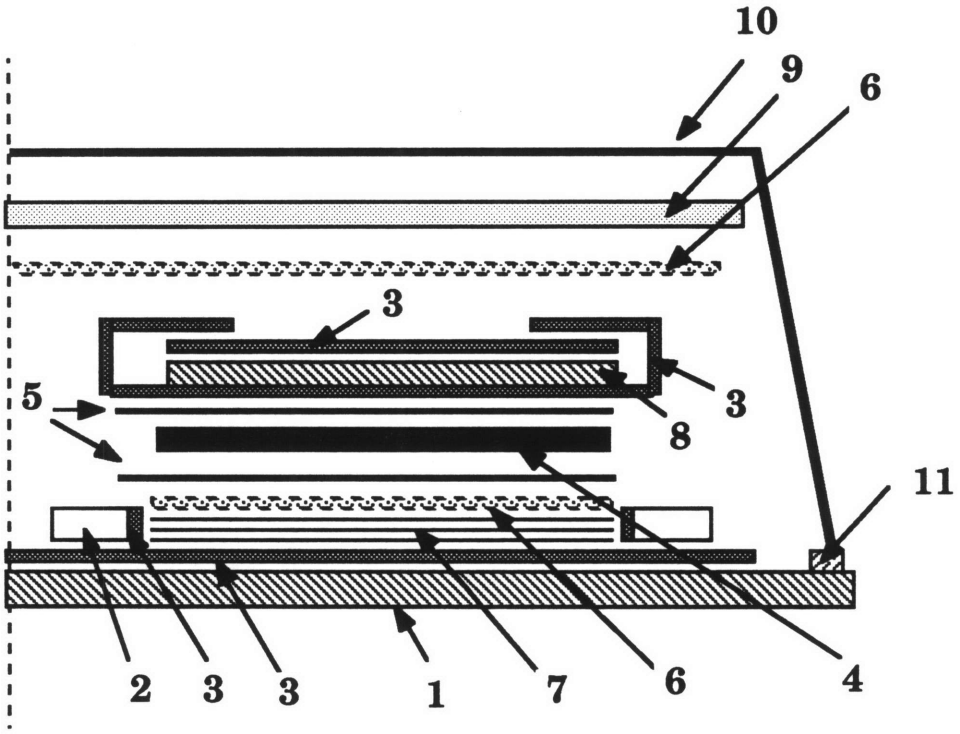

1. Aluminum Caul Plate coated with mold release
2. Corprene (Cork) dams
3. "Guaranteed" Non-Porous Teflon
4. Laminate
5. Peel-Ply
6. Porous Teflon
7. Paper Bleeders
8. Aluminum Top Plate
9. Fiberglass Airbreather
10. Vacuum Bagging
11. Vacuum Tape

Figure 3.4 Cure assembly cross-section for a laminate cure.

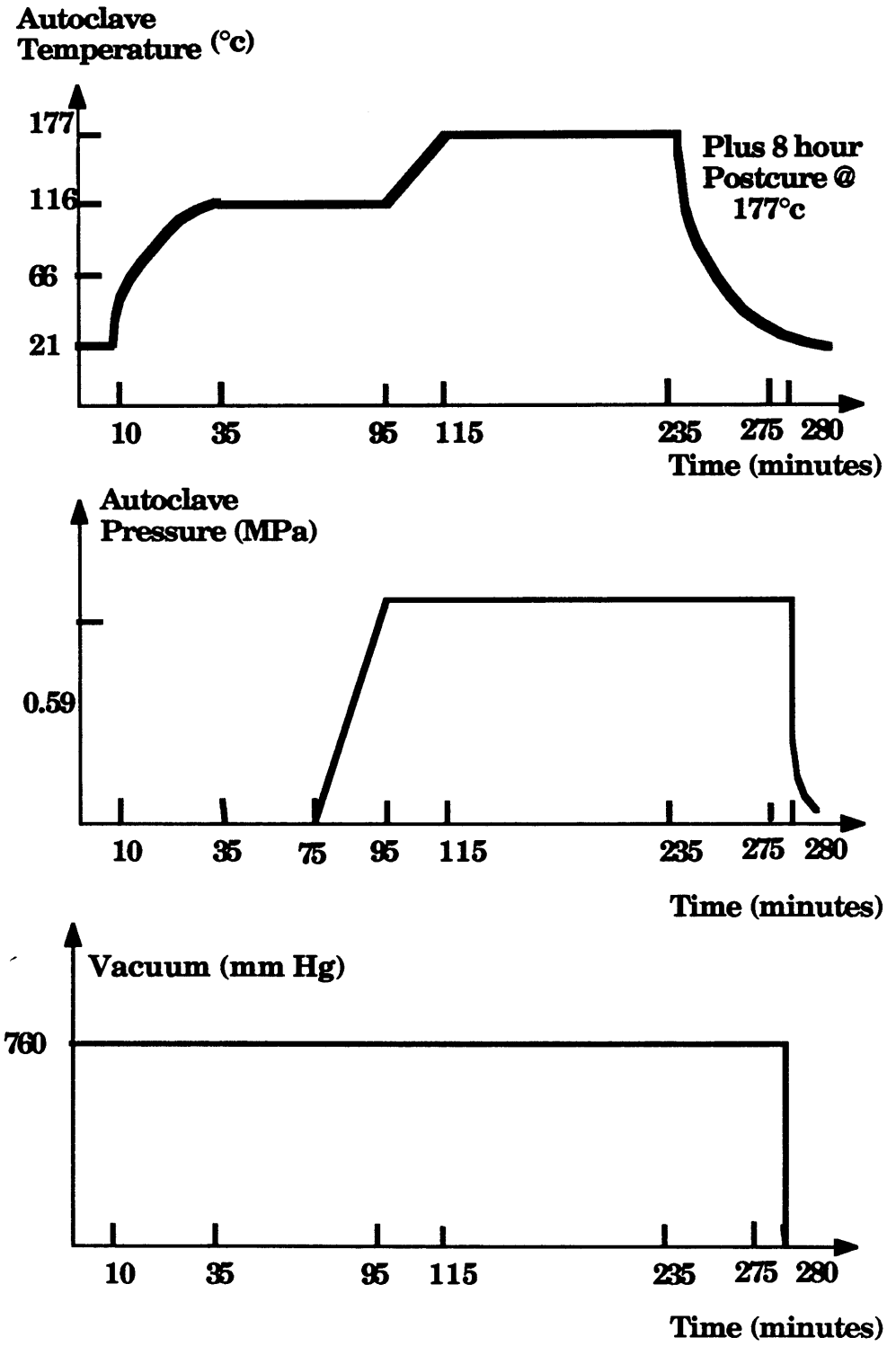

Figure 3.5 Altered cure cycle for the AS4/3501-6 graphite/epoxy laminate used in this study.

last point, involving the time of pressure application, is the only alteration as compared to the original cycle wherein the 0.59 MPa external pressure is applied throughout the cure cycle. This change in the cycle was made to minimize the movement of the film adhesive during its flow stage. The pressure, when applied 40 minutes into the flow stage results in the slow pressurization of the autoclave till it achieved its full value of 0.59 MPa just as the flow stage would end. After the cure assembly has been disassembled, the laminates were placed in an unpressurized oven with the peel-ply for an eight-hour postcure at 177°C to complete the cure of the 3501-6 epoxy.

3.2.3 Final Preparation

The resulting cured pieces, which are 70 mm wide and 350 mm long, are milled with a water-cooled diamond-blade. On milling the specimen widthwise at its ends, the location of the film adhesive is visible in the cross-section at both its ends. The specimens were checked in this fashion to ensure the alignment of the film adhesive. The specimens were scribed to mark a 50 mm wide and 350 mm long specimen with the desired width of the film adhesive at the edge of the specimen. The specimens were milled along these scribe lines with a slow table speed of about 20 mm/min to ensure that no damage was introduced at the edge of the specimen during the cutting operation.

After the specimens were cut to the required size, thickness and width measurements were taken from the test section of each coupon at the marked points shown in Figure 3.6. Thickness measurements were taken at 9 points with a digital micrometer and width measurements were taken with dial calipers. These measurements were then averaged to provide a single pair of measured dimensions for each coupon. The measured thickness did not show

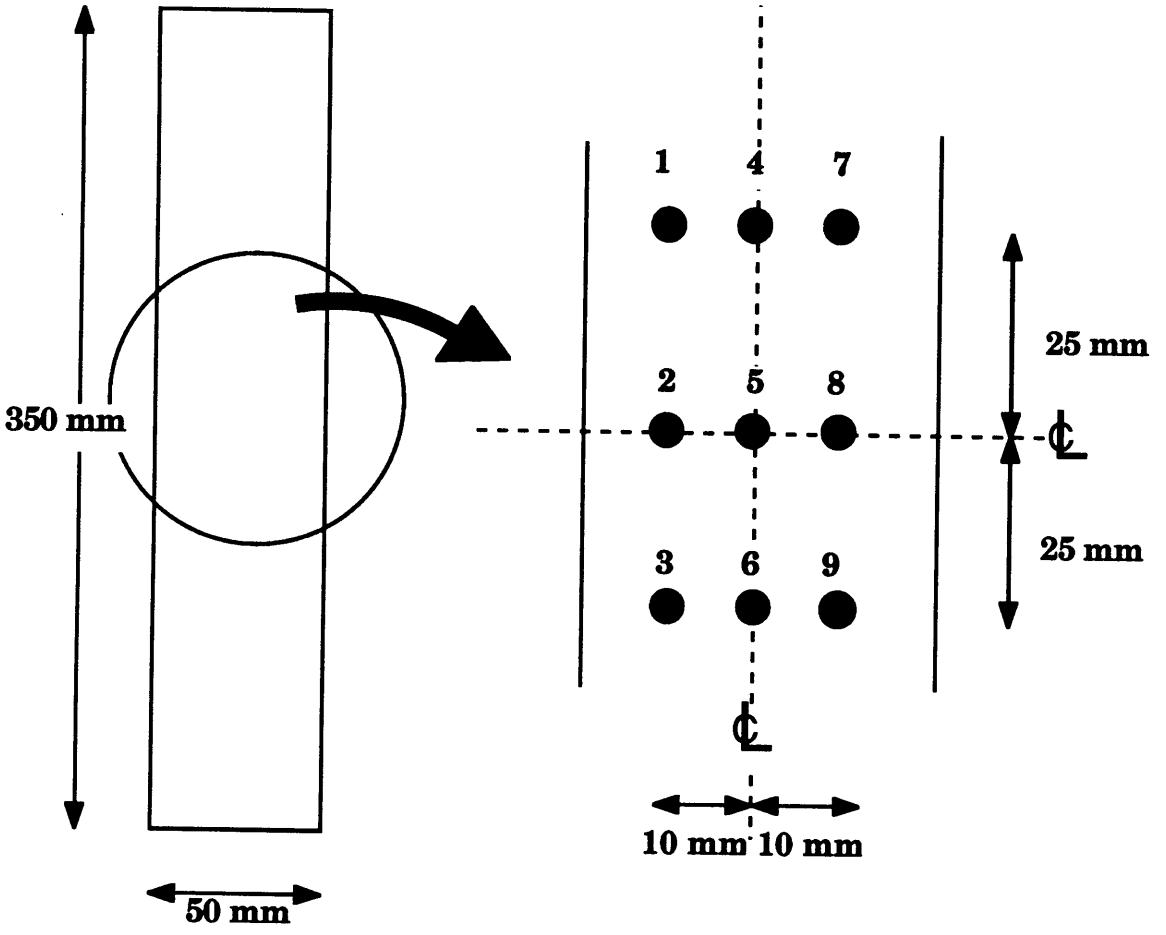

Figure 3.6 Location of specimen width and thickness measurements.

significant variation within a specimen, however it was seen to be about 12 to 14% less than the nominal thickness (5.628 mm) of the specimen without the film adhesive. For stress calculations purposes however, the nominal thickness of the specimens without the film adhesive were chosen.

The specimen edge, when observed under the microscope, revealed considerable local variation in the thickness of the cocured film adhesive layers in the laminates, as is shown in the micrograph in Figure 3.7. This was also reported by Weems [32] in his study. It was found to be impossible to eliminate these local variations.

The loading tabs are $[0/90]_{ns}$ cross-ply laminates of Scotchply 1002 fiberglass/epoxy, which are obtained as precured 380 mm by 610 mm sheets of various ply thicknesses. Nineteen-ply thick tabs, which measure 4.5 mm in thickness were chosen. The fiberglass/epoxy sheets were cut into rectangular pieces 75 mm long and 50 mm wide and these pieces bevelled on a belt sander to a 30° angle so that the tabs, when placed on the test specimen would taper towards the test section, as shown in Figure 3.1. These loading tabs were bonded to the specimens with FM123-2 film adhesive from American Cyanamid. The FM123-2 film adhesive was cured in the autoclave using the cure assembly shown in Figure 3.8. Steel cover plates 380 mm long were used to help apply even pressure over the tab. The adhesive was cured at 107°C for two hours, with an external pressure of 0.069 MPa plus a 30 mm Hg vacuum providing the recommended 0.35 MPa pressure on the bond surfaces.

After the bond cure, the specimens were polished at the edges to give them a smooth finish. The polishing was done with a felt bob mounted on a drill press and dipped into a colloidal solution of Kaopolite-SP, an abrasive with a particle size of 0.7 microns. Each edge was polished twice and then quickly rinsed to prevent the abrasive from drying on the edge of the specimen. The

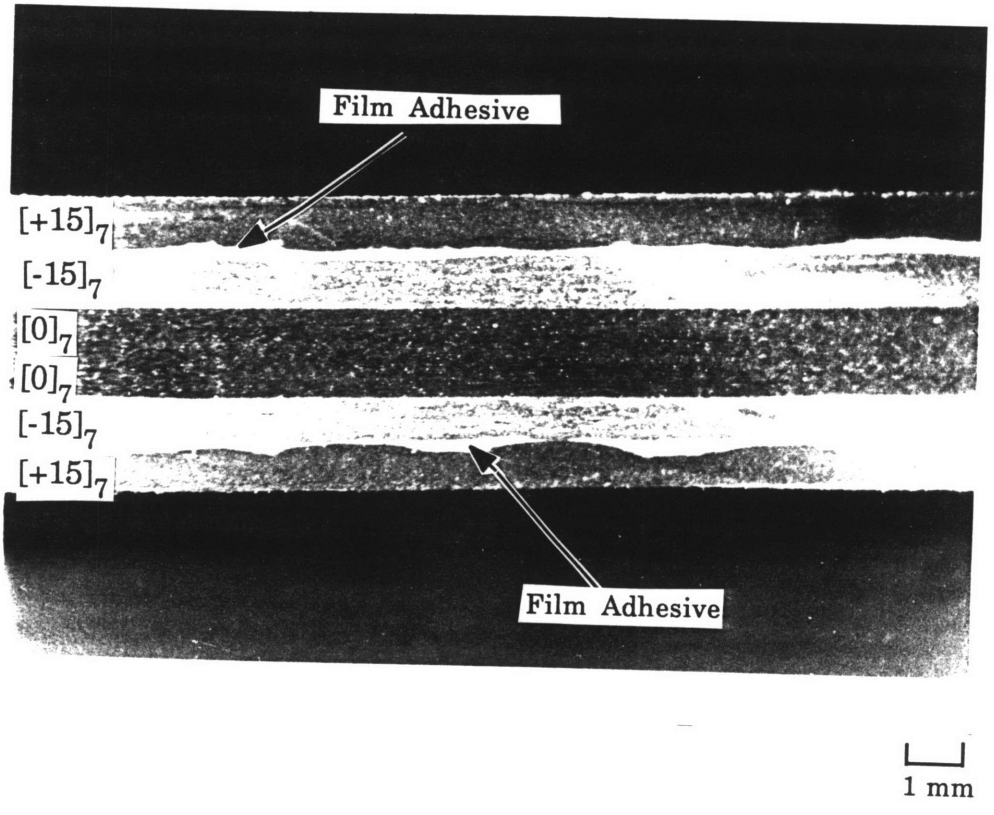

Figure 3.7 Photomicrograph illustrating the variation of film adhesive thickness at the edge of the specimen after cure.

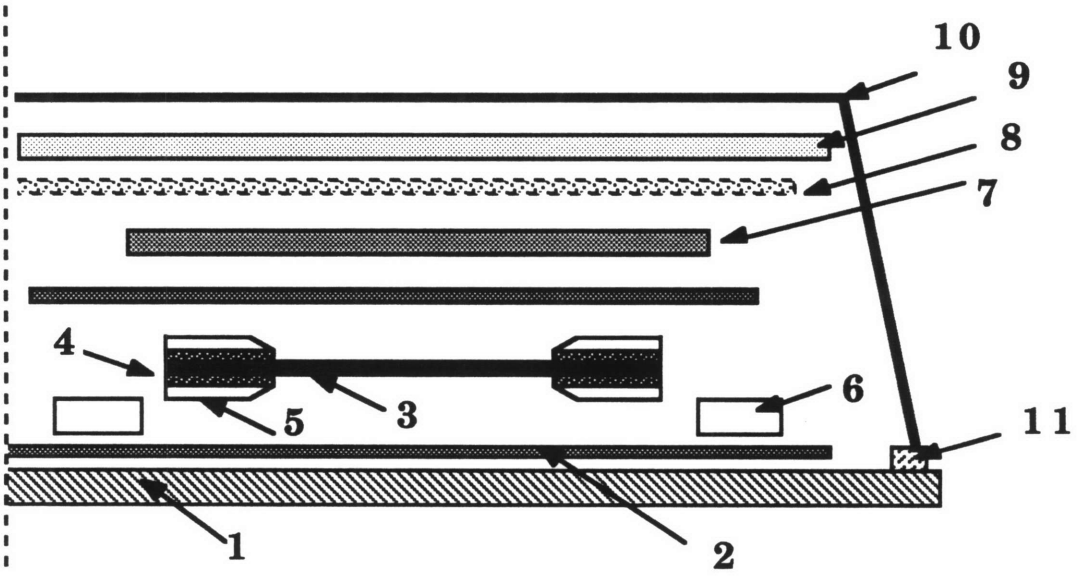

1. Aluminum Caul Plate
2. "Guaranteed" Non-Porous Teflon
3. Laminate
4. FM123-2 Film Adhesive
5. Fiberglass/Epoxy Loading Tabs
6. Support Tabs
7. Steel Cover Plate
8. Porous Teflon
9. Fiberglass Airbreather
10. Vacuum Bagging
11. Vacuum Tape

Figure 3.8 Cure assembly cross-section for a tab bond cure.

smoothly polished edges enabled better replicas of the edge to be obtained during the edge replication procedure described further herein.

3.3 Instrumentation

The final step in the specimen preparation procedure was the instrumentation of the specimen with strain gages. All specimens were outfitted with two primary strain gages at the center of the test section, one aligned with the longitudinal (loading) axis, the other aligned with the transverse axis. These gages provided the longitudinal and transverse strain data used to calculate the elastic constants of the specimen. The standard strain gage configuration is shown in Figure 3.9. All the strain gages used were Micro-Measurements EA-06-125AD-120 gages. The gages were bonded onto the specimens at room temperature with M-Bond 2000 adhesive system.

3.4 Testing

3.4.1 General Test Technique

The testing system used in this investigation consists of an MTS 810 hydraulic test machine interfaced with a DEC 11/34 computer. The testing machine has 100,000 pounds (445 kN) capacity and is equipped with hydraulic grips. The computer is set up for both data acquisition and test control.

At the beginning of each test, the specimen was placed in the testing machine and gripped at its upper end only, with the lower grip being placed, but not closed, around the lower end of the specimen. This is defined as the zero load, zero strain condition. A machinist's square was used to ensure that the longitudinal axis of the specimen was parallel to the loading axis, by using

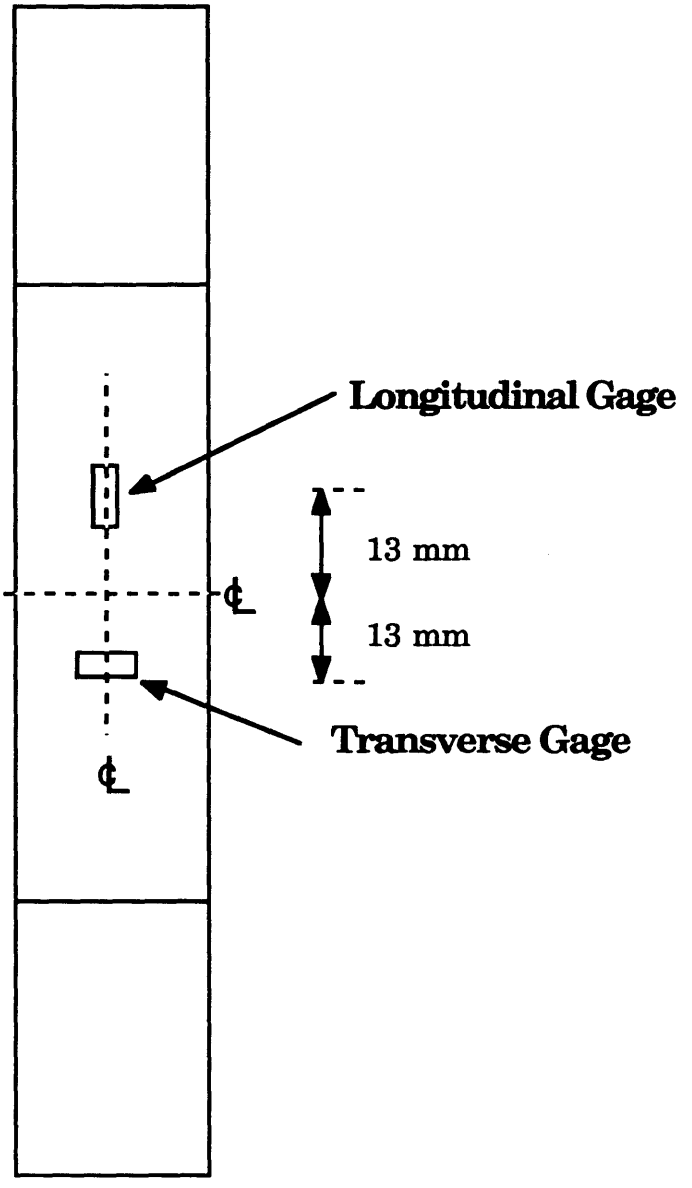

Figure 3.9 Standard strain gage locations.

one edge of the specimen and the upper grip of the machine as references for the square. In the unloaded condition, the load and strain channels are zeroed and all active strain gage conditioners balanced and calibrated. Calibration of the strain gage conditioners was accomplished by placing a precision decade resistor in parallel with the active gage to simulate a strain of a certain magnitude, then adjusting the conditioner gain until the computer read the desired value. After all calibration was complete, the lower grip was closed. The specimen were loaded at a constant stroke rate of 1.09 mm/min, producing a strain rate of approximately 5000 microstrain/minute similar to standard tests. The resolution of the raw data obtained from the computer was 12.5 microstrain for strain, 2.44×10^{-4} inches (0.0062 mm) for stroke and 48.5 pounds (215.7 N) for the load. The resolution of the load data depends on the load range used, which in turn was governed by the maximum expected failure load. The expected failure load in this case was close to 50,000 pounds, thus the machine had to be set at 100% of its load capacity which was 100,000 pounds. The data files also contain marks inserted manually whenever any visible or audible damage was detected.

All the tests done in this study used the "Load Drop Program" wherein the computer was used for data acquisition and also for running the test. This was used in association with the edge replication procedure which enabled the determination of the load at which delamination initiated, and the location of the initiation on the specimen edge. After final failure of the specimen, the edges of the specimen were examined to look at the size of the film adhesive strip at the test section. In almost all cases, the size of the film adhesive at the test section could be measured from the traces of the film adhesive which were of a different color than the rest of the laminate. This measurement was made to ensure the validity of the specimen. In cases where the specimen did not

have proper placement of the film adhesive strip at its edge, the specimen data was discarded.

3.4.2 Load Drop Program and Edge Replication

This load drop computer program to control the testing was developed at TELAC. The occurrence of damage in a laminate will result in a drop in the modulus of the specimen. This change in modulus manifests itself in the form of an instantaneous drop in the load when the specimen is loaded in displacement (stroke) control. Hence, a drop in load in a quasistatically loaded specimen may indicate the occurrence of damage. Damage initiation may be detected in this manner if the load drop is not immediately obscured by the increase in load due to normal loading of the specimen.

The load drop program allows the termination of the test when a load drop is detected, and thus helps to control the testing. The program's ability to detect load drops depends on the magnitude of the load drop, the loading rate and the time interval chosen between data points. The load data is obtained by the computer from the testing machine through analog-to-digital converters, which digitize the analog voltage data, representing the applied load with discrete computer units. The load equivalent to a computer unit depends on the load range selected. The program compares each new load datum with the previous one, and if the new point's value is lower, the test is halted.

It is necessary that the load drop be larger than the normal increase in load, in the time interval between data points, by at least one computer unit, otherwise the drop will be obscured as illustrated in Figure 3.10. If the time interval is too short, however, the noise in the system can be larger than the normal rise in load, resulting in erroneous stops. Trial and error were used to find a time interval which was short enough to provide the necessary

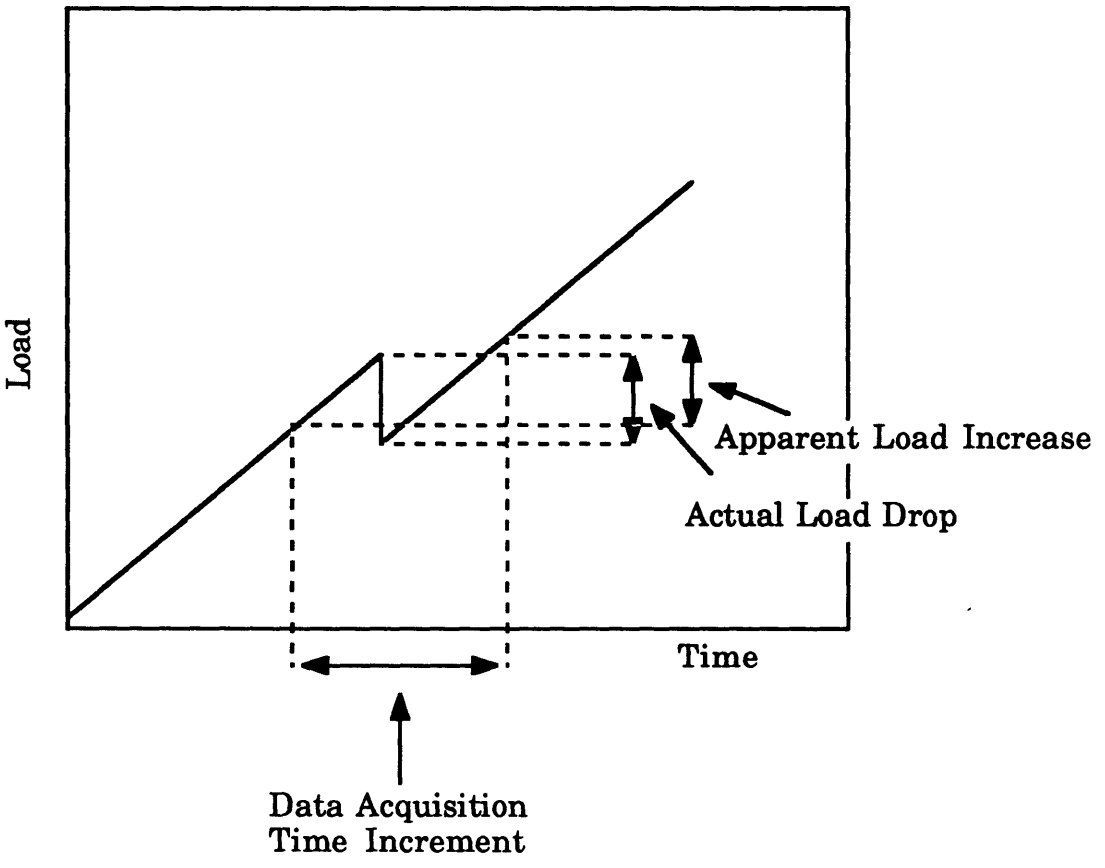

Figure 3.10 Illustration of load increase obscuring a load drop.

sensitivity, but long enough to avoid problems with noise. The interval chosen tended to err on the side of being short; this resulted in the first few load drops for a specimen being erroneous, but ensured that the first sign of damage was detected. The time interval used was 0.18 seconds.

On encountering a load drop, the computer halts the test and reduces the stroke to half the stroke, to allow edge replicas to be taken. This unloading prevents the specimen from getting any further damage, while still keeping the specimen under load to ensure that any cracks and delaminations are open so as to show up better on the edge replica.

Edge replication is a procedure in which a piece of clear acetate film is used to record the surface texture of the specimen's edge. The specimen edges are polished before testing to give a clear replica. The acetate tape, when softened with acetone and pressed against the specimen edge, flows into the flaws such as transverse cracks and delaminations. When the acetate hardens, it forms a permanent record of these flaws which can be examined under a microscope.

In the replicas of the free edge, different plies and the interply matrix layer can be identified due to their different surface texture. The replicas are illuminated from a light source behind and to the side during inspection under the microscope. Delamination initiations and angle ply splits appear as bright thin lines. An SZ-Tr Olympus Zoom Stereo Microscope, with a magnification range of 10X to 60X was used to examine the edge replicas.

In all cases, an initial edge replica was taken when the specimen was gripped in the hydraulic grips. This replica was used as a reference to ensure that the specimen was undamaged before the start of the test. An edge replica was taken at every subsequent load drop at which the computer halted the test. These edge replicas were not taken for the case of the teflon implanted

specimens as the delamination was initiated via those implants in the specimens.

3.5 Data Reduction

The raw data files, as created by the data acquisition program, contain load in pounds, stroke in inches, and strain in microstrain, These raw data files are backed up to off-line storage after each testing session, before data reduction.

The first step in data reduction is to snip off any extraneous data points, which were recorded after final failure of the specimen or even before loading of the specimen began. The load data was converted to stress units (MPa) using the graphite/epoxy specimen nominal thickness. The failure loads and stroke of the specimen were recorded from the data files.

With the data reduced to the required form, the elastic modulus and the Poisson's ratios are determined from the linear regressions of the stress versus longitudinal strain, respectively. In these cases, a special program was used to determine the linear regions of maximum correlation, with the elastic constants being taken as the slope of the first significant linear region.

CHAPTER 4

ANALYTIC DETERMINATION OF INTERLAMINAR STRESSES AT PLY DROPOFFS

4.1 Previous Work on Interlaminar Stresses at Ply Dropoffs

Relatively little work has been done in the area of ply dropoffs in laminates. Most of the work done in this area involves the use of the finite element method to model the complicated geometry that arises at a dropoff.

Chan and Ochoa [30] used the method of terminating critical internal plies near the edges to suppress delamination at the free edges of the laminate. The laminates used in the study were $[30/-30_2/30/90]_S$ and $[\pm 35/0/90]_S$, with the 90° ply terminating just before the free edge. The analysis to investigate the stress distribution due to ply termination used a quasi three-dimensional finite element formulation, with an eight noded isoparametric element. The tapered laminate geometry was based on the examination of a test coupon cross-section under the microscope. The 90° ply was terminated at a distance from the free edge equivalent to a width of twenty-eight plies. Immediately adjacent to the terminated 90° ply, a triangular region of four ply thicknesses in length and one ply in height is modelled as a resin-rich region. The laminate considered for analysis was $[\pm 35/0/90]_S$. Through the thickness graphs at various locations on the laminate indicate σ_{zz}, the interlaminar normal stress, and σ_{2z} the interlaminar shear stress, to be the highest in the region before the ply termination. A study of the interlaminar stress near the midplane shows the σ_{zz} to be highest just before the dropoff. The σ_{2z} stresses are less than half the

normal stress, and their peaks occur in the resin-rich region. The authors do not make any mention of the σ_{1z} interlaminar stress.

Kemp and Johnson [35] used a two-dimensional generalized plane deformation finite element model to study the interlaminar stresses at a ply drop and hence predict the initiation of failure. The influence of various parameters were considered in this study and laminates with various permutations of these parameters were studied. Two different layups, symmetric and nonsymmetric plydrops, were considered. Within each of these four possible combinations of layup and symmetry, one, two and three plies were dropped, and aspect ratios of 1/3, 1/4, 1/5 and 1/6 were considered for the triangular resin-rich region formed at the dropoff. The results were presented for the basic layup, $[\pm 45/0/90/0_3/90/0/\pm 45]_s$, with the $[0_3]$ dropped off. The aspect ratio of the resin-rich region is 1/3. The laminate was subject to an axial strain of ε_1 (in tension), which was normal to the dropped ply, and the resulting axial strain distribution through-the-thickness of the laminate displayed a maximum in the thick section before the ply dropoff. Through the thickness σ_{1z} distributions indicate it to be maximum just before and after the dropoff. At both these locations, the stress shows two peaks, one at the interface above the dropped ply and another below the dropoff. At the interface below the dropped ply, the shear stress σ_{1z} has two peaks, one in the thick section before the dropoff and one in the thin section.

The interlaminar normal stress, σ_{zz}, shows a maximum at almost exactly the same locations as the shear stress, σ_{2z}. The magnitudes of the two stresses are also similar. Decreasing the aspect ratio of the resin region results in the reduction of both the stresses. The values for applied axial strain were computed for two failure modes with the maximum stress failure criterion used to predict interlaminar failure in the pure resin regions

surrounding the droped plies, and a three dimensional Tsai-Wu tensor polynomial criterion, used to predict intralamina failure. Most cases were seen to be resin failure cases, just above or below the dropped ply depending on the laminate layup.

The work of Adams et al. [36] includes experimental as well as analytical results conducted on a laminate typical of that used in a wing skin. The laminate considered had a $[0_{16}/(\pm 45)_5/90_4]_S$ configuration. Two 0° plies were dropped but at different locations through-the-thickness. A materially-nonlinear finite element analysis was used to predict the stress distributions near the ply dropoff. Thermal residual stresses resulting from the curing process were included. The interlaminar stress resultants were found to be small in comparison to the in-plane stress resultants. The tests and analysis showed little reduction in strength due to ply dropoffs.

Curry, Johnson and Starnes [37] experimentally and analytically studied the effect of ply dropoffs on the strength of graphite/epoxy laminates in both tension and compression. The specimens were fabricated with all the dropped plies lumped together in the center of a sixteen-ply quasi-isotropic layup, such that one surface remained flat and the other changed abruptly to accomodate the thickness change at the dropoff. Experiments were conducted on specimens which differed in the configuration of the dropped plies only. The analysis of interlaminar stresses was carried out by a global-local finite element model. It was observed experimentally that the strength of a laminate with dropped plies was less than the strength of its thin section, and the compression specimens exhibited a lower strength than a tension specimen for the same configuration and width. The greater the stiffness change between the thick and thin sections at the dropped ply location the greater is the reduction in strength. The delamination was seen to initiate at the upper

interface at the end of the dropped ply. The analysis showed this as the location close to the maximum of the interlaminar normal and shear stresses. The normal and shear stresses were seen to be of the same order of magnitude.

Fish [38] used glass-epoxy specimens in his studies of internal ply dropoffs. Five different layups were chosen, two layups with and the remaining without significant free edge effects. The dropoff edge was normal to the loading direction. The plies dropped were staggered over some distance and were not all dropped at the same location. A hybrid finite element method was used in the analytical study of the interlaminar stresses at the dropoff. In most cases, the highest interlaminar stresses were found before the last step of plies dropped off, and the interface was the upper interface of the dropped ply. The σ_{2z} stress was negligibly small compared to the σ_{1z} stress. On the lower interface, where the stresses were lower, σ_{1z} and σ_{zz} had about the same magnitude.

Most of the previous work involves extensive modelling and analysis using the finite element approach to the problem. The current study, however, precipitates in the development of a closed form solution by the development of a simplified model. This should enable a quick study of the state of interlaminar stress, and constitute a useful preliminary design tool.

4.2 Problem Formulation

The presence of an in-plane stress gradient has been shown by Saeger [39] to cause out-of-plane stresses. In the current problem of delamination suppression by the use of film adhesive strips, it is observed that the film adhesive strip has to be terminated at some location inside the laminate. The termination, or "dropoff", of the film adhesive strip implies that

the in-plane load which the dropped ply carried, has to be redistributed amongst the remaining plies of the laminate. The in-plane load is therefore altered i.e., there exists an in-plane stress gradient within the laminate which gives rise to interlaminar stresses. Thus, the interlaminar stresses that arise in the case of a ply dropoff must be evaluated to ensure that they do not cause delamination in the composite laminate, the resulting in-plane stress concentrations also need to be examined for the possibility of intralamina failure.

The methodology used in developing solutions for the interlaminar stresses at a ply dropoff is based on the Reduced Eigenfunction Stress Technique (REST) developed by Saeger [39]. The fundamental principle behind this technique is the development of a companion problem, to be superposed on any existing solution to provide a more accurate solution to the problem. A typical example would be the case of interlaminar stresses at the stress-free edge of composite laminates. Classical Laminated Plate Theory provides a planar solution and does not indicate the presence of any interlaminar or out-of-plane stresses. The stresses obtained from this theory satisfy the equations of equilibrium only in an integral sense at the free edge as individual ply equilibrium is not satisfied. Therefore, any ply of a laminate subjected to in-plane loading in one direction and stress free in the transverse direction will show the presence of some "residual" stresses σ_{22} and σ_{12} in each ply at the free edge. These residual stresses are not zero on a point-by-point basis, but integrate to zero through the laminate thickness. In actuality, however, the stress-free condition is to be satisfied at the free edge by each individual ply. To satisfy the stress-free requirement, a companion problem is formulated. The companion problem is defined as a problem in which a laminate is subjected to a loading which is the negative of the residual stresses at the free

edge. Using the principle of superposition, the solution to the companion problem is superposed on the Classical Laminated Plate Theory solution with the resulting sum being a solution which satisfies equilibrium on a ply-by-ply basis and also satisfies the stress-free boundary conditions at the free edge, since the stresses at the free edge in the companion problem are the negative of the residual stresses. This addition of the two solutions is possible because both the solutions are equilibrium stress states in themselves, and their addition also results in another equilibrium state. A pictorial representation of this approach is shown in Figure 4.1.

One form of the REST approach involves formulating the companion problem by assuming arbitrary functions for the in-plane stresses in each individual ply,

$$\sigma^{i}_{\alpha\beta}=F^{i}_{\alpha\beta}(x_1,x_2) \qquad \alpha,\beta=1,2 \tag{4.1a}$$

The in-plane stresses are assumed to be independent of the z-direction in each ply and the equations 4.1a are used in the equilibrium equations to obtain the unknown out-of-plane stresses in terms of these functions. All the stresses are thus in terms of the unknown functions, the interlaminar shear stresses end up linear in z, and the interlaminar normal stresses end up quadratic in z, within a ply.

These stresses are utilized to obtain the complementary energy, Π_c, of the laminate,

$$\Pi_c=\frac{1}{2}\iiint_{v}\sum_{i=1}^{n}\sigma^{(i)}_{pq}S^{*}_{pqkl}\sigma^{(i)}_{kl} \qquad p,q,k,l=1,2,3 \tag{4.1b}$$

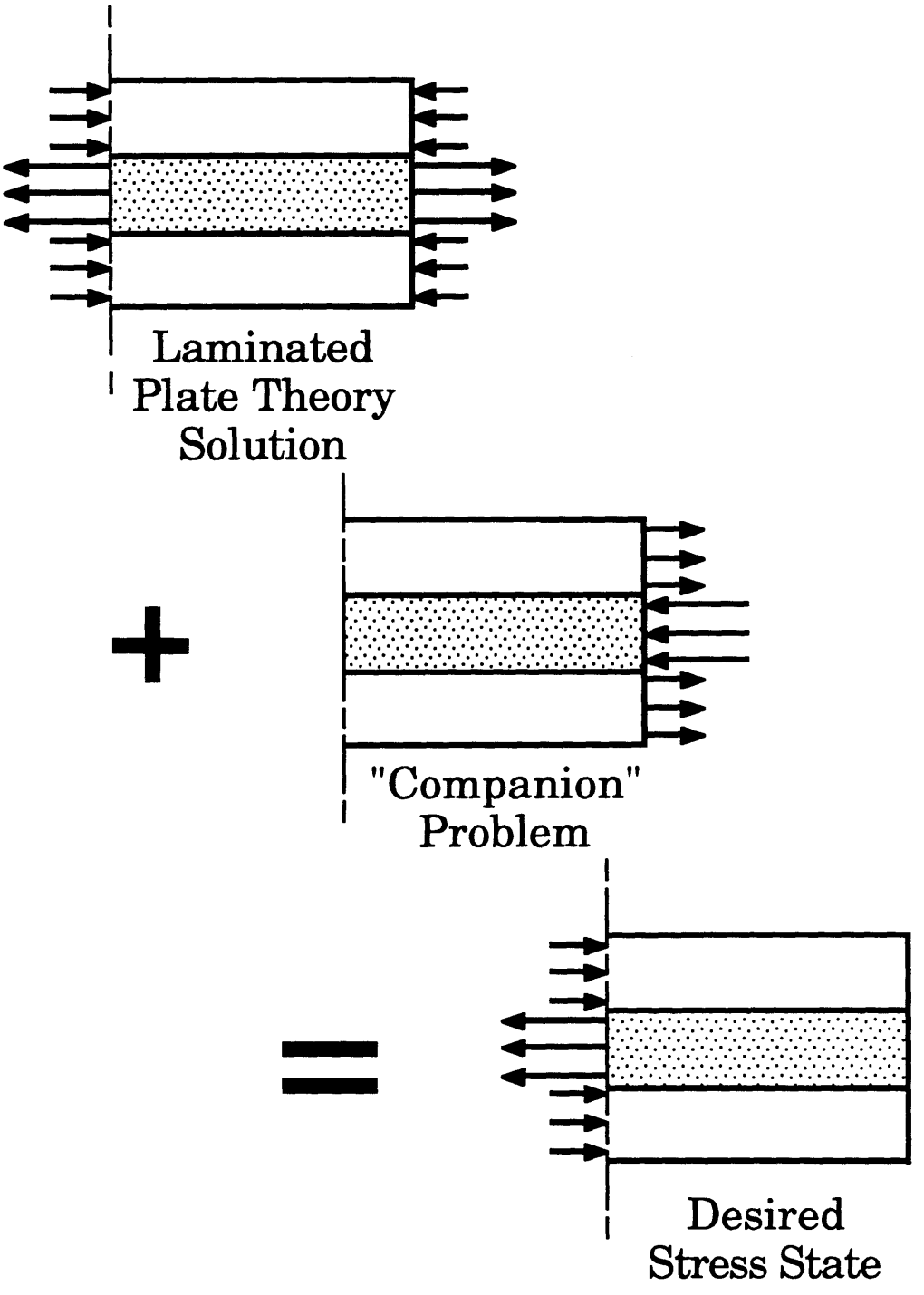

Figure 4.1 Illustration of the solution technique adopted by the REST approach using the principle of superposition.

where S^*_{pqkl} are the components of the compliance tensors.

The variational principle is then applied to the complementary energy by setting,

$$\delta\Pi_c=0 \tag{4.1c}$$

This, by the principle of minimum energy, should lead to the "best" possible solution for the functions $F^i_{\alpha\beta}$, which satisfy ply equilibrium and the boundary conditions. The governing equations resulting from setting the variational equal to zero are a set of homogeneous, coupled, fourth-order partial differential equations. These resulting equations are difficult to solve analytically, unless some simplifications are made in the functions assumed for the in-plane stresses. The absence of a gradient stress field in the x_1-direction of the laminate leads to considerable simplification. This is tantamount to assuming the laminate to be two-dimensional and any cross-section in the x_1-direction is exactly similar to any other. This modifies the governing equations from partial to ordinary differential equations which can be solved analytically to obtain expressions for the interlaminar stresses.

4.3 Simplified Problem Model

The geometry of the ply dropoff problem tends to be complicated due to the various shapes of the resin pockets at the dropoff region. The geometry not only results in complex equations, but is also difficult to determine and may vary depending on the angle of the ply dropped, the number of plies dropped, and other variables. An illustration of a $[\pm 15_7/0_7]_s$ specimen with a film adhesive strip placed at the free edge and terminating within the laminate is

shown in Figure 4.2. A cross-section of this specimen is considered in Figure 4.3a. The region before the dropoff of the film adhesive is termed as region A, the intermediate region during the tapering of the film adhesive is known as the "dropoff region", and the region after is termed as region B.

The simplified model adopted in this analysis is that the dropoff region is collapsed completely and the stresses are matched between all the plies which continue from region A to region B. The stresses in the dropped ply are assumed to go to zero at the dropoff, as is illustrated in Figure 4.3b.

4.4 Assumptions in the model

The assumptions associated with the present problem can be classified into two types, those associated with the simplified problem model and those associated with the method of solution.

The first in the problem model is that the dropped ply is unloaded of its in-plane stresses σ_{22} and σ_{12} in the direction of the dropoff, by transfering stresses to the neighboring plies by the mechanism of interlaminar shear stresses, σ_{1z} and σ_{2z}. The edge of the dropped ply thus behaves like a free edge at the interface of region A and B with the stresses σ_{12}, σ_{22} and σ_{2z} equal to zero at the interface, as is illustrated in Figure 4.3b. It should be noted that the in-plane stresses σ_{11}, σ_{22} and σ_{12} are not involved in the transfer of stresses from the dropped ply to the adjacent plies, only the interlaminar shear stresses perform this task.

Second, it is assumed that there is no significant variation in the stresses in the dropoff region arising due to the tapered geometry of the plies in this region and hence this dropoff region can be eliminated for purposes of the analysis. The stresses in the plies can therefore be matched directly

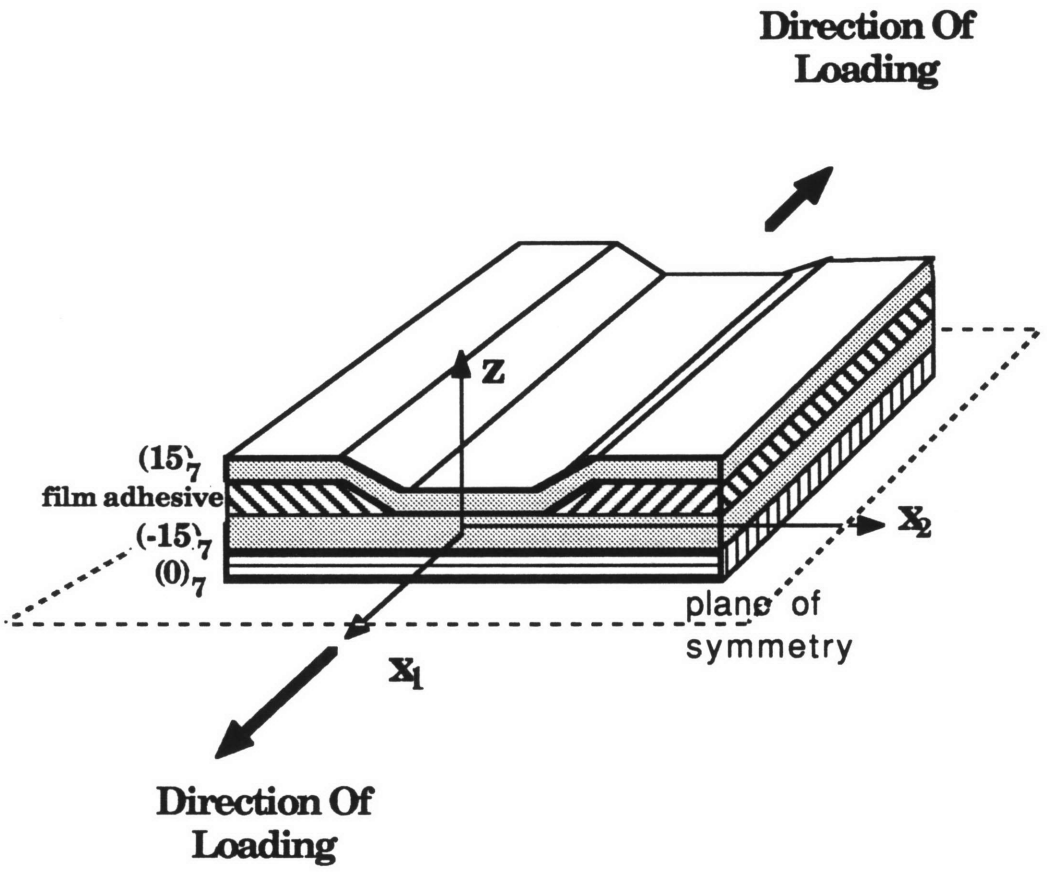

Figure 4.2 Illustration of the specimen with film adhesive strips dropped off along with the coordinate system adopted.

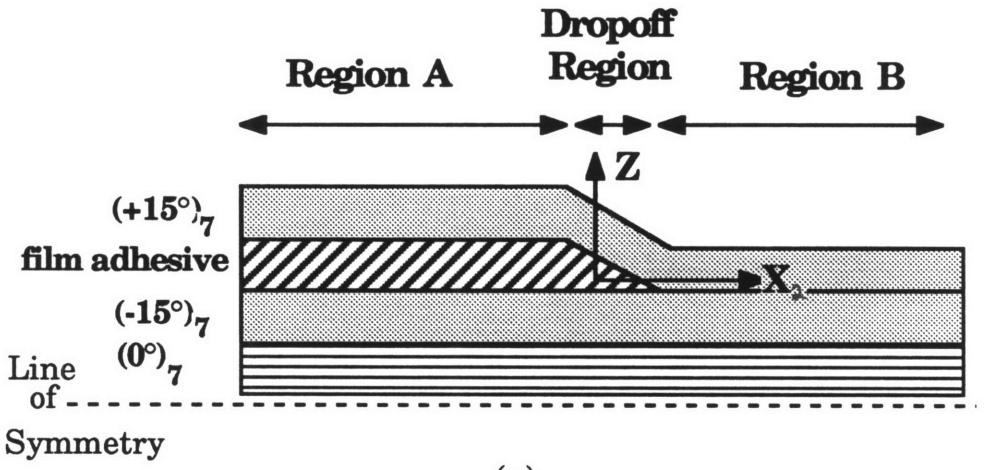

(a)

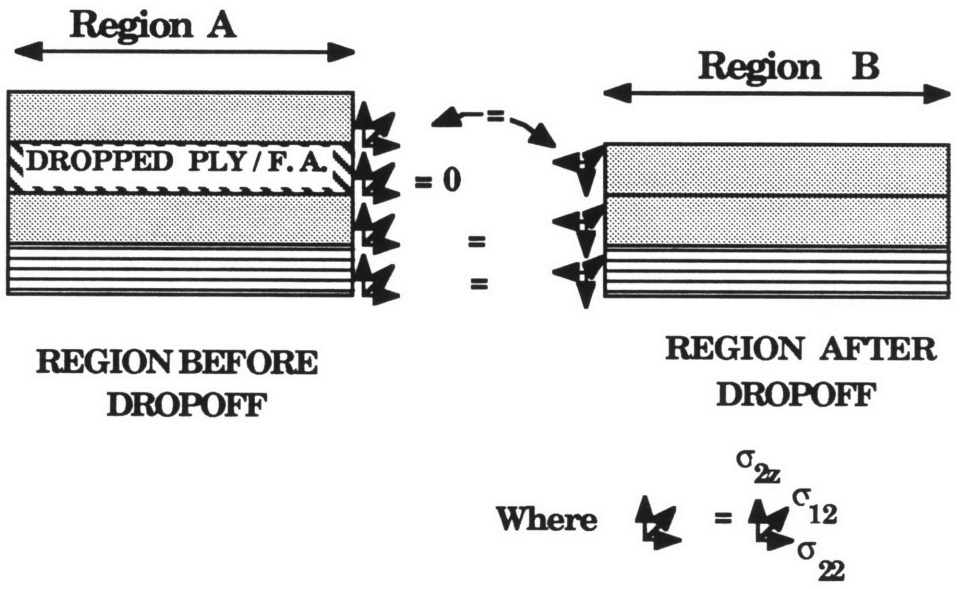

(b)

Figure 4.3 Illustrations of (a) actual specimen in cross-section indicating the three regions in the analysis; and (b) simplified problem model adopted for the analysis.

between region A and B as illustrated in Figure 4.3b. The dropped ply in this case being a film adhesive, does not carry significant in-plane load to begin with, and the assumption that the dropped end of this ply behaves like a free edge with stresses dropping to zero seems to be applicable in this case. In cases where actual load-carrying plies are dropped off, it has been shown by Curry et al. [37] that there is an accumulation of resin in the 'dropoff' region. Since the resin is not capable of carrying much load, it is likely that the ply would have transferred most of its stresses to the adjacent plies by the mechanism of interlaminar stresses prior to this resin accumulation. Therefore, the assumption about the stresses in the dropped ply receeding to zero seem to be valid, even in cases where significant load-bearing plies of the laminate are dropped off.

The third assumption made is that there are no gradient stress fields along the loading axis (x_1) shown in Figure 4.2. This assumption is valid in the case of a specimen subject to simple tension as there are no gradients in the x_1-direction and hence there is no difference in the behavior of any x_1-axis location of the specimen. This simplifies the problem from a three-dimensional to a two-dimensional problem and the governing equations turn out as ordinary differential equations instead of partial differential equations. The new axis system utilized is defined in the cross-section of the specimen shown in Figure 4.3a.

The previous three assumptions are with regard to the model adopted in this context. The other assumptions are associated with the solution technique adopted in this problem.

In the Reduced EigenFunction Stress technique [39] used for the analysis, the interlaminar shear stresses within a ply are a linear interpolation, in the z-direction, of the stresses at the ply interfaces. As a

consequence, on using the equations of equilibrium to obtain the other stresses, the in-plane stresses are seen to be independent of the z-direction within a ply, and the interlaminar normal stresses are quadratically interpolated in the z-direction.

4.5 Overview of the Analysis

An overview of the methodolgy involved in the analysis of the dropoff problem is outlined in the flowchart in Figure 4.4. The entire process of solution is outlined in four discrete steps.

The first step involves the simplication of the problem. The simplified problem model described in section 4.3 is utilized for this purpose. The laminate model now consists of two regions A and B which refer to the regions before and after the dropoff, respectively, as is shown in Figure 4.3a and b. These two regions can now be dealt with individually, as indicated by the two branches of the flowchart in Figure 4.4. The analysis consists of separation of the problem into an in-plane and an out-of-plane problem. The Classical Laminated Plate Theory is used to obtain the solution to the in-plane stresses. The companion problem is formulated using these stresses. The Reduced Eigenfunction Stress technique is used to obtain the solution for the out-of-plane stresses from the companion problem. The two solutions are finally superposed to obtain the complete solution to the problem. Since the in-plane solution is fully known, only the companion problem is considered in the individual regions. Arbitrary unknown functions which are functions of the x-coordinate illustrated in Figure 4.3b are used to define the stresses. The final aim of the analysis is to determine the companion stresses in the individual regions by solving for the unknown functions.

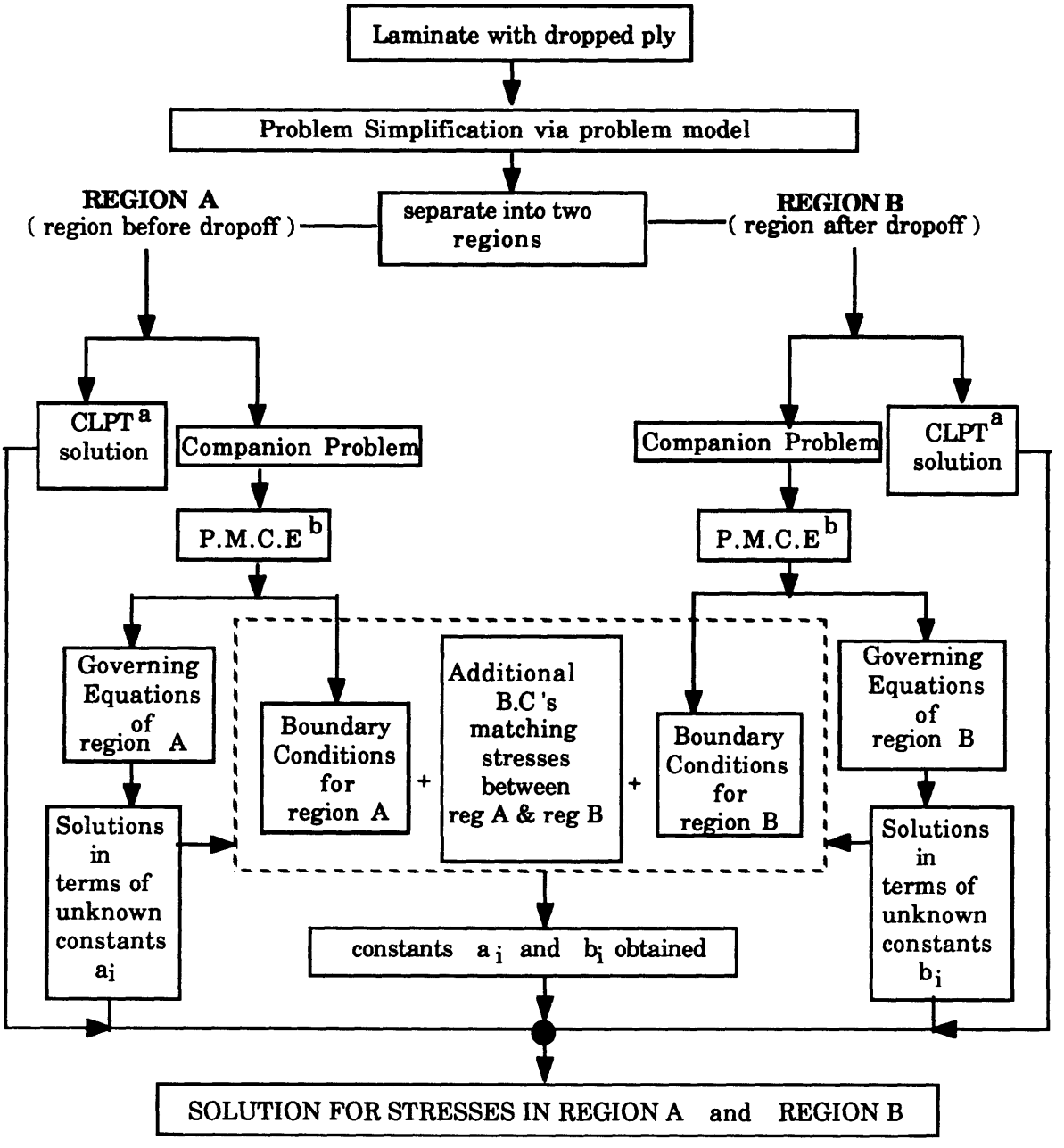

[a] Classical Laminated Plate Theory

[b] Principle of Minimum Complimentary Energy

Figure 4.4 Flowchart for the method of analysis used for determining the interlaminar stresses in laminate with ply dropoffs.

The second step involves obtaining the governing differential equations in terms of the unknown funtions for the two regions, A and B, separately. The complementary energies of the regions are formulated and the variational principle is applied to the complementary energy. This results in the governing equation and the boundary conditions for each individual region as is shown in the flowchart in Figure 4.4. The governing equations turn out to be a set of simultaneous differential equations in terms of the unknown functions. The solution to these equations provide the expressions for the unknown functions. These solutions, however, involve constants a_i in region A and b_i in region B, which remain to be determined from the boundary conditions of the problem.

The third step involves the determination of the constants by using the equations incorporating the boundary conditions obtained on taking the variational principle. The two regions, A and B, which have been individually dealt with, are now brought together by creating an additional set of boundary conditions requiring the stresses σ_{2z}, σ_{12} and σ_{22} to match at the interface of region A and region B as is shown in the problem model in Figure 4.3b. This results in an additional set of boundary condition equations. Thus, there are, in all, three sets of boundary condition equations to be satisfied viz., one set each obtained from applying the variational principle to the individual regions, and another set resulting from matching the stresses between the two regions. These set of equations can be solved to obtain the constants involved in the solutions of both the regions.

Step four involves the substitution of these constants, a_i and b_i, to obtain the complete solution to the problem. Thus, knowing the functions that were assumed for the stresses to begin with, the complete solution for the stresses in the problem is now known.

4.6 The Governing Equations of the Companion Problem

The governing equations that are obtained for the companion problem, can be applied to obtain the interlaminar stresses in any problem with a residual stress loading. Therefore, the formulation in section 4.6.1 is for a general case, and the specific applications to the ply dropoff problem are considered in section 4.6.2.

4.6.1 Formulation for a General Case

Consider a symmetric laminate with 2n plies in the "thick section" (region A), and a ply dropped off symmetrically to give a "thin section" (region B) consisting of 2(n-1) plies. It is for simplicity that only one ply drop is considered.

As mentioned in section 4.5, the regions A and B can be considered as two separate regions subjected to the same longitudinal strain (ε^{L}_{11}). Classical Laminated Plate Theory can be applied separately, to each individual region, and results in ply stresses which are different for the same type of ply from region A to region B. It can be seen from the model in Figure 4.3b that the regions A and B share the same stresses σ_{22} , σ_{12} and σ_{2z} at the interface of the two regions and the stresses in the dropped ply go to zero. Two companion problems need to be developed which when superposed on the Classical Laminated Plate Theory solutions of the individual regions, would result in the satisfaction of the above requirements of stresses matching at the interface as illustrated in Figure 4.5. Therefore, the aim in this section is to develop the governing equations to the companion problem and solve them to obtain the companion stresses.

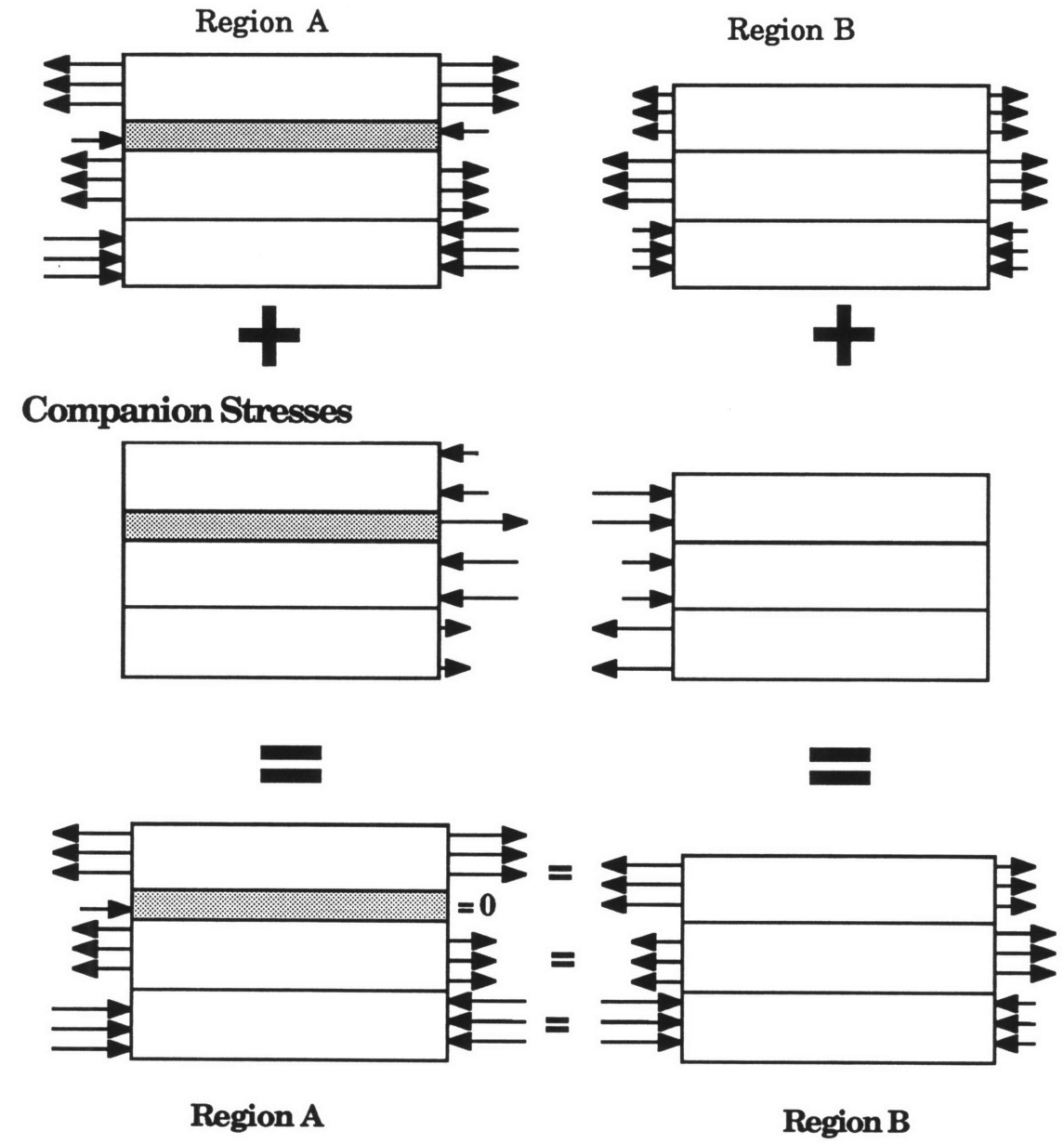

Figure 4.5 The ply dropoff problem modelled as a superposition of the laminated plate theory and the companion problem for each individual region.

Since the two regions are similar, the process of obtaining the governing equations is dealt with in a generalized manner and with no reference to any particular region. The resulting equations are applicable to both regions. For the case of a symmetric laminate with 2n plies, only half the laminate is considered due to symmetry. Its complementary energy is given by,

$$\Pi_c = \frac{1}{2} \iiint_V \sum_{i=1}^{n} \sigma_{pq}^{(i)} S_{pqkl} \sigma_{kl}^{(i)} \qquad p,q,k,l = 1,2,3 \tag{4.2}$$

where σ_{pq} are the companion stresses and S_{pqkl} is the compliance matrix

If the laminate is subject to a strain of ε^L_{11}, then in order that this applied strain does not change when a companion problem is superposed on this, the contribution of the companion problem to ε_{11} must be zero,

$$\varepsilon_{11} = 0 = S^{(i)}_{1111}\sigma^{(i)}_{11} + S^{(i)}_{1122}\sigma^{(i)}_{22} + S^{(i)}_{1133}\sigma^{(i)}_{33} + S^{(i)}_{1112}\sigma^{(i)}_{12} \tag{4.3a}$$

Note that $S^{(i)}_{1113}$ and $S^{(i)}_{1123}$ are always zero. Equation 4.3a can be used to express the stress σ_{11} in terms of the other stresses as follows,

$$\sigma^{(i)}_{11} = -\frac{S^{(i)}_{1122}}{S^{(i)}_{1111}}\sigma^{(i)}_{22} - \frac{S^{(i)}_{1133}}{S^{(i)}_{1111}}\sigma^{(i)}_{33} - \frac{S^{(i)}_{1112}}{S^{(i)}_{1111}}\sigma^{(i)}_{12} \tag{4.3b}$$

This equation 4.3b can be substituted into the complementary energy expression in 4.2, to obtain,

$$\Pi_c = \frac{1}{2} \iiint_V \sum_{i=1}^{n} \sigma_{pq}^{(i)} S^*_{pqkl} \sigma_{kl}^{(i)} \tag{4.4}$$

or, expressing this in vector form,

$$\Pi_c = \iiint_V \frac{1}{2} \left\{ \sum_{i=1}^{n} \left(\underline{\sigma}^{(i)} \right)^T \underline{S}^{*(i)} \left(\underline{\sigma}^{(i)} \right) \right\} \, dV \tag{4.5}$$

where

$$\left(\underline{\sigma}^{(i)} \right) = \left\{ \sigma_{22}^{(i)} \quad \sigma_{33}^{(i)} \quad \sigma_{23}^{(i)} \quad \sigma_{13}^{(i)} \quad \sigma_{12}^{(i)} \right\}^T \tag{4.6}$$

and

$$\underline{S}^{*(i)} = \begin{bmatrix} S^{*(i)}_{2222} & S^{*(i)}_{2233} & 0 & 0 & S^{*(i)}_{2212} \\ S^{*(i)}_{2233} & S^{*(i)}_{3333} & 0 & 0 & S^{*(i)}_{3312} \\ 0 & 0 & S^{*(i)}_{2323} & S^{*(i)}_{2313} & 0 \\ 0 & 0 & S^{*(i)}_{2313} & S^{*(i)}_{1313} & 0 \\ S^{*(i)}_{2212} & S^{*(i)}_{3312} & 0 & 0 & S^{*(i)}_{1212} \end{bmatrix} \tag{4.7}$$

This $\underline{S}^{*(i)}$ is referred to as the modified compliance matrix

The various stresses in the stress vector in equation 4.6 are interrelated by the equations of equilibrium, which is a prerequisite condition to be satisfied by the stresses in Π_c. The differential equations of equilibrium are,

$$\begin{aligned} \frac{\partial \sigma_{11}^{(i)}}{\partial x_1} + \frac{\partial \sigma_{12}^{(i)}}{\partial x_2} + \frac{\partial \sigma_{1z}^{(i)}}{\partial x_z} &= 0 \\ \frac{\partial \sigma_{12}^{(i)}}{\partial x_1} + \frac{\partial \sigma_{22}^{(i)}}{\partial x_2} + \frac{\partial \sigma_{2z}^{(i)}}{\partial x_z} &= 0 \end{aligned} \tag{4.8}$$

$$\frac{\partial \sigma_{13}^{(i)}}{\partial x_1} + \frac{\partial \sigma_{23}^{(i)}}{\partial x_2} + \frac{\partial \sigma_{3z}^{(i)}}{\partial x_z} = 0$$

where the axes x_1, x_2, and z are those defined in Figure 4.2. These equilibrium equations can be simplified on the basis of the earlier mentioned assumption, about the absence of a gradient stress field in the direction of loading (x_1) of the specimen. This causes all the partial derivatives in the x_1-direction to be zero and results in a simplification of equations 4.8 and the new relations between the various stresses are,

$$\frac{\partial \sigma_{12}^{(i)}}{\partial x} = -\frac{\partial \sigma_{1z}^{(i)}}{\partial z} \tag{4.9a}$$

$$\frac{\partial \sigma_{22}^{(i)}}{\partial x} = -\frac{\partial \sigma_{2z}^{(i)}}{\partial z} \tag{4.9b}$$

$$\frac{\partial \sigma_{2z}^{(i)}}{\partial x} = -\frac{\partial \sigma_{zz}^{(i)}}{\partial z} \tag{4.9c}$$

where the coordinate x illustrated in Figure 4.3a has been used in place of x_1.

The simplified relations in equation 4.9a convey that only one of the stresses σ_{12} or σ_{1z} need be known to determine the other; similarly equations 4.9b and 4.9c indicate that only one of the stresses σ_{22}, σ_{2z} and σ_{1z} need to be known in order to determine the other two. Thus, the next step is to determine any two of the above mentioned sets of stresses, in terms of some arbitrary functions and determine all the remaining stresses by the use of equations 4.9a-c in terms of these arbitrary funtions.

The ith ply of the laminate is considered, as is shown in Figure 4.6. The top interface of the ply is termed as the (i)th interface and the bottom interface

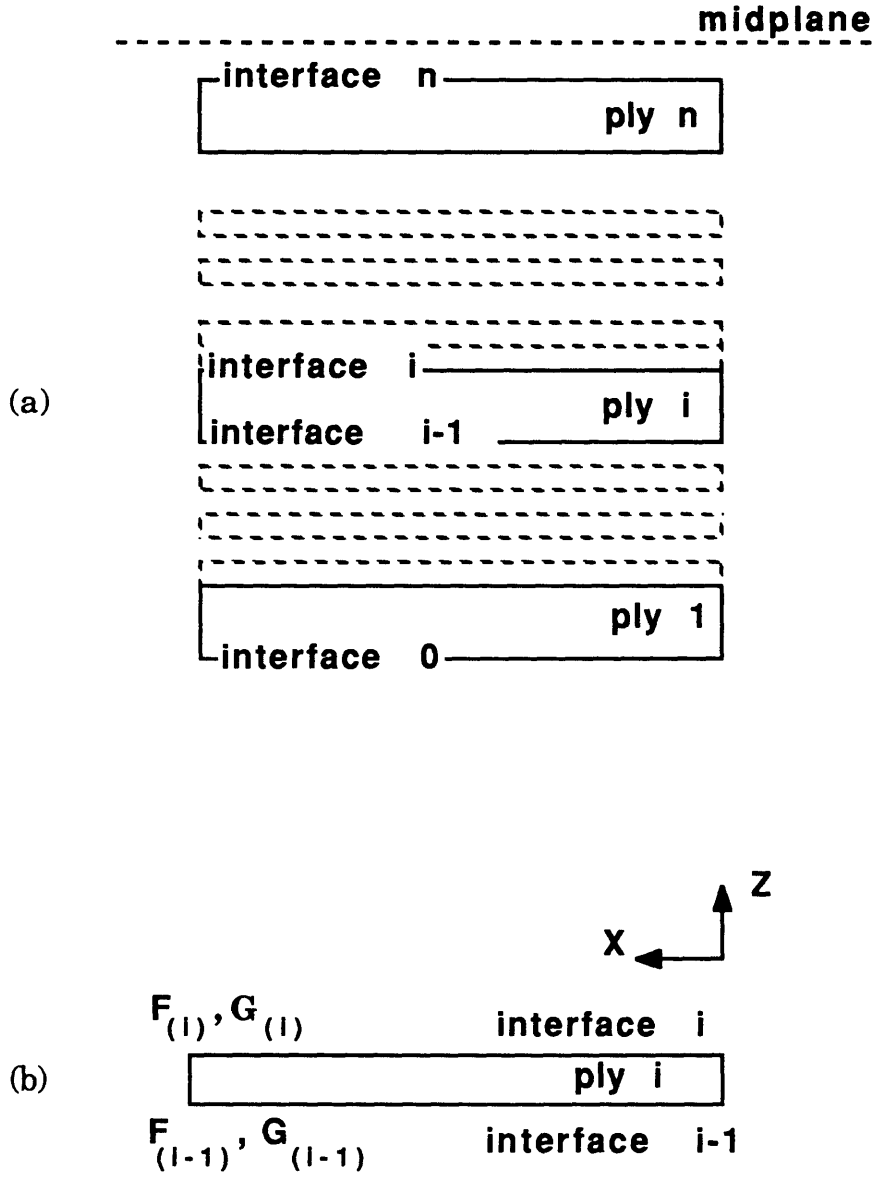

Figure 4.6 Illustration of (a) the various interfaces in the laminate; and (b) the functions F and G defined at the interfaces of the ith ply of the laminate.

as the (i-1)th interface. Two arbitrary unknown functions $F_i(x)$ and $G_i(x)$ are defined at the ith interface such that,

$$\sigma_{2z} \text{ (at the interface i)} = F'_i(x) \tag{4.10a}$$

$$\sigma_{1z} \text{ (at the interface i)} = G'_i(x) \tag{4.10b}$$

where the prime indicates differentiation with respect to the x-direction.

The stresses being derived here are the companion stresses and the conditions imposed on the companion problem is that it must recover the far-field solution, when the companion problem is superposed on the Classical Laminated Plate theory solution, to form the complete solution to the problem as is illustrated in Figure 4.5. This condition requires that the functions $F_i(x)$ and $G_i(x)$ must approach zero for large values of x (i.e as x tends to ∞). It is seen further that the companion stresses involve up to the second derivative of the function $F_i(x)$ and the first derivative of the function $G_i(x)$. Hence the conditions satisfied by these two functions are as follows,

$$\begin{aligned} &\lim_{x\to\infty} F_i(x) \to 0 \\ &\lim_{x\to\infty} F'_i(x) \to 0 \\ &\lim_{x\to\infty} F''_i(x) \to 0 \end{aligned} \tag{4.11a}$$

and,

$$\begin{aligned} &\lim_{x\to\infty} G_i(x) \to 0 \\ &\lim_{x\to\infty} G'_i(x) \to 0 \end{aligned} \tag{4.11b}$$

Since the stresses σ_{2z} and σ_{1z} have been defined at the various interfaces, the stress in any ply can now be written as the linear interpolation of the stresses at its interface. The stresses $\sigma^{(i)}_{2z}$ and $\sigma^{(i)}_{1z}$ in the ith ply can be written as follows,

$$\sigma^{(i)}_{2z} = F'_i\left(\frac{z}{h_i}+\frac{1}{2}\right) - F'_{i-1}\left(\frac{z}{h_i}-\frac{1}{2}\right) \tag{4.12a}$$

$$\sigma^{(i)}_{1z} = G'_i\left(\frac{z}{h_i}+\frac{1}{2}\right) - G'_{i-1}\left(\frac{z}{h_i}-\frac{1}{2}\right) \tag{4.12b}$$

where h_i is the thickness of the i^{th} ply. Having obtained these stresses, all other stresses can be obtained by the substitution of equations 4.12a and 4.12b into equation 4.9a-c.

The stress $\sigma^{(i)}_{12}$ is obtained on substituting equation 4.12b into the equilibrium equation 4.9a and integrating both sides of the equation,

$$\sigma^{(i)}_{12} = \frac{G_{i-1}}{h_i} - \frac{G_i}{h_i} \tag{4.12c}$$

the constant of integration vanishes due to the constraint imposed by equation 4.11b requiring the companion stresses to go to zero in the far-field.

The expression for $\sigma^{(i)}_{2z}$ can be substituted into equation 4.9b to obtain the stress $\sigma^{(i)}_{22}$ and into equation 4.9c to obtain the stress $\sigma^{(i)}_{zz}$. In both the cases, integration is performed and the resulting constants are set to zero by the dictates of equation 4.10a. The resulting expressions for the stresses $\sigma^{(i)}_{22}$ and $\sigma^{(i)}_{zz}$ are as follows,

$$\sigma_{22}^{(i)} = \frac{F_{i-1}}{h_i} - \frac{F_i}{h_i} \tag{4.12d}$$

$$\sigma_{zz}^{(i)} = \frac{h_i F''_{i-1}}{2}\left(\frac{z}{h_i} + \frac{1}{2}\right)^2 - \frac{h_i F''_i}{2}\left(\frac{z}{h_i} - \frac{1}{2}\right)^2 - \sum_{j=1}^{n} F''_j\left(h_j h_{j-1} + h^2{}_j\right) \tag{4.12e}$$

All the stresses have now been obtained in terms of the functions F_i and G_i. There are, in all, (n-1) interfaces that need to be considered as the laminate has 2n plies and is symmetric. Hence, (n-1) funtions of each type need to be defined within the laminate to obtain the interlaminar stresses in the n plies of the laminate, and they are described by F_1 through F_{n-1} and G_1 through G_{n-1}.

The stresses, being in terms of these functions, can be substituted into the expression for Π_c to obtain the complementary energy in terms of these functions. The variational of the complementary energy is taken as follows,

$$\delta\Pi_c\left(F_i, F'_i, F''_i, G_i, G'_i\right) = 0 \qquad \text{where} \qquad i = 1,..,(n-1) \tag{4.13}$$

On taking the variational, two sets of equations arise. Both sets involve various derivatives of the functions mentioned in equation 4.12 . These two sets of equations are one, the set of governing differential equations to the problem :

$$f\left(F_i, F_i'', F_i'''', G_i, G_i''\right) = 0 \tag{4.14a}$$

and, two, the boundary conditions to the problem :

$$g\,(\,F_i, F_i'', F_i'''', G_i, G_i'') = 0 \qquad (4.14b)$$

The governing equations can be solved to obtain the solutions for the functions F_i and G_i. However, these solutions involve constants which are determined from the boundary conditions of the problem. These constants are normally determined by substituting the solutions for F_i and G_i into the boundary condition equations defined by equation 4.14b. In this case, however, it should be remembered that the analysis dealt with herein must be repeated twice to obtain the governing equations and boundary conditions for both the regions A and B. The solutions obtained for the governing equations has two sets of unknown constants, one from region A and the other from B, which are to be determined from the boundary conditions.

Besides the two sets of boundary conditions obtained on taking the variational for regions A and B, there also exist a third set of additional boundary conditions requiring the matching of stresses $\sigma^{(i)}_{22}$, $\sigma^{(i)}_{2z}$ and $\sigma^{(i)}_{12}$ at the interface between the plies of the two regions, except for the stresses in the dropped ply which must be set to zero at the dropoff. Thus, these three sets of boundary conditions must be satisfied in order that the constants in the solutions to the functions F_i and G_i can be completely determined. Once these functions are determined, the stresses in all the plies can be easily determined by substituting these functions back into the equations 4.11a-e.

The present section looks into the governing equations, the boundary conditions are dealt with in the next section. The governing differiential equations obtained from the variational of the complementary energy taken in equation 4.13 are as follows,

$$\begin{bmatrix} [\alpha 11] & [\varnothing] \\ [\varnothing] & [\varnothing] \end{bmatrix}\begin{Bmatrix} \{F''''\} \\ \{G''''\} \end{Bmatrix}+\begin{bmatrix} [\beta 11] & [\beta 12] \\ [\beta 12] & [\beta 22] \end{bmatrix}\begin{Bmatrix} \{F''\} \\ \{G''\} \end{Bmatrix}+ \begin{bmatrix} [\eta 11] & [\eta 12] \\ [\eta 12] & [\eta 22] \end{bmatrix}\begin{Bmatrix} \{F\} \\ \{G\} \end{Bmatrix}=\begin{Bmatrix} 0 \end{Bmatrix} \tag{4.15}$$

where,

$$\{F\}=\begin{Bmatrix} F_1 \\ \vdots \\ F_{(n-1)} \end{Bmatrix} \tag{4.16a}$$

and

$$\{G\}=\begin{Bmatrix} G_1 \\ \vdots \\ G_{(n-1)} \end{Bmatrix} \tag{4.16b}$$

and the matrices indicated by, [αij], [βij] and [ηij] (where i and j take the values 1 and 2) are (n-1) by (n-1) square matrices consisting of constants which are dependent on the material used and the layup of the laminate being analyzed. The matrix [ø] indicates a (n-1) by (n-1) null matrix. The elements of all the matrices employed are given below,

$$\alpha 11_{ij}=\begin{cases} e_j\left(e_i g_i - 2L_3^i h_i\right)+L_1^i+L_1^{i+1} & \text{for} \quad j=i \\ e_i\left(e_j g_j + L_3^j h_j - L_3^{j+1} h_{j+1}\right)-L_2^j & \text{for} \quad j=i+1 \\ e_i\left(e_j g_j + L_3^j h_j - L_3^{j+1} h_{j+1}\right) & \text{for} \quad n-1 \geq j > i+1 \end{cases} \tag{4.17}$$

$$\beta 11_{ij} = \begin{cases} 2e_i\left(-L_8^{i+1}h_{i+1}\right) + L_4^i + L_4^{i+1} & \text{for} \quad j = i \\ e_i\left(L_8^j h_j - L_8^{j+1}h_{j+1}\right) + L_5^{i+1} & \text{for} \quad j = i+1 \\ e_i\left(L_8^j h_j - L_8^{j+1}h_{j+1}\right) & \text{for} \quad n-1 \geq j > i+1 \end{cases} \tag{4.18}$$

$$\beta 12_{ij} = \begin{cases} 0 & \text{for} \quad j < i-1 \\ L_7^i & \text{for} \quad j = i-1 \\ \left(-e_i L_{12}^{i+1}h_{i+1} + L_6^i + L_6^{i+1}\right) & \text{for} \quad j = i \\ \left(e_i(L_{12}^{i+1}h_{i+1} - L_{12}^{i+2}h_{i+2}) + L_7^{i+1}\right) & \text{for} \quad j = i+1 \\ e_i\left(L_{12}^j h_j - L_{12}^{j+1}h_{j+1}\right) & \text{for} \quad n-1 \geq j > i+1 \end{cases} \tag{4.19}$$

$$\beta 22_{ij} = \begin{cases} -2\left(L_{11}^i + L_{11}^{i+1}\right) & \text{for} \quad j = i \\ -L_{11}^{i+1} & \text{for} \quad j = i+1 \\ 0 & \text{for} \quad n-1 \geq j > i+1 \end{cases} \tag{4.20}$$

$$\eta 11_{ij} \begin{cases} \left(L_9^i + L_9^{i+1}\right) & \text{for} \quad j = i \\ -L_9^{i+1} & \text{for} \quad j = i+1 \\ 0 & \text{for} \quad n-1 \geq j > i+1 \end{cases} \tag{4.21}$$

$$\eta 12_{ij} = \begin{cases} 0 & \text{for} \quad j < i-1 \\ -L_{10}^i & \text{for} \quad j = i-1 \\ \left(L_{10}^i + L_{10}^{i+1}\right) & \text{for} \quad j = i \\ -L_{10}^i & \text{for} \quad j = i+1 \\ 0 & \text{for} \quad n-1 \geq j > i+1 \end{cases} \tag{4.22}$$

$$\eta 22_{ij} = \begin{cases} \left(L_{13}^{i} + L_{13}^{i+1}\right) & \text{for} \quad j = i \\ -L_{13}^{i+1} & \text{for} \quad j = i+1 \\ 0 & \text{for} \quad n-1 \geq j > i+1 \end{cases} \tag{4.23}$$

The constants e_i, g_i and L_i are given below,

$$e_i = \frac{1}{2}\left(h_i + h_{i+1}\right) \tag{4.24}$$

$$g_i = \sum_{j=i+1}^{n} L_{14}^{j}(h_j^2) \tag{4.25}$$

$$L_1^i = S_{3333}^{*(i)} \frac{h_i^3}{10} \tag{4.26a}$$

$$L_2^i = S_{3333}^{*(i)} \frac{h_i^3}{60} \tag{4.26b}$$

$$L_3^i = S_{3333}^{*(i)} \frac{h_i}{3} \tag{4.26c}$$

$$L_4^i = \frac{2}{3} S_{2233}^{*(i)} h_i - \frac{8}{3} S_{2233}^{*(i)} h_i \tag{4.26d}$$

$$L_5^i = -\frac{2}{3} S_{2233}^{*(i)} h_i - \frac{4}{3} S_{2233}^{*(i)} h_i \tag{4.26e}$$

$$L_6^i = \frac{2}{3} S_{3312}^{*(i)} h_i - \frac{8}{3} S_{1323}^{*(i)} h_i \tag{4.26f}$$

$$L_7^i = -\frac{2}{3} S_{3312}^{*(i)} h_i - \frac{4}{3} S_{1323}^{*(i)} h_i \tag{4.26g}$$

$$L_8^i = 2S_{2233}^{*(i)} / h_i \tag{4.26h}$$

$$L_9^i = 2S_{2222}^{*(i)} / h_i \tag{4.26i}$$

$$L^{i}_{10} = 4S^{*(i)}_{2212}/h_i \tag{4.26j}$$

$$L^{i}_{11} = \frac{4}{3}S^{*(i)}_{1313}h_i \tag{4.26k}$$

$$L^{i}_{12} = 4S^{*(i)}_{3312}/h_i \tag{4.26l}$$

$$L^{i}_{13} = 8S^{*(i)}_{1212}/h_i \tag{4.26m}$$

$$L^{i}_{14} = 2S^{*(i)}_{3333}/h_i \tag{4.26n}$$

The governing equations of 4.15, are a set of homogeneous, simultaneous, fourth order differential equations, the standard solution to which is of the form,

$$\begin{Bmatrix}\{F\}\\ \{G\}\end{Bmatrix} = \{c\}\, e^{-\lambda x} \tag{4.27}$$

where {c} is a vector consisting of constants and λ are the eigenvalues of the solution. The complete solution is determined by substituting the assumed solution given in equation 4.27 into the equations of 4.15. This leads to a polynomial in λ of order 3(n-1) which can be solved to obtain the 3(n-1) roots of the polynomial. This results in 3(n-1) eigenvalues which can be individually substituted back into equation 4.15 to obtain the 3(n-1) eigenvectors associated with them. Thus, the solution to the governing equation is of the form,

$$\begin{Bmatrix}\{F\}\\ \{G\}\end{Bmatrix} = \sum_{j=1}^{3(n-1)} a_j \{\phi\}_j e^{-\lambda_j x} = \sum_{j=1}^{3(n-1)} a_j \begin{Bmatrix}\{\phi^F\}_j\\ \{\phi^G\}_j\end{Bmatrix} e^{-\lambda_j x} \tag{4.28}$$

where,

$$\{\phi\}_j = \begin{Bmatrix}\{\phi^F\}_j\\ \{\phi^G\}_j\end{Bmatrix} \tag{4.29}$$

and the individual elements of $\{\phi^F\}_j$ and $\{\phi^G\}_j$ are defined by,

$$\{\phi^F\}_j = \begin{Bmatrix}\phi^F_{1,j}\\ \vdots \\ \phi^F_{3(n-1),j}\end{Bmatrix} \quad \text{and} \quad \{\phi^G\}_j = \begin{Bmatrix}\phi^G_{1,j}\\ \vdots \\ \phi^G_{3(n-1),j}\end{Bmatrix} \tag{4.30}$$

The a_j are unknown constants determined by the boundary conditions particular to the problem, and $\{\phi\}_j$ refers to the eigenvector. It is seen from equations 4.28 and 4.29 that the eigenvector has been split into two parts $\{\phi^F\}_j$ and $\{\phi^G\}_j$. This is for convenience alone, as an indication that each part refers to the functions {F} and {G} respectively.

The solution for any individual F_i or G_i can be separately expressed as,

$$F_i = \sum_{j=1}^{3(n-1)} a_j \phi^F_{i,j} e^{-\lambda_j x} \tag{4.31}$$

and

$$G_i = \sum_{j=1}^{3(n-1)} a_j \phi^G_{i,j} e^{-\lambda_j x} \tag{4.32}$$

4.6.2 Application to the Ply Dropoff Model

As has been reiterated throughout, the solution of equation 4.28 is for the case of any general laminate. For the specific purpose of the ply dropoff problem model, this analysis can be applied separately to each individual region A and B to obtain separate governing equations and solutions to the regions. The solutions for the two regions are provided below by adding additional superscripts to the eigenvalues and eigenvectors. The additional superscript 'a' indicates that it belongs to region A and the additional superscript 'b' indicates the solution belongs to region B.

The solution for region A, which is a symmetric 2n-ply laminate in the form of equation 4.28 is,

$$\begin{Bmatrix} \{F_a\} \\ \{G_a\} \end{Bmatrix} = \sum_{j=1}^{3(n-1)} a_j \begin{Bmatrix} \{\phi^{Fa}\}_j \\ \{\phi^{Ga}\}_j \end{Bmatrix} e^{-\lambda_j^a x} \tag{4.33a}$$

The solution for region B, which is a symmetric 2(n-1)-ply laminate formed after ply dropoff, is:

$$\begin{Bmatrix} \{F_b\} \\ \{G_b\} \end{Bmatrix} = \sum_{j=1}^{3(n-2)} b_j \begin{Bmatrix} \{\phi^{Fb}\}_j \\ \{\phi^{Gb}\}_j \end{Bmatrix} e^{-\lambda_j^b x} \tag{4.33b}$$

The next step in obtaining the complete solution is the determination of the constants expressed in vector form as {a} and {b}, using the boundary conditions.

4.7 Boundary Conditions and Final Solution

It was stated in section 4.6 that there are, in all, three sets of boundary conditions that have to be utilized in this problem. Two sets result from taking the variational principle separately in regions A and B and an additional set arises on matching the stress at the interfaces of region A and region B, as was shown in the problem model in Figure 4.3b. These three sets of boundary conditions are mathematically cumbersome to deal with and hence an alternative way of obtaining them in a simpler form is to rewrite a new complementary energy for the entire laminate consisting of region A and region B, obtained by a linear addition of the complementary energies of the individual regions. In this complementary energy, the additional boundary condition resulting from matching the stresses σ_{22}, σ_{12} and σ_{2z} between regions A and B are incorporated by means of Lagrange multipliers. The variational principle is then applied to this new complementary energy to obtain the boundary conditions to the problem. In schematic form, the new complementary energy is as follows,

$$\Pi_c = (\Pi_c)_A + (\Pi_c)_B + \psi \text{ (Boundary Condition Matching)} \qquad (4.34)$$

here, $(\Pi_c)_A$ is the complementary energy of region A, $(\Pi_c)_B$ is the complementary energy of region B, and ψ is the Lagrange multiplier.

It should be specifically mentioned that the variational principle is not being applied twice, but rather, is being used to obtain equations for boundary conditions which have already been obtained before, in a mathematically convenient form. This is easily seen on applying the variational principle to the new Π_c that the resulting three sets of equations are exactly what had been previously obtained,

$$\delta\Pi_c = 0 \tag{4.35}$$

therefore,

$$\delta(\Pi_c)_A = 0 \tag{4.36a}$$

$$\delta(\Pi_c)_B = 0 \tag{4.36b}$$

$$\delta\psi \text{ (Boundary Conditions matching)} = 0 \tag{4.36c}$$

Equations 4.36a and 4.36b would recover the same governing equations and boundary conditons, for their individual regions, as obtained in the previous section. However, if the solution in equations 4.33a and 4.33b are substituted into 4.36a and 4.36b respectively, then the governing equations are identically satisfied leaving only the boundary conditions in terms of the constants {a} and {b}. Equation 4.36c leads to the additional boundary conditions.

The next step is to define the boundary conditions for matching regions A and B as mentioned in equation 4.36c in terms of the constants {a} and {b} before formulating the new Π_c. There are, in all three stresses to be matched, σ_{22}, σ_{12} and σ_{2z}. However, the stresses to be matched must be the total stresses at the interface consisting of both the companion problem stresses and the Classical Laminated Plate Theory solution. Only matching the companion

stresses will not provide a proper match at the interface of the two regions because the the Classical Laminated Plate Theory solutions are not the same for both the regions, as they have different layups.

The first stress considered here is σ_{22}, and if the interface at which the two laminates meet is termed as the z-axis (i.e. the location x equal to zero) as illustrated in Figure 4.3a and b, the stresses are matched as follows,

$$\left\{\begin{matrix}\sigma^1_{22}\\ \vdots \\ \sigma^d_{22}\\ \vdots \\ \sigma^{n-1}_{22}\end{matrix}\right\}_{regA} + \left\{\begin{matrix}\sigma^1_{22L}\\ \vdots \\ \sigma^d_{22L}\\ \vdots \\ \sigma^{n-1}_{22L}\end{matrix}\right\}_{regA} = \left\{\begin{matrix}\sigma^1_{22}\\ \vdots \\ 0\\ \vdots \\ \sigma^{n-2}_{22}\end{matrix}\right\}_{regB} + \left\{\begin{matrix}\sigma^1_{22L}\\ \vdots \\ 0\\ \vdots \\ \sigma^{n-2}_{22L}\end{matrix}\right\}_{regB} \tag{4.37}$$

where, σ^i_{22} indicates the companion stress in the ith ply, σ^i_{22L} indicates the Classical Laminated Plate Theory stress in the i^{th} ply and the superscript 'd' indicates the dropped ply.

There are two things that must be noted in equation 4.37. The first is that since the dropped ply does not exist in region B, it is replaced by a zero, indicating that the stresses in the region A go to zero in the dropped ply at the dropoff. The second is that although the region A has n plies only (n-1) seem to have been considered for matching purposes. This is because, the Classical Laminated Plate Theory and the Companion Problem both satisfy integral equilibrium. For example, in region A ,

$$\sum_{j=1}^{n} \sigma^j_{22} = 0 \tag{4.38}$$

hence determining stresses in any (n-1) plies will provide the stress in the nth ply. Similarly, since region B has (n-1) plies, only (n-2) stresses need to be matched. The expression 4.37 can be rewritten as,

$$[I_{1A}]\{\sigma_{22}\}_{regA} + \{\sigma_{22L}\}_{regA} = [I_{1B}]\{\sigma_{22}\}_{regB} + \{\sigma_{22L}\}_{regB} \qquad (4.39)$$

where,

$$\{\sigma_{22}\} = \begin{Bmatrix} \sigma_{22}^{1} \\ \vdots \\ \sigma_{22}^{n-1} \end{Bmatrix} \qquad (4.40a)$$

$[I_{1A}]$ is an (n-1) by (n-1) identity matrix and $[I_{1B}]$ is a rectangular matrix of size (n-1) by (n-2), which is a slightly modified version of an identity matrix, with the following elements,

$$\begin{aligned} (I_{1B})_{ij} &= \delta_{ij}(1-\delta_{id}) && \text{for } i \le d \\ &= \delta_{i(j+1)} && \text{for } i > d \end{aligned} \qquad (4.40b)$$

where δ_{ij} is the kronecker delta. The subscript 'd' indicates the dropped ply and the purpose of the term $(1-\delta_{id})$ in equation 4.40b is to enable the stress in the dropped ply to go to zero.

Equation 4.39 is to be modifed so as to express the companion stresses in terms of the function F_i and consequently in terms of the unknown constants {a}. The expression for σ_{22} is taken from 4.12d to be,

$$\sigma_{22}^{(i)}(x) = \frac{F_{i-1}}{h_i} - \frac{F_i}{h_i} \tag{4.41a}$$

This can be written in vector form as,

$$\left\{\sigma_{22}^{(i)}(0)\right\} = \begin{bmatrix} \frac{1}{h_i} & \frac{-1}{h_i} \end{bmatrix} \begin{Bmatrix} F_{i-1}(0) \\ F_i(0) \end{Bmatrix} \tag{4.41b}$$

where the stresses have been evaluated at the specific location x equal to zero. Equation 4.41b is only for one single ply, whereas the vectors in equation 4.39 consists of (n-1) plies of the laminate. Stacking together the stresses for the various plies the following expression is obtained,

$$\left\{\sigma_{22}(0)\right\} = [I_2] \quad \{F(0)\} \tag{4.42}$$

where $[I_2]$ is an (n-1) by (n-1) square matrix defined as,

$$I_{2ij} = \begin{cases} 0 & \text{for} \quad j < i-1 \\ -1/h_i & \text{for} \quad j = i-1 \\ 1/h_i & \text{for} \quad j = i \\ 0 & \text{for} \quad j > i \end{cases} \tag{4.43a}$$

and

$$\{F(0)\} = \begin{Bmatrix} F_1(0) \\ \vdots \\ F_{(n-1)}(0) \end{Bmatrix} \tag{4.43b}$$

The next step is to use the solution in equation 4.31 to express F_i in terms of the unknown constants {a} as follows,

$$F_i(x) = \sum_{j=1}^{3(n-1)} a_j \phi^F_{(i),j} e^{-\lambda_i x} \tag{4.44a}$$

which at location x equal to zero becomes,

$$F_i(0) = \sum_{j=1}^{3(n-1)} a_j \phi^F_{(i),j} = \left\{\phi^F\right\}^T_i \{a\} \tag{4.44b}$$

Once again, equation 4.44b is for a single funtion F_i. This can be put into a vector form as follows,

$$\{F(0)\} = \left[\Phi^F\right]\{a\} \tag{4.45}$$

where,

$$\left[\Phi^F\right] = \begin{bmatrix} \left\{\phi^F\right\}^T_1 \\ \vdots \\ \left\{\phi^F\right\}^T_{3(n-1)} \end{bmatrix} \tag{4.46}$$

The expression in equation 4.45 is substituted into equation 4.42 to give an equation for the companion stress vector $\{\sigma_{22}\}$ in terms of the unknown constants {a} as,

$$\{\sigma_{22}\} = [I_2][\Phi^F]\{a\} \tag{4.47}$$

For region A, the matrix $[I_2]$ is termed $[I_{2A}]$ and is of size (n-1) by (n-1). For region B, the matrix is termed $[I_{2B}]$ and is of size (n-2) by (n-2).

Therefore, the boundary condition equation expressed in equation 4.39 is now in terms of the unknown constants {a} and {b} and the expression is,

$$[I_{1A}][I_{2A}][\Phi^F]_A\{a\} + \{\sigma_{22L}\}_{regA} = [I_{1B}][I_{2B}][\Phi^F]_B\{b\} + \{\sigma_{22L}\}_{regB} \tag{4.48a}$$

Rearranging yields,

$$[I_{1A}][I_{2A}][\Phi^F]_A\{a\} - [I_{1B}][I_{2B}][\Phi^F]_B\{b\} = \{\sigma_{22L}\}_{regB} - \{\sigma_{22L}\}_{regA} \tag{4.48b}$$

or,

$$[I_{1A}][I_{2A}][\Phi^F]_A\{a\} - [I_{1B}][I_{2B}][\Phi^F]_B\{b\} = \Delta\{\sigma_{22L}\} \tag{4.49}$$

where,

$$\Delta\{\sigma_{22}\} = \{\sigma_{22L}\}_{reg\,A} - \{\sigma_{22L}\}_{reg\,B} \tag{4.50}$$

Thus, equation 4.49 presents the equation which results in the matching of the stress σ_{22} at the interface between region A and B.

The matching of the stress σ_{12} at the interface of the two regions is performed in exactly the same manner as σ_{22} and results in a similar equation given below,

$$\left[I_{1A}\right]\left[I_{2A}\right]\left[\Phi^{G}\right]_{A}\{a\} - \left[I_{1B}\right]\left[I_{2B}\right]\left[\Phi^{G}\right]_{B}\{b\} = \Delta\left\{\sigma_{12L}\right\} \tag{4.51}$$

where,

$$\left[\Phi^{G}\right] = \begin{bmatrix} \left\{\phi^{G}\right\}_{1}^{T} \\ \vdots \\ \left\{\phi^{G}\right\}_{3(n-1)}^{T} \end{bmatrix} \tag{4.52a}$$

and,

$$\Delta\{\sigma_{12}\}=\{\sigma_{12L}\}_{\text{reg A}} - \{\sigma_{12L}\}_{\text{reg B}} \tag{4.52b}$$

The matching of the stress σ_{2z} varies from the previous two because this stress, as obtained within a ply, is a linear interpolation in the z-direction of the stresses at the interface as is indicated in expression 4.11a. Therefore, to ensure a match of this stress between region A and region B, it is necessary that the stresses not in the individual plies, but at the individual ply interfaces be matched. This ensures that the σ_{2z} stresses between individual plies are matched exactly. In order that this stress goes to zero in the dropped ply (referred to as ply 'd'), the stresses at both the interfaces of the dropped ply (viz. ply interfaces 'd-1' and 'd') should go to zero. Since these interfaces

merge into interface (d-1) in the region B, as shown in Figure 4.7, the stress at that interface must also go to zero. The equations resulting from the matching of the stress σ_{2z} at the interface are as follows,

$$(F'_j)_{\text{reg A}} = (F'_j)_{\text{reg B}} \qquad \text{for } 1 \le j < d-1 \tag{4.53a}$$

$$(F'_{(d-1)})_{\text{reg A}} = (F'_{(d-1)})_{\text{reg B}} = 0 \tag{4.53b}$$

$$(F'_d)_{\text{reg A}} = 0 \tag{4.53c}$$

$$(F'_j)_{\text{reg A}} = (F'_{(j-1)})_{\text{reg B}} \qquad \text{for } (n-1) \ge j > d \tag{4.53d}$$

Expressing this in vector form results in:

$$\begin{Bmatrix} F'_1(0) \\ \vdots \\ F'_{d-1}(0) \\ F'_d(0) \\ 0 \\ \vdots \\ F'_{(n-1)}(0) \end{Bmatrix}_{\text{reg A}} = \begin{Bmatrix} F'_1(0) \\ \vdots \\ 0 \\ 0 \\ F'_{d-1}(0) \\ \vdots \\ F'_{(n-2)}(0) \end{Bmatrix}_{\text{reg B}} \tag{4.54}$$

This can also be expressed as,

$$[I_{3A}]\,\{F'(0)\}_{\text{reg A}} = [I_{3B}]\,\{F'(0)\}_{\text{reg B}} \tag{4.55}$$

where,

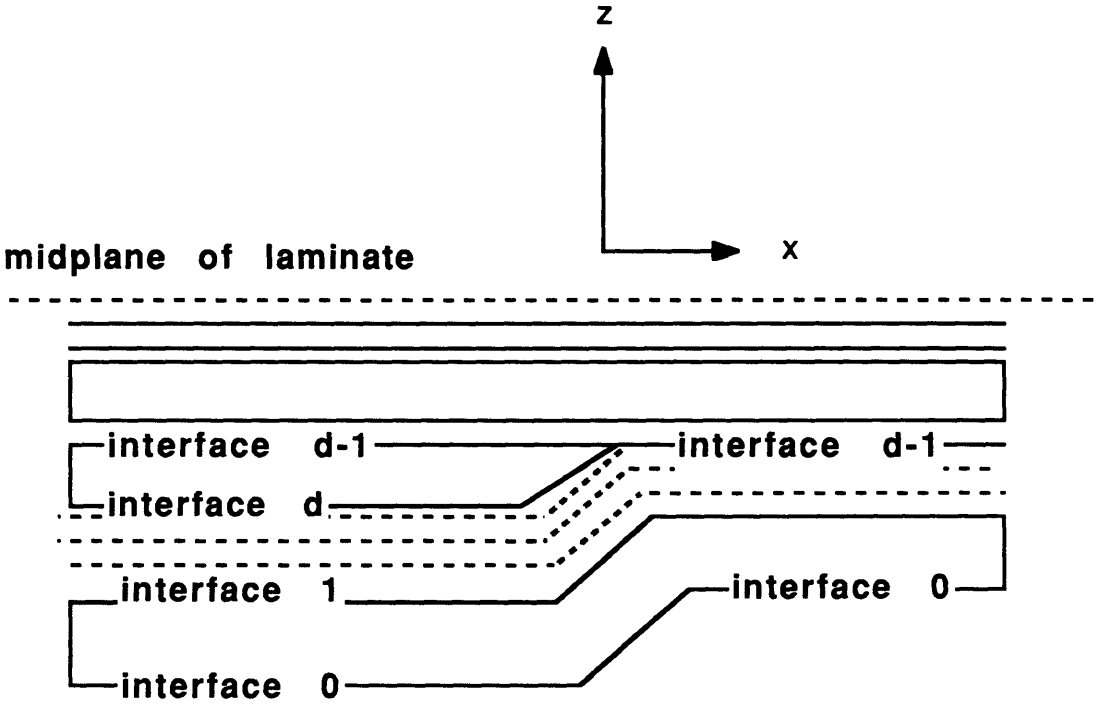

Figure 4.7 Illustration of the two interfaces of the dropped ply (d and d-1) merging into a single interface (d-1) after dropoff.

$$\left\{F'(0)\right\} = \begin{Bmatrix} F'_1(0) \\ \vdots \\ F'_{(n-1)}(0) \end{Bmatrix} \tag{4.56a}$$

$[I_{3A}]$ is an (n) by (n-1) rectangular matrix with the elements,

$$I_{3Aij} = \begin{cases} \delta_{ij}\left[1 - \delta_{i(d+1)}\right] & \text{for} \quad i \le d \\ \delta_{i(d+2)} & \text{for} \quad i \le d \end{cases} \tag{4.56b}$$

$[I_{3B}]$ is a rectangular matrix of size (n) by (n-2) with the following elements,

$$I_{3Bij} = \begin{cases} \delta_{ij}\left[1 - \delta_{id}\right]\left[1 - \delta_{i(d+1)}\right] & \text{for} \quad i \le d \\ \delta_{i(j+2)} & \text{for} \quad i \le d \end{cases} \tag{4.56c}$$

where δ_{ij} is again the kronecker delta.

The next step is to obtain the {F'(0)} in terms of the constants {a} and {b}. Differentiating the expression for F(x) in equation 4.31 gives,

$$F'_i(x) = \sum_{j=1}^{3(n-1)} a_j (-\lambda_i)\, \phi^F_{(i),j}\, e^{-\lambda_i x} \tag{4.57}$$

At x equal to zero this becomes,

$$F'_i(0) = \sum_{j=1}^{3(n-1)} a_j (-\lambda_i)\, \phi^F_{(i),j} \tag{4.58a}$$

Expressing this in vector form,

$$\left\{F'(0)\right\} = \left[\Phi^{F'}\right]\{a\} \tag{4.58b}$$

where,

$$\left[\Phi^{F'}\right] = \begin{bmatrix} -\lambda_1 \left\{\phi^F\right\}_1^T \\ \vdots \\ -\lambda_{3(n-1)} \left\{\phi^F\right\}_{3(n-1)}^T \end{bmatrix} \tag{4.59}$$

Substituting equation 4.58b into equation 4.55, the final equation for matching the stresses σ_{2z} between the regions A and B is obtained in terms of the constants {a} and {b} as follows,

$$\left[I_{3A}\right]\left[\Phi^{F'}\right]_A \{a\} = \left[I_{3B}\right]\left[\Phi^{F'}\right]_B \{b\} \tag{4.60}$$

Thus, all the additional boundary conditions mentioned in equation 4.34 are now in terms of the constants {a} and {b} according to equations 4.49, 4.51 and 4.60. These are to be used with the aid of Lagrange multipliers to obtain the total Π_c as in equation 4.34,

$$\begin{aligned} \Pi_c = \iiint_V & \left[\sum_{j=1}^{n} \left(\sigma_{pq}^j S_{pqkl}^{*j} \sigma_{kl}^j \right)_A + \sum_{j=1}^{n-1} \left(\sigma_{pq}^j S_{pqkl}^{*j} \sigma_{kl}^j \right)_B \right] dV \\ & - \left\{ \left[I_{1A}\right]\left[I_{2A}\right]\left[\Phi^F\right]_A \{a\} - \left[I_{1B}\right]\left[I_{2B}\right]\left[\Phi^F\right]_B \{b\} - \Delta\left\{\sigma_{22L}\right\} \right\}^T \{\psi_1\} \\ & - \left\{ \left[I_{1A}\right]\left[I_{2A}\right]\left[\Phi^G\right]_A \{a\} - \left[I_{1B}\right]\left[I_{2B}\right]\left[\Phi^G\right]_B \{b\} - \Delta\left\{\sigma_{12L}\right\} \right\}^T \{\psi_2\} \\ & - \left\{ \left[I_{3A}\right]\left[\Phi^{F'}\right]_A \{a\} - \left[I_{3B}\right]\left[\Phi^{F'}\right]_B \{b\} \right\}^T \{\psi_3\} \end{aligned} \tag{4.61}$$

In the first two terms of equation 4.61, only the companion stress contribution from region A and B are considered and their contribution to the complementary energy are given by the terms,

$$(\Pi_c)_A = \iiint_V \sum_{j=1}^{n} \left(\sigma^j_{pq} S^{*j}_{pqkl} \sigma^j_{kl} \right)_A dV \tag{4.62a}$$

$$(\Pi_c)_B = \iiint_V \sum_{j=1}^{n-1} \left(\sigma^j_{pq} S^{*j}_{pqkl} \sigma^j_{kl} \right)_B dV \tag{4.62b}$$

These terms involve only the companion stresses, whereas, when the two regions A and B are being matched, the complete solution consisting of the Classical Laminated Plate theory stresses and the companion problem stresses must be included. Only the companion stresses have been considered in this case because it can be shown that the only additional contributions on adding the Classical Laminated Plate solution are constants which add on to equation 4.62a and 4.62b. On taking the variational to obtain the boundary condition equations, as in equation 4.35, only the terms with companion stresses contribute.

Returning to the complementary energy in equation 4.61, the companion stresses σ_{ij} have to be expressed in terms of the unknown constants {a} and {b}. The stresses have earlier been defined in equation 4.12a-e in terms of the functions F_i and G_i. These functions F_i and G_i have in turn been determined by equations 4.31 and 4.32. Thus, the stresses σ_{ij} can be expressed in terms of the constants {a} and {b}, making the expression for Π_c as follows,

$$\begin{aligned}\Pi_c = \quad & \{a\}^T[\Omega_a]\{a\} + \{b\}^T[\Omega_b]\{b\} \\ & - \left\{\left[\Gamma_{1A}\right]\{a\} - \left[\Gamma_{1B}\right]\{b\} - \Delta\left\{\sigma_{22L}\right\}\right\}^T \{\psi_1\} \\ & - \left\{\left[\Gamma_{2A}\right]\{a\} - \left[\Gamma_{2B}\right]\{b\} - \Delta\left\{\sigma_{12L}\right\}\right\}^T \{\psi_2\} \\ & - \left\{\left[\Gamma_{3A}\right]\{a\} - \left[\Gamma_{3B}\right]\{b\}\right\}^T \{\psi_3\}\end{aligned} \tag{4.63}$$

where,

$$\left[\Gamma_{1A}\right] = \left[I_{1A}\right]\left[I_{2A}\right]\left[\Phi^F\right]_A \tag{4.64a}$$

$$\left[\Gamma_{1B}\right] = \left[I_{1B}\right]\left[I_{2B}\right]\left[\Phi^F\right]_B \tag{4.64b}$$

$$\left[\Gamma_{2A}\right] = \left[I_{1A}\right]\left[I_{2A}\right]\left[\Phi^G\right]_A \tag{4.64c}$$

$$\left[\Gamma_{2B}\right] = \left[I_{1B}\right]\left[I_{2B}\right]\left[\Phi^G\right]_B \tag{4.64d}$$

$$\left[\Gamma_{3A}\right] = \left[I_{3A}\right]\left[\Phi^{F'}\right]_A \tag{4.64e}$$

$$\left[\Gamma_{3B}\right] = \left[I_{3B}\right]\left[\Phi^{F'}\right]_B \tag{4.64f}$$

and the matrices $[\Omega_A]$ and $[\Omega_B]$ are defined in general as follows,

$$\Omega_{mn} = \sum_{i=1}^{n} S^{*(i)}_{2222}\left[M1^{(i)}_{mn}\right] + S^{*(i)}_{2233}\left[M6^{(i)}_{mn} + M6^{(i)}_{nm}\right] + S^{*(i)}_{1212}\left[M7^{(i)}_{mn} + M7^{(i)}_{nm}\right]$$
$$+ S^{*(i)}_{3333}\left[M2^{(i)}_{mn}\right] + S^{*(i)}_{3312}\left[M8^{(i)}_{mn} + M8^{(i)}_{nm}\right]$$
$$+ S^{*(i)}_{2323}\left[M5^{(i)}_{mn}\right] + S^{*(i)}_{2313}\left[M9^{(i)}_{mn} + M9^{(i)}_{nm}\right] \qquad (4.65)$$
$$+ S^{*(i)}_{1313}\left[M4^{(i)}_{mn}\right] + S^{*(i)}_{1212}\left[M3^{(i)}_{mn}\right]$$

where the constants designated by M are,

$$M1^{(i)}_{pq} = \frac{h_i}{(\lambda_p + \lambda_q)}\left\{\left(\phi^F_{i-1,p} - \phi^F_{i,p}\right)\left(\phi^F_{i-1,q} - \phi^F_{i,q}\right)\right\} \qquad (4.66a)$$

$$M2^{(i)}_{pq} = \frac{(\lambda_p\lambda_q)^2}{(\lambda_p + \lambda_q)}\left\{\left(\phi^F_{i-1,p}\phi^F_{i-1,q} + \phi^F_{i,p}\phi^F_{i,q}\right)\left(\frac{h_i^5}{20}\right)\right.$$
$$- \left(\phi^F_{i-1,p}\phi^F_{i,q} - \phi^F_{i,p}\phi^F_{i-1,q}\right)\left(\frac{h_i^5}{120}\right)$$
$$+ \frac{h_i^3}{6}\left(\phi^F_{i-1,q} - \phi^F_{i,q}\right)\sum_{j=1}^{i-1}\frac{\phi_{j,p}}{2}\left(h_j + h_{j-1}\right) \qquad (4.66b)$$
$$+ \frac{h_i^3}{6}\left(\phi^F_{i-1,p} - \phi^F_{i,p}\right)\sum_{j=1}^{i-1}\frac{\phi_{j,q}}{2}\left(h_j + h_{j-1}\right)$$
$$\left. + h_i\left[\sum_{j=1}^{i-1}\frac{\phi_{j,p}}{2}\left(h_j + h_{j-1}\right)\right]\left[\sum_{j=1}^{i-1}\frac{\phi_{j,q}}{2}\left(h_j + h_{j-1}\right)\right]\right\}$$

$$M3^{(i)}_{pq} = \frac{h_i}{(\lambda_p + \lambda_q)}\left\{\left(\phi^G_{i-1,p} - \phi^G_{i,p}\right)\left(\phi^G_{i-1,q} - \phi^G_{i,q}\right)\right\} \qquad (4.66c)$$

$$M4^{(i)}_{pq} = \frac{(\lambda_p \lambda_q)}{(\lambda_p + \lambda_q)} \left\{ \left(\phi^G_{i-1,p} \phi^G_{i-1,q} + \phi^G_{i,p} \phi^G_{i,q} \right) \left(\frac{h_i^3}{3} \right) + \left(\phi^G_{i-1,p} \phi^G_{i,q} - \phi^G_{i,p} \phi^G_{i-1,q} \right) \left(\frac{h_i^3}{6} \right) \right\} \tag{4.66d}$$

$$M5^{(i)}_{pq} = \frac{(\lambda_p \lambda_q)}{(\lambda_p + \lambda_q)} \left\{ \left(\phi^F_{i-1,p} \phi^F_{i-1,q} + \phi^F_{i,p} \phi^F_{i,q} \right) \left(\frac{h_i^3}{3} \right) + \left(\phi^F_{i-1,p} \phi^F_{i,q} - \phi^F_{i,p} \phi^F_{i-1,q} \right) \left(\frac{h_i^3}{6} \right) \right\} \tag{4.66e}$$

$$M6^{(i)}_{pq} = \frac{(\lambda_q)^2}{(\lambda_p + \lambda_q)} \left\{ \left(\phi^F_{i-1,p} - \phi^F_{i,p} \right) \left(\frac{h_i^3}{6} \phi^F_{i-1,q} - \frac{h_i^3}{6} \phi^F_{i,q} + h_i \sum_{j=1}^{i-1} \frac{\phi_{j,q}}{2} \left(h_j + h_{j-1} \right) \right) \right\} \tag{4.66f}$$

$$M7^{(i)}_{pq} = \frac{h_i}{(\lambda_p + \lambda_q)} \left\{ \left(\phi^G_{i-1,p} - \phi^G_{i,p} \right) \left(\phi^G_{i-1,q} - \phi^G_{i,q} \right) \right\} \tag{4.66g}$$

$$M8^{(i)}_{pq} = \frac{(\lambda_q)^2}{(\lambda_p + \lambda_q)} \left\{ \left(\phi^G_{i-1,p} - \phi^G_{i,p} \right) \left(\frac{h_i^3}{6} \phi^F_{i-1,q} - \frac{h_i^3}{6} \phi^F_{i,q} + h_i \sum_{j=1}^{i-1} \frac{\phi_{j,q}}{2} \left(h_j + h_{j-1} \right) \right) \right\} \tag{4.66h}$$

and

$$M9_{pq}^{(i)} = \frac{(\lambda_p \lambda_q)}{(\lambda_p + \lambda_q)} \left\{ \left(\phi^G_{i-1,p} \phi^F_{i-1,q} + \phi^F_{i,p} \phi^G_{i,q} \right) \left(\frac{h_i^3}{3} \right) + \left(\phi^G_{i-1,p} \phi^F_{i,q} - \phi^G_{i,p} \phi^F_{i-1,q} \right) \left(\frac{h_i^3}{6} \right) \right\} \tag{4.66i}$$

Thus, the Π_c is now entirely in terms of known eigenvalues, eigenvectors evaluated earlier for regions A and B, and it also contains five unknown vectors {a}, {b}, $\{\psi_1\}$, $\{\psi_2\}$ and $\{\psi_3\}$. These constants can be evaluated from the five sets of equations that result on taking the variational. Taking the variation with respect to {a} and setting it to zero gives:

$$[\Omega_a]\{a\} - [\Gamma_{1A}]^T \{\psi_1\} - [\Gamma_{2A}]^T \{\psi_2\} - [\Gamma_{3A}]^T \{\psi_3\} = \{0\} \tag{4.67a}$$

similarly for {b}:

$$[\Omega_b]\{b\} - [\Gamma_{1B}]^T \{\psi_1\} - [\Gamma_{2B}]^T \{\psi_2\} - [\Gamma_{3B}]^T \{\psi_3\} = \{0\} \tag{4.67b}$$

for $\{\psi_1\}$:

$$[\Gamma_{1A}]\{a\} - [\Gamma_{1B}]\{b\} = \Delta \underline{\sigma}_{22L} \tag{4.67c}$$

for $\{\psi_2\}$:

$$[\Gamma_{2A}]\{a\} - [\Gamma_{2B}]\{b\} = \Delta \underline{\sigma}_{12L} \tag{4.67d}$$

for $\{\psi_3\}$:

$$[\Gamma_{3A}]\{a\} - [\Gamma_{3B}]\{b\} = \{0\} \tag{4.67e}$$

These five sets of equations 4.67a-e can be expressed in a matrix form as follows,

$$\begin{bmatrix} [\Omega_a] & \varnothing & [\Gamma_{1A}]^T & [\Gamma_{2A}]^T & [\Gamma_{3A}]^T \\ \varnothing & [\Omega_b] & [\Gamma_{1B}]^T & [\Gamma_{2B}]^T & [\Gamma_{3B}]^T \\ [\Gamma_{1A}] & [\Gamma_{1B}] & \varnothing & \varnothing & \varnothing \\ [\Gamma_{2A}] & [\Gamma_{2B}] & \varnothing & \varnothing & \varnothing \\ [\Gamma_{3A}] & [\Gamma_{3B}] & \varnothing & \varnothing & \varnothing \end{bmatrix} \begin{Bmatrix} \{a\} \\ \{b\} \\ \{\psi_1\} \\ \{\psi_2\} \\ \{\psi_3\} \end{Bmatrix} = \begin{Bmatrix} \varnothing \\ \varnothing \\ \Delta \underline{\sigma}_{22L} \\ \Delta \underline{\sigma}_{12L} \\ \varnothing \end{Bmatrix} \tag{4.70}$$

The equations in 4.68 are a set of simultaneous equations which can be solved for the unknown constants, {a}, {b}, $\{\psi_1\}$, $\{\psi_2\}$, and $\{\psi_3\}$. Only the constants {a} and {b} are of interest, because these were the only unknowns that needed to be determined in the expressions 4.33a and 4.33b for the functions F_i and G_i in the regions A and B. These functions having been fully determined, it is now easy to obtain the stresses σ_{22}, σ_{2z}, σ_{zz}, σ_{12} and σ_{1z} because these are expressed only in terms of the functions F_i and G_i as is seen from the expressions for the stresses in equations 4.12a-e. The general expression for any stress in either region with a total of 2n plies, is of the form,

$$\sigma_{ij} = \sum_{k=1}^{3(n-1)} A_k e^{-\lambda_k x} \tag{4.69}$$

where λ_k are complex eigenvalues and can be expressed as,

$$\lambda_k = \beta_k + i\omega_k \tag{4.70}$$

and A_k are known constants.

Substituting equation 4.70 into equation 4.69 yields the expression,

$$\sigma_{ij} = \sum_{k=1}^{3(n-1)} e^{-\beta_k x} \{ A_{1k} \cos(\omega_k x) + A_{2k} \sin(\omega_k x) \} \tag{4.71}$$

Thus, the stresses in any ply in region A and B can be obtained as in equation 4.71. The ω_k define the various modes contributing to the stresses and the β_k indicate the decay rates of these modes. Thus, the solution provides a feel for the various contributing terms. The number of terms in the solution is seen to be a function of the number of plies, and hence the magnitude and time required for the solution increases with the number of plies involved in the laminate being analyzed.

Another factor to be taken note of during the analysis is that the Classical Laminated Plate theory solution is to be added on to the companion problem to provide the complete solution to the problem. The results of the in-plane stresses are different in region A and B because they have different layups and are subjected to the same ε^L_{11}. Also, if σ_{11} is being applied instead of ε^L_{11} then care must be taken to ensure that the σ_{11} of region A and B are related as follows,

$$(\sigma_{11})_B = \{ (S_{1111})_A / (S_{1111})_B \} (\sigma_{11})_A \tag{4.72}$$

This would ensure that the ε^L_{11} in the two regions are the same.

4.8 Computer Implementation

The analysis was programmed on a Digital Electronics Corporation μvax II. The software package is named DOSE, for DropOff Stress Evaluator. One of the standard packages used for evaluating the eigenvalues and eigenvectors is EISPACK®. Another matrix manipulating package, LINPACK®, is used for matrix inversions, and some other matrix operations. The programming language used is FORTRAN.

The input to the program consists of the laminate information from the region A and the region B, and the ply to be dropped is also indicated. The various plies of the laminate, their thicknesses and the material properties must be provided in the input file. The Classical Lamianted Plate Theory predicted stresses σ_{22L} and σ_{12L} in each ply, in each region along the laminate axes are also required by the program.

The output from the main program essentially consists of the eigenvalues, eigenvectors and constants {a} and {b}. There is, however, a postprocessor program which takes these results and provides the interlaminar stresses, σ_{2z}, σ_{1z} and σ_{zz} at any interface of the laminate.

The run time for the present case of a $[+15_7/FA/-15_7/0_7]_s$ laminate which is modelled as four plies with the film adhesive ply dropped off, is 8 seconds of CPU time for obtaining the eigenvalues and eigenvectors at all the interfaces for both regions A and region B. The postprocessing which consists of utilizing the eigenvalues and eigenvectors to obtain the plots of the stresses σ_{22}, σ_{12}, σ_{2z}, σ_{zz}, and σ_{1z} requires about 5 seconds of CPU time for each interface of the laminate. Thus, for the entire laminate, the stresses can be obtained in about 28 seconds of CPU time.

The complete listing of the program code is provided in Appendix A.

4.9 Verification of Analysis Methodology

The verification procedure adopted for DOSE was to compare the results for the case of a free edge problem with the results obtained by Saeger and Lagace [14]. The modification that is to be adopted in the program just lies in altering the boundary conditions. Instead of considering two regions A and B, only one single region is considered for the laminate, and the stresses at the edge of the laminate in the companion problem are set equal to the residual stresses for the laminate as obtained for Classical Laminated Plate Theory. Thus, when the companion problem solution is superposed on the Classical Laminated Plate Theory solution, the resulting solution should satisfy a stress-free boundary condition at the free edge.

In the method adopted by Saeger and Lagace [14], the solution approach to the companion problem uses the same two functions F and G to define the stresses in every ply of the laminate. The ratios of the in-plane stresses between various plies is a constant. Since only two functions are used for the analysis, the solution is always made up of only two eigenvalues, independent of the number of plies in the laminate. In the current approach, however, there is a laminate dependence that enters the analysis, as here the functions F_i and G_i are defined individually for every interface between plies. Thus, the more the number of plies in the laminate, the more the number of functions and hence the number of eigenvalues in the solution. The in-plane stresses in the companion problem are therefore not related by a simple ratio in this case, thus allowing the stresses in each ply more independence in their behavior. The current method can also be used to discretize a ply further into subplies thus providing more interfaces at which the functions F_i and G_i can be defined, allowing more accurate solutions to the problem. This, however, at

the expense of considerable computer time which increases as the cube of the number of plies.

For the case of a symmetric four ply laminate, say $[\theta_1/\theta_2]_s$, there exists only one interface, the θ_1/θ_2 interface at which the functions F and G are defined. Hence, for this case there are only two functions defined for the entire laminate. The analysis for any laminate of this type by either the approach of Saeger and Lagace [14] or the current approach should lead to similar results for the interlaminar stresses. This case has been adopted for verification of the current method and three laminates have been selected for the purpose, $[0/90]_s$, $[-45/45]_s$, and $[0/30]_s$, made of AS4/3501-6 graphite/epoxy. The properties of the materials used in the analysis are listed in Table 3.2.

The first is a cross-ply laminate, the second an angle ply laminate and the third case is a general unbalanced laminate. The interlaminar stresses σ_{2z}, σ_{zz} and σ_{1z} at the free edge were evaluated for the three laminates at the θ_1/θ_2 ply interface.

The results are compared in Figures 4.8, 4.9 and 4.10. In these figures the symbols represent the results from the current method and the legends represent the results obtained from the analysis by Saeger and Lagace [14]. The results are seen to match very well for the case of the $[0/90]_s$ and for the $[-45/45]_s$ laminates as are seen in Figure 4.8 and 4.9 respectively. The results obtained for the case of the $[0/30]_s$ in Figure 4.10 show a slight discrepency in the results particularly for the stress σ_{zz} at the free edge, (at location x/h equal to zero). This is attributed to the numerical error that was involved in the analysis which uses numerical techniques (for example the matrix inversion procedures used, etc.) as opposed to algebraic techniques used by Saeger and Lagace [14] in the computer implementation. It should also be noticed that

this discrepency arises in σ_{zz} which is almost an order smaller in magnitude than the σ_{1z} stress.

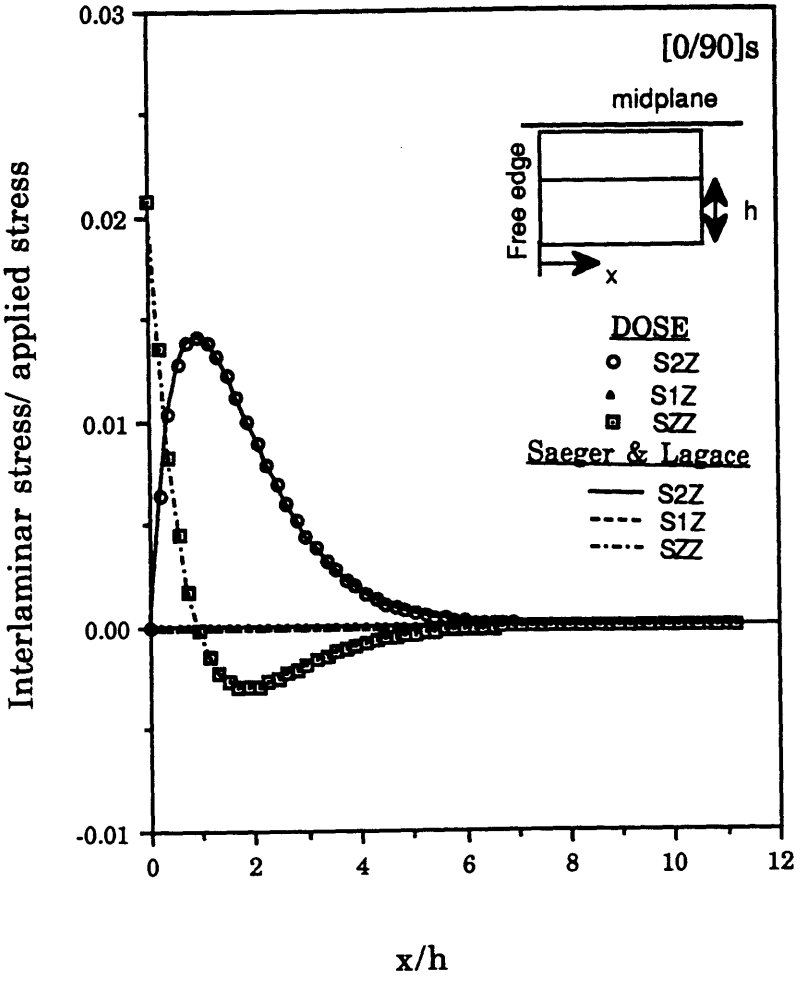

Figure 4.8 Comparison of interlaminar stresses obtained by DOSE with previous results for $[0/90]_s$ laminate.

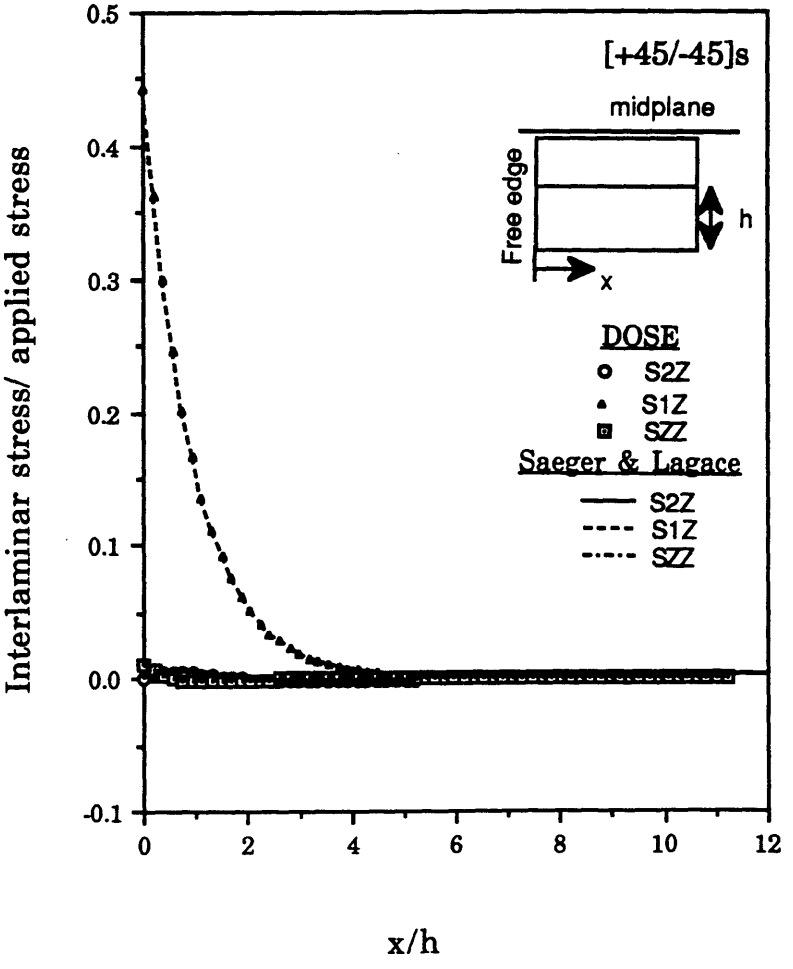

Figure 4.9 Comparison of interlaminar stresses obtained by DOSE with previous results for $[+45/-45]_s$ laminate.

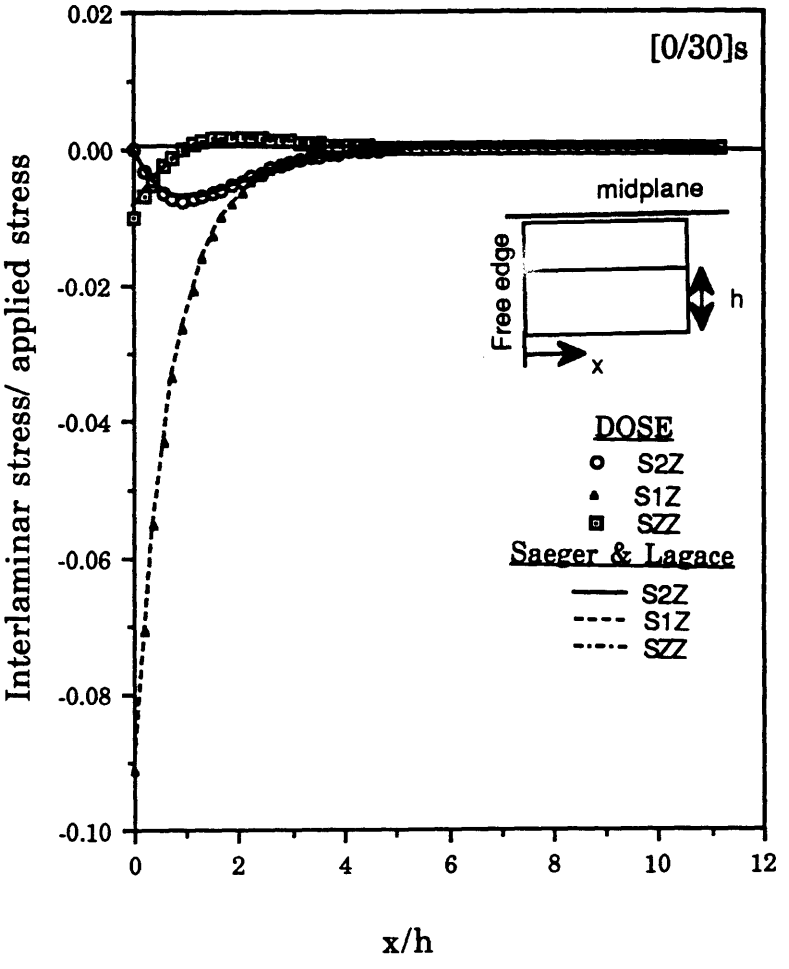

Figure 4.10 Comparison of interlaminar stresses obtained by DOSE with previous results for $[0/30]_s$ laminate.

CHAPTER 5

RESULTS

5.1 Experimental Results

The experimental results for the various specimens tested are provided herein. Predicted values for the delamination initiation stresses and the in-plane fracture stresses are also provided along with the experimental results. The Force Balance Method developed by Kassapoglou and Lagace [13] was used to evaluate the interlaminar stresses at the free edges of the laminate. These stresses were then used in an average stress criterion called the Quadratic Delamination Criterion developed by Brewer and Lagace [20]. The Quadratic Delamination Criterion requires the use of various strength parameters, the out-of-plane shear strength S_{1z} is taken to be the same as the in-plane shear strength S_{12} with a magnitude of 105 MPa. The through-the-thickness strength Z^t is taken to be 43 MPa, as measured by Weems and Lagace [40]. The other out-of-plane shear strength S_{2z}, is not needed due to the much smaller magnitude of the σ_{2z} stresses.

Delamination initiation is predicted to occur at about 466 MPa for specimens without any film adhesive implants and at 639 MPa for specimens with full widths of film adhesive. In-plane fracture stresses were determined using Classical Laminated Plate theory and the Tsai-Wu stress interaction criterion [41] applied on a ply-by-ply basis to predict first ply failure. In-plane failure stresses of 1790 MPa and 1684 MPa were predicted for specimens without any implants and with film adhesive implants, respectively. These

calculations were performed assuming a full specimen width strip of film adhesive and the nominal thickness of the specimens.

The experiments for specimens with film adhesive strips were aimed at observing the loads at which initiation occurred. No specific attempt was made to study the growth of the delamination subsequent to the initiation. In the case of the specimens with the teflon implants, only the final failure load was of interest, as the delamination was implanted and, thus, initiated to begin with. No specific attempt was made to study the growth of the delamination crack length.

5.1.1 Control Group

The specimens without any implants within them are termed the control group of specimens. The results obtained from these specimens are taken as the reference for all further tests performed in this study. The results for delamination initiation and fracture stresses obtained for the case of the control laminates are summarized in Table 5.1.

An undamaged specimen on being loaded would, at a certain load, exhibit delamination and angle ply splits as an indication of damage. Angle ply splits, is the term used for the transverse cracks that appear in the angle plies viz., +15° and -15° at the free edge, and progress into the ply along the fiber direction. Due to the already present delamination, this leads to the opening of a small triangular shaped region of the ply. The interface that opened up was in all cases the +15°/-15° interface. At this point, the edge of the specimen was no longer flat, due to the delaminated ply separating away in certain regions, and edge replicas could not be obtained. The load at which this delamination occurred was termed as the delamination initiation load. The average delamination initiation load measured is 411 MPa with a

Table 5.1 Test Results for $[\pm 15_7/0_7]_s$ specimens with no implants

Test Number	Delamination Initiation Stress (MPa)	Fracture Stress (MPa)
1	412	486
2	377	467
3	384	478
4	471	512
Average	411 (10.4 %)[a]	486 (3.9%)

a Numbers in parentheses are coefficients of variation.

coefficient of variation of 10.4%. This shows good correlation with the predicted delamination initiation stress of 466 MPa. Once initiated, the delamination progressed rapidly into the laminate and the specimen normally failed within a 20%-30% rise in load above the delamination initiation load. Examination of the specimen after failure indicated extensive delamination at the +15°/-15° interface and fiber failure in the laminate. Thus, the specimen exhibits significant out-of-plane behavior in terms of delamination which results in the reduction in the strength of the laminate and failure at a load much earlier than the predicted in-plane failure load.

The in-plane fracture stress as predicted by the Tsai-Wu criterion is 1790 MPa, whereas the measured average fracture stresses is seen to be 486 MPa with a coefficient of variation of 3.9%. Thus, the specimens fail at stresses which are only about 25% of the predicted in-plane failure.

A typical stress-strain curve for the $[\pm 15_7/0_7]_s$ control specimen is shown in Figure 5.1. The average longitudinal modulus (E_L) measured for the control specimens is 110 MPa as compared to 125 MPa predicted by the Classical Laminated Plate theory using the nominal specimen thickness of 5.628 mm for both the cases. This shows a discrepency of about 12% between the measured and the predicted value. This difference is explained by the 12% to 14% difference in the actual specimen and the nominal specimen thickness used in calculating the modulus. The stress-strain curves were linear up to failure. The curve shown in Figure 5.1 is only up to the first load drop exhibited by the specimen. The photograph of a typical mode of failure of the control specimen is shown in Figure 5.2. Delamination associated with some fiber breakage was the mode of failure observed in the specimens.

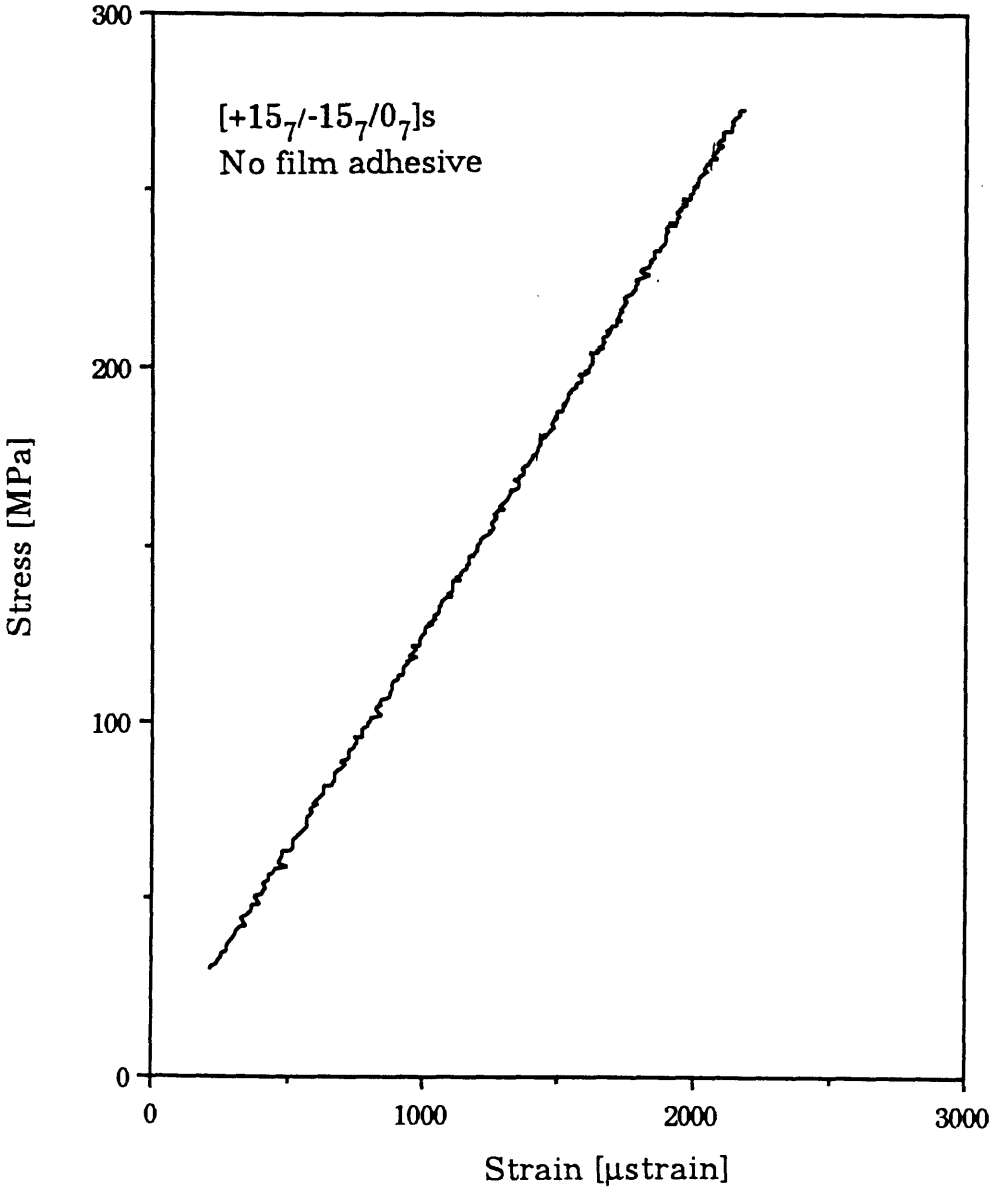

Figure 5.1 Typical stress-strain plot for $[15_7/-15_7/0_7]_s$ specimens without film adhesive

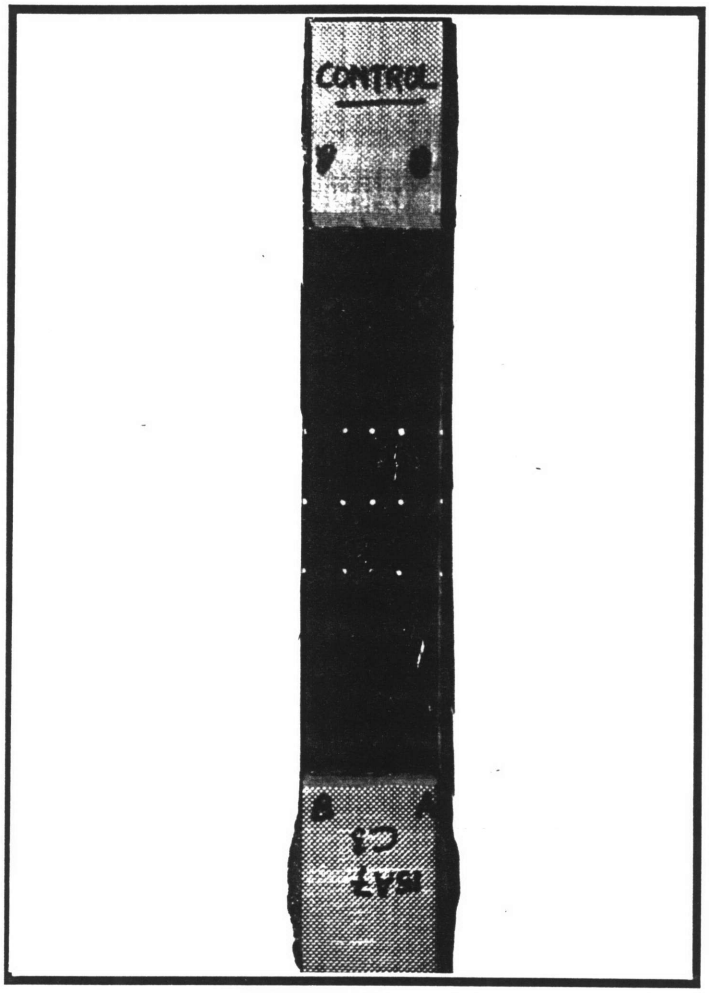

Figure 5.2 Photograph of a typical failure of a $[15_7/-15_7/0_7]_s$ without film adhesive.

5.1.2 Specimens with Film Adhesive Implants

The following results are for the specimens listed in Table 3.2. The results for the specimens with full plies of film adhesive placed at the ±15° interface are presented in Table 5.2. The results for specimens with film adhesive strips of sizes 3 mm (1/3 the boundary layer width), 6 mm (2/3 the boundary layer width) and 9 mm (equal to the boundary layer width) are presented in Tables 5.3, 5.4, and 5.5, respectively.

A delamination initiation stress of 639 MPa is predicted for all the three types of specimens. This is due to the fact that the predictions for delamination initiation, using the software packages mentioned earlier and in-plane failure using the Tsai-Wu criterion, assume that the film adhesive layer is an entire ply as they cannot take into consideration the presence of finite width strips of film adhesive.

On testing the specimen with full width film adhesive layers, no visible or audible damage was heard in specimen numbers two, three and four and hence they showed delamination initiation occuring only at final failure. The specimen number one, however, did show damage in the edge replicas at loads before the final failure loads. The delamination was seen at the +15°/-15° interface and angle ply splits were also seen in both the +15° and the -15° plies.

The average delamination initiation load for specimens with full width film adhesive is 646 MPa with a coefficient of variation of 5.2%. This correlates well with the Quadratic Delamination Criterion prediction for delamination initiation stress of 639 MPa and is seen to be higher than that of the control specimens by about 50%, using the latter as the baseline. The fracture stresses in this category are exceedingly close to the delamination initiation loads and the final failure occurred as a combination of delamination progressing through the +15°/-15° interface along with some fiber failure. The final failure

Table 5.2 Test Results for $[\pm 15_7/0_7]_s$ specimens with full plies of film adhesive at the +15°/-15° interface

Test Number	Delamination Initiation Stress (MPa)	Fracture Stress (MPa)
1	620	752
2	668	668
3	614	614
4	680	680
Average	646 (5.2%)[a]	679 (8.4%)

[a] Numbers in parentheses are coefficients of variation.

Table 5.3 Test Results for $[\pm 15_7/0_7]_s$ specimens with 9 mm wide film adhesive strips placed adjacent to the free edge at the +15°/-15° interface

Test Number	Delamination Initiation Stress (MPa)	Fracture Stress (MPa)
1	627	752
2	715	715
3	565	724
4	680	680
Average	647 (10.1%)[a]	718 (4.1%)

[a] Numbers in parentheses are coefficients of variation.

Table 5.4 Test Results for $[\pm 15_7/0_7]_s$ specimens with 6 mm wide film adhesive strips placed adjacent to the free edge at the +15°/-15° interface

Test Number	Delamination Initiation Stress (MPa)	Fracture Stress (MPa)
1	499	716
2	507	645
3	680	680
4	735	735
Average	605 (19.9%)[a]	694 (5.7%)

[a] Numbers in parentheses are coefficients of variation.

Table 5.5 Test Results for $[\pm 15_7/0_7]_s$ specimens with 3 mm wide film adhesive strips placed adjacent to the free edge at the +15°/-15° interface

Test Number	Delamination Initiation Stress (MPa)	Fracture Stress (MPa)
1	582	678
2	736	736
3	605	676
4	744	744
Average	667 (12.8%)[a]	708 (5.2%)

[a] Numbers in parentheses are coefficients of variation.

is still prompted by delamination, and the average failure stress of these specimens is 679 MPa with a coefficient of variation of 8.4%, whereas the in-plane failure predicted by the Tsai-Wu criterion is at 1807 MPa. Thus, delamination is still responsible for the early failure of the specimen. However, the delamination initiation load has been delayed by the presence of the film adhesive layer.

The stress-strain curve for a typical specimen in this category is shown in Figure 5.3 and the measured longitudinal modulus (E_L) is about 103 GPa as compared to the expected 125 GPa as predicted by the Classical Laminated Plate theory. This implies a difference of about 18% between the expected and measured values of the modulus. The graphite/epoxy cross-sectional area, which has a nominal thickness of 5.628 mm was used in the calculation of the modulus for both the measured and predicted value. This explains the discrepency between the measured and calculated value, as it was mentioned earlier that the differences in the actual and measured thicknesses were of the order of 12% to 14%, and hence the apparent discrepency between the measured and predicted values. It is seen that the change in modulus due to the addition of the film adhesive is not very significant.

The photograph of a failed specimen is shown in Figure 5.4. These specimens show much more fiber breakage than the control specimens due to the higher load at which these specimens fail.

In general, the specimens with film adhesive strips of various sizes showed the same behavior as the specimens with a full ply of film adhesive with respect to delamination initiation and failure. The interface where delamination was initiated is the +15°/-15° interface. The results of the test for these specimens are summarized in Tables 5.2 through 5.5. A comparison

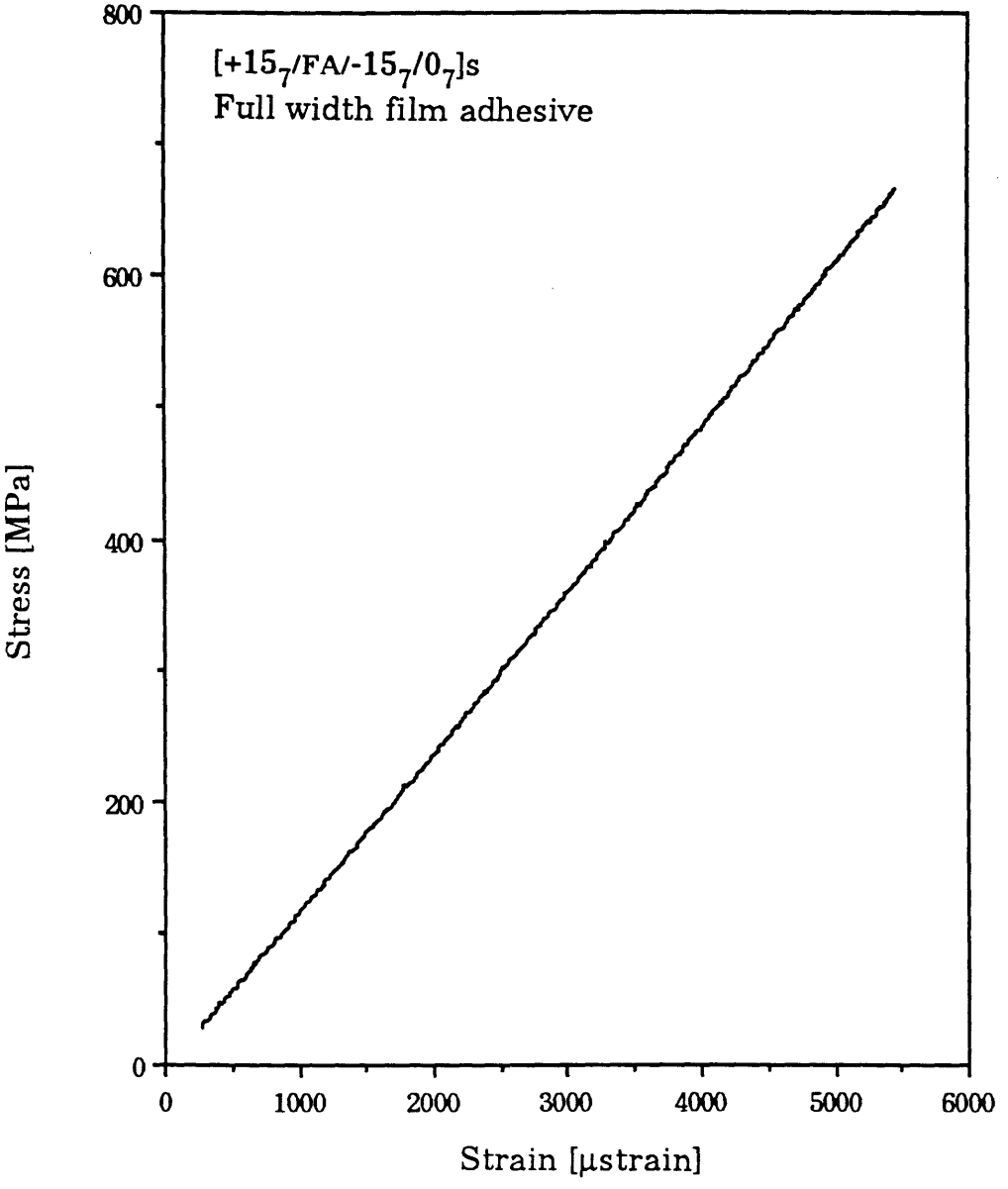

Figure 5.3 Typical stress-strain plot for $[15_7/FA/-15_7/0_7]_s$ specimens with full width film adhesive ply.

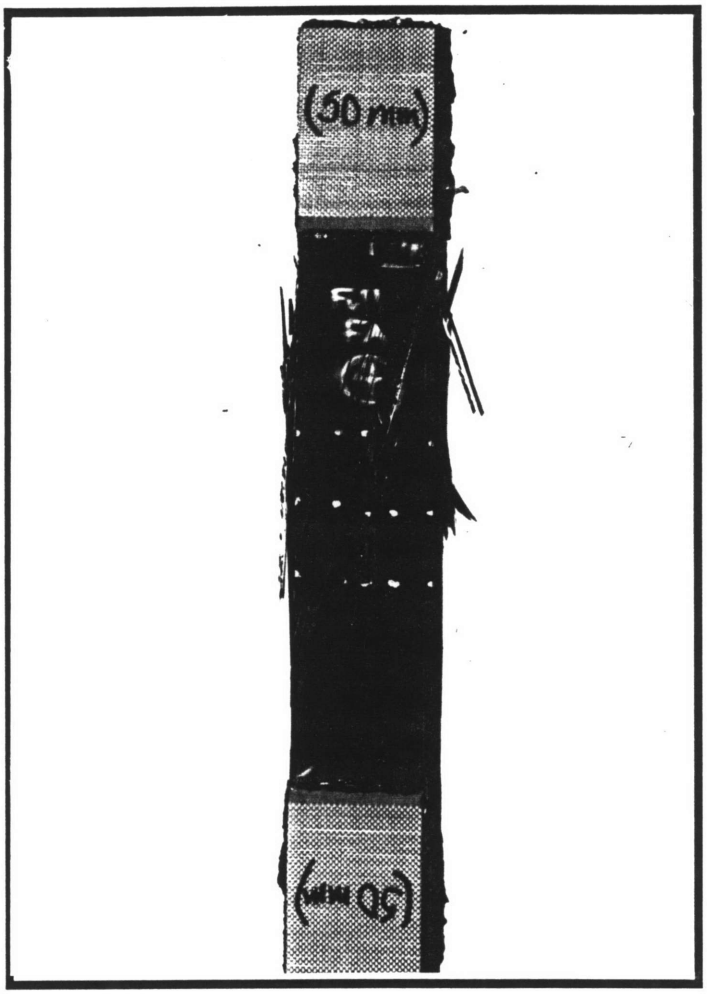

Figure 5.4 Photograph of a typical failure of a $[15_7/FA/-15_7/0_7]_s$ with a full width film adhesive.

between the average stresses of all the film adhesive specimens and the control specimens is made in Table 5.6.

For specimens with 9 mm wide strips of film adhesive, two specimens (viz., specimen number two and four) exhibited angle ply splits and delamination, before failure The average delamination initiation stress for this category of specimens is 647 MPa with a coefficient of variation of 10.1%, as compared to the average delamination initiation stress of 411 MPa, for specimens without any film adhesive. This implies a 55% increase in the delamination initiation load with reference to the control specimens. This increment is obtained by the use of 9 mm wide strips of film adhesives instead of entire plies of film adhesive. The average fracture stress for these specimens was 718 MPa with a coefficient of variation of 4.1%. Thus, there seems to be no significant difference in the behavior of the specimens with full plies of film adhesive and those with the 9 mm wide strips of film adhesive with regards to either the average delamination initiation stress or the average fracture stress.

For specimens with 6 mm wide film adhesive strips, again, there are two specimens in which delamination initiated (specimen number one and two) before final failure as is indicated in Table 5.4. This set of specimens show an average delamination initiation stress of 605 MPa with a coefficient of variation of 19.9% and an average fracture stress of 694 MPa with a coefficient of variation of 5.7%. The delamination initiation stress is close to the predicted stress of 639 MPa, and again a 45% improvement is seen in the delamination initiation load as compared to the control specimens. The fracture stress is still far lower than the predicted in-plane fracture stress of 1684 MPa, with the final failure indicating delamination as a mode of failure.

Table 5.6 Average Delamination initiation and fracture stresses for $[\pm 15_7/0_7]_s$ specimens with and without film adhesive implants

Width of Film adhesive (mm)	Average Delamination Initiation Stress (MPa)	Average Fracture Stress (MPa)
0	411 (10.4%)[a]	486 (3.9%)
50	646 (5.2%)	679 (8.4%)
9	647 (10.1%)	718 (4.1%)
6	605 (19.9%)	694 (5.7%)
3	667 (12.8%)	708 (5.2%)

[a] Numbers in parentheses are coefficients of variation.

The results in Table 5.5 for specimens with 3 mm wide film adhesive strips indicate three specimens (specimen numbers one, two and three) in which angle ply splits and delamination were observed before final failure. This set of laminates show an average delamination initiation stress of 667 MPa with a coefficient of variation of 12.8% and an average fracture stress of 708 MPa with a coefficient of variation of 5.2%. The delamination initiation stress is close to the predicted stress of 639 MPa, and implies a 60% improvement in the delamination initiation stress as compared to the control specimens. Like the previous three types of specimens with implants, the fracture stress is still far lower than the predicted in-plane fracture stress of 1684 MPa, with delamination as a mode of failure.

In general, therefore, specimens with film adhesive implants show good correlation with the predicted delamination initiation stresses but do not achieve the predicted in-plane failure stress. If a comparison is made of the behavior of the laminates with film adhesive to the control specimens, in general an increase in delamination initiation stress in excess of 40% is observed and an increase of the same order is obtained in the final fracture stress.

Comparing the family of specimens with film adhesive implants of various widths it can be seen that their behaviors are similar and the differences in the delamination initiation stresses and the fracture stresses are seen to be less than 10%. Thus, despite the fact that the dropoff takes place at various distances from the free edge in the specimens with different film adhesive widths, there seems to be little effect of the same to be observed in the results.

Typical stress-strain curves for specimens with 9 mm, 6 mm and 3 mm wide film adhesive implants are shown in Figures 5.5, 5.6, and 5.7,

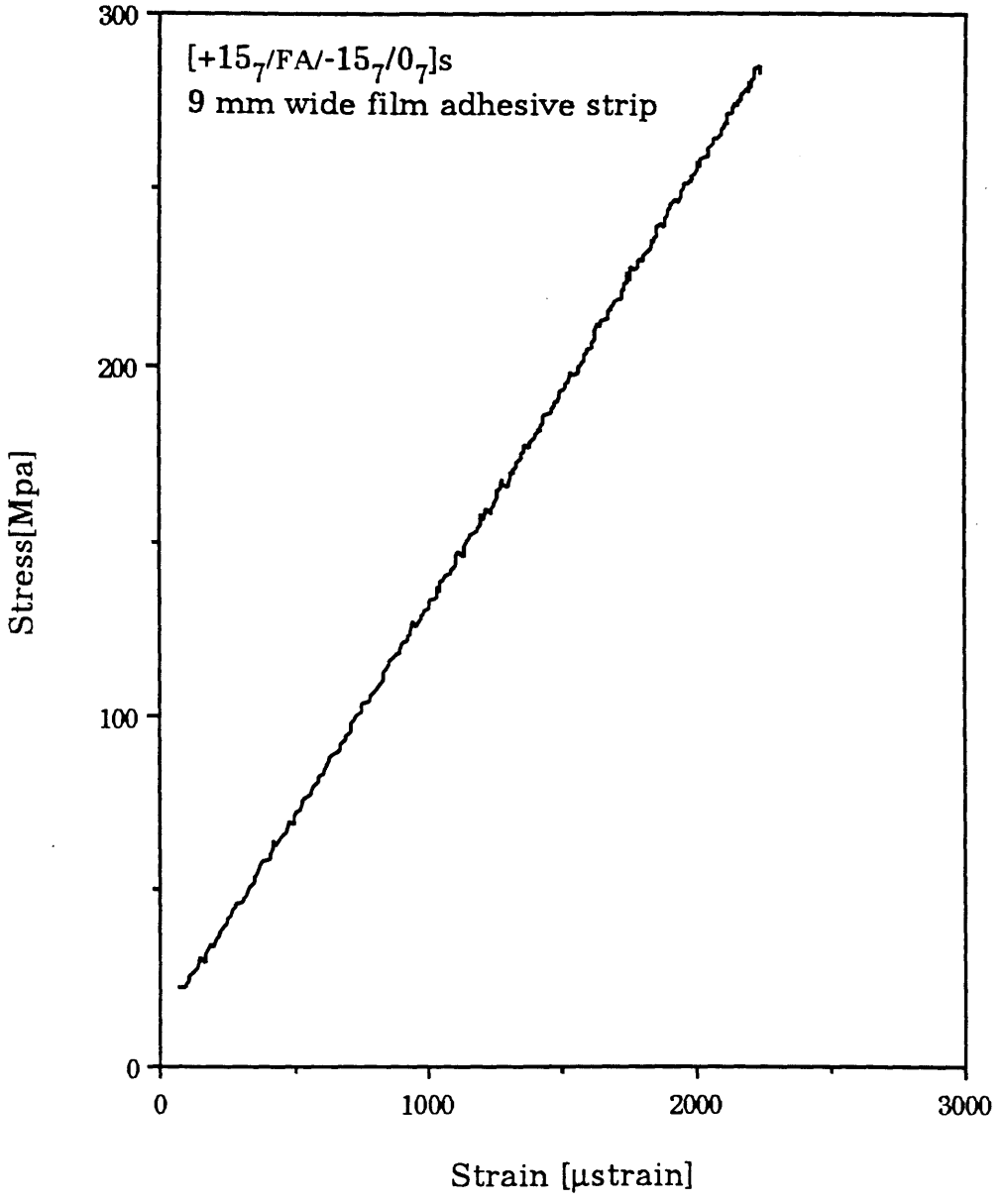

Figure 5.5 Typical stress-strain plot for $[15_7/FA/-15_7/0_7]_s$ specimens with 9 mm wide film adhesive ply strips at the +15°/-15° interface.

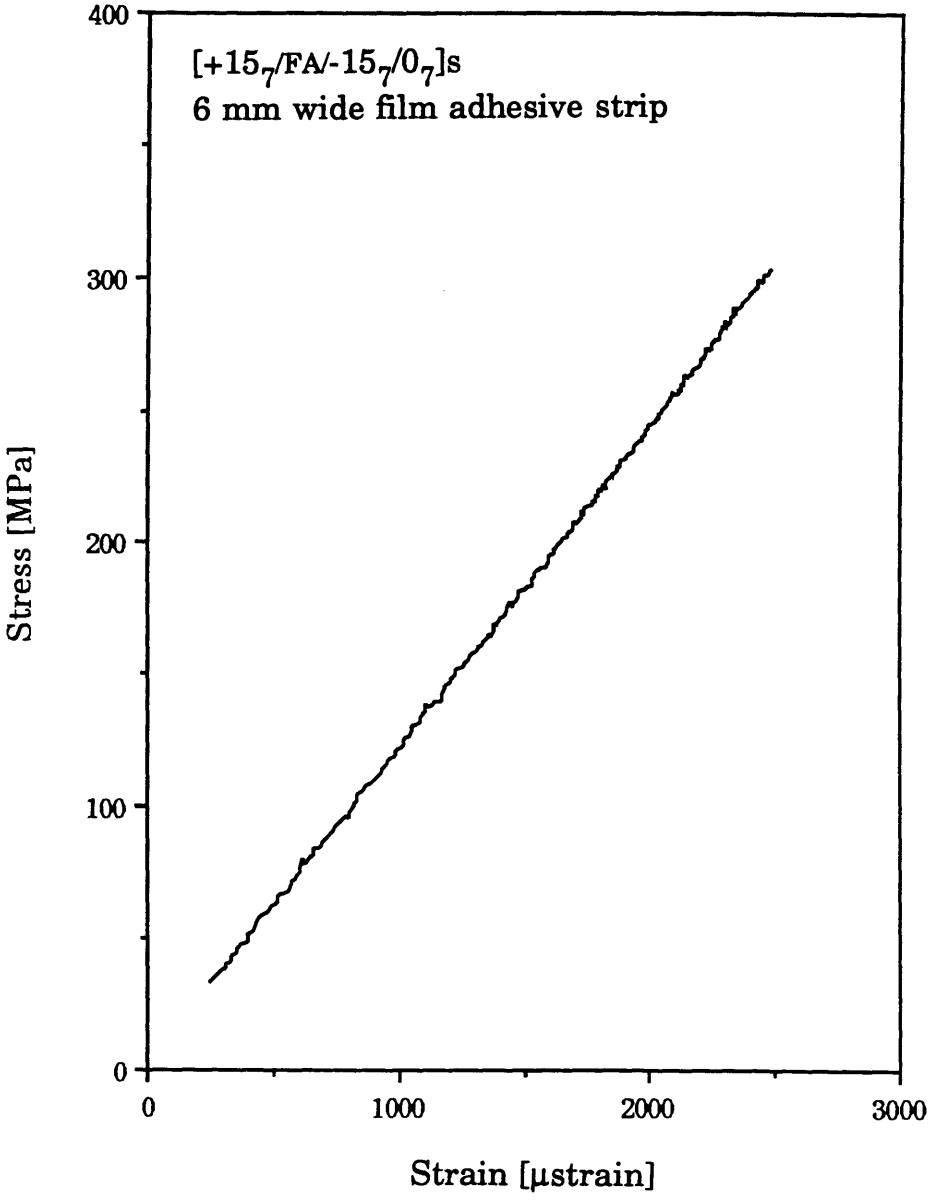

Figure 5.6 Typical stress-strain plot for $[15_7/FA/-15_7/0_7]_s$ specimens with 6 mm wide film adhesive ply strips at the +15°/-15° interface.

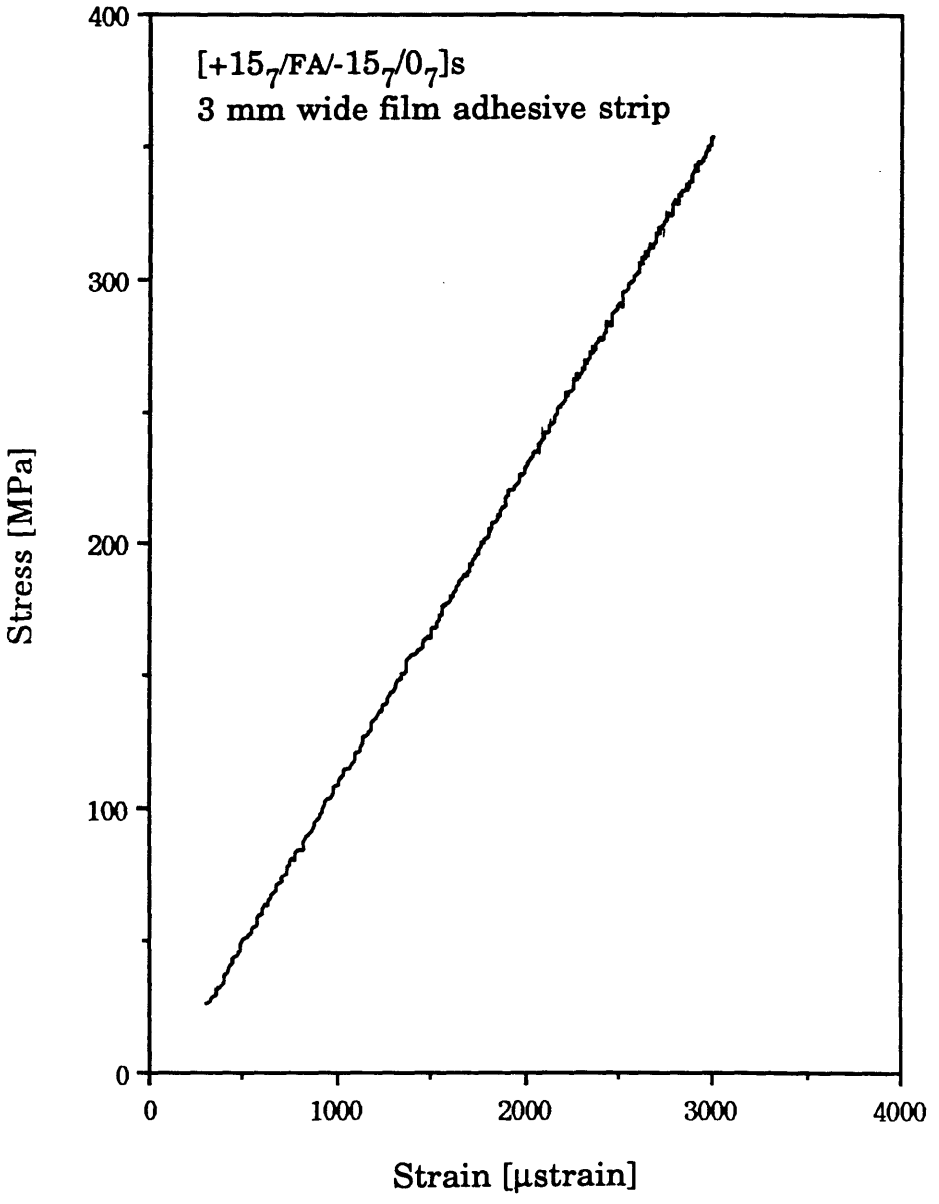

Figure 5.7 Typical stress-strain plot for $[15_7/FA/-15_7/0_7]_s$ specimens with 3 mm wide film adhesive ply strips at the +15°/-15° interface.

respectively. These specimens show, on average longitudinal moduli (E_L) of 109 GPa, 109 GPa, and 110 GPa, respectively. A nominal thickness of 5.628 mm was used for these calculations.

The modulus values of these specimens can be predicted by assuming them to be a combination of three laminates, the two edge regions with film adhesive strips can be considered as separate laminates of the $[+15_7/FA/-15_7/0_7]_s$ type, and the remaining region can be considered as a $[+15_7/-15_7/0_7]_s$ laminate without any film adhesive. The resulting longitudinal modulus E_L can be obtained by the use of the following expression,

$$E_L = \frac{\sum_{i=1}^{3} E_i A_i}{\sum_{i=1}^{3} A_i} \tag{5.1}$$

where E_i is the longitudinal modulus of each section, and A_i is the cross-sectional area of the laminate.

Using equation 5.1, and a nominal thickness of 5.628 mm gave 125 GPa as the longitudinal modulus, E_L, irrespective of the size of the width of the film adhesive strip. There is again a difference, of about 12%, between the predicted and measured values due to the 12% to 14% difference in the measured and the nominal thickness of these specimens. All the specimens including the specimens with strips of film adhesive indicate linear behavior till failure. The stress-strain curves shown in Figures 5.5 through 5.7 are up to the first load drop encountered during the testing of the specimen.

The various specimens did not exhibit much difference in their fracture behavior, as was described earlier. Figures 5.8 through 5.10 show photographs of the failed specimens with 9 mm, 6 mm and 3 mm wide film adhesive implants respectively. Their failure mode is very similar to that of

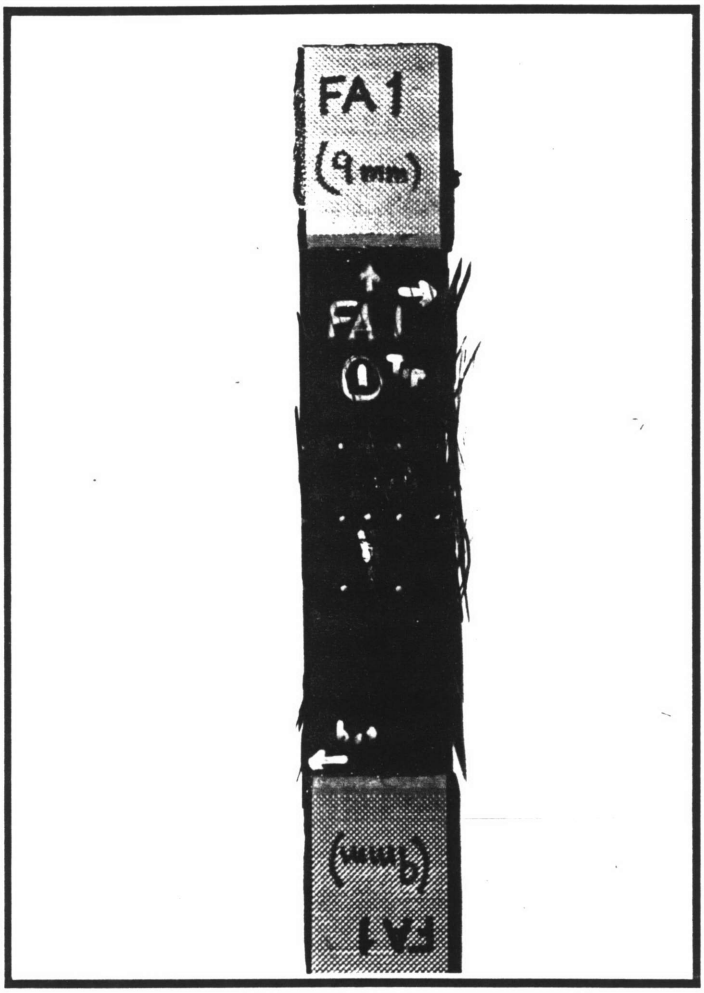

Figure 5.8 Photograph of a typical failure of a $[15_7/-15_7/0_7]_s$ with 9 mm wide film adhesive strips.

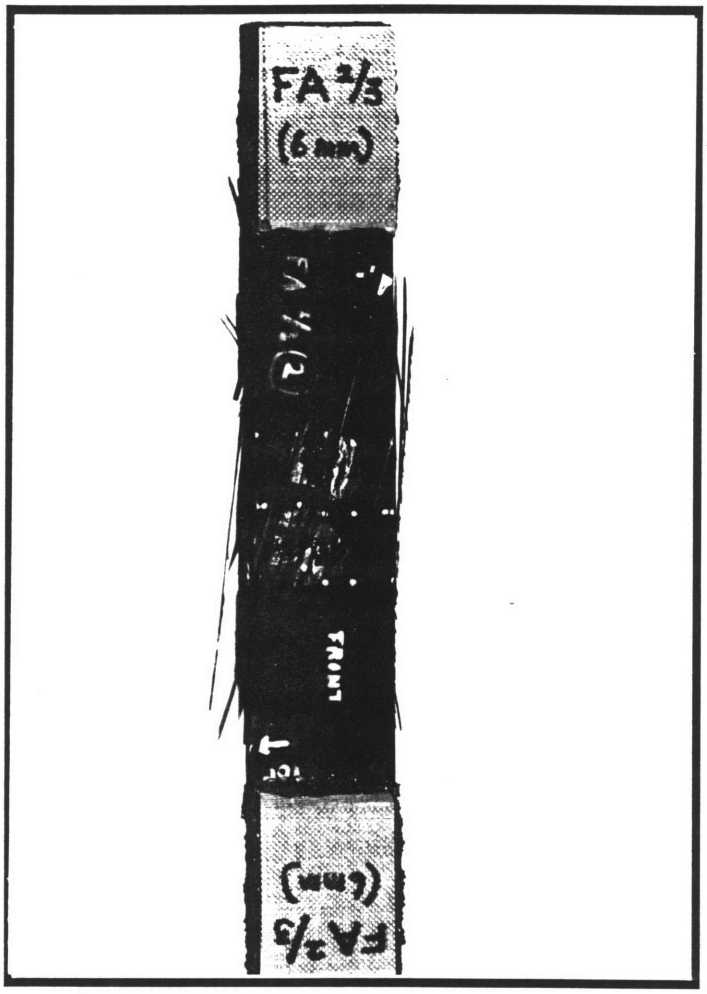

Figure 5.9 Photograph of a typical failure of a $[15_7/-15_7/0_7]_s$ with 6 mm wide film adhesive strips.

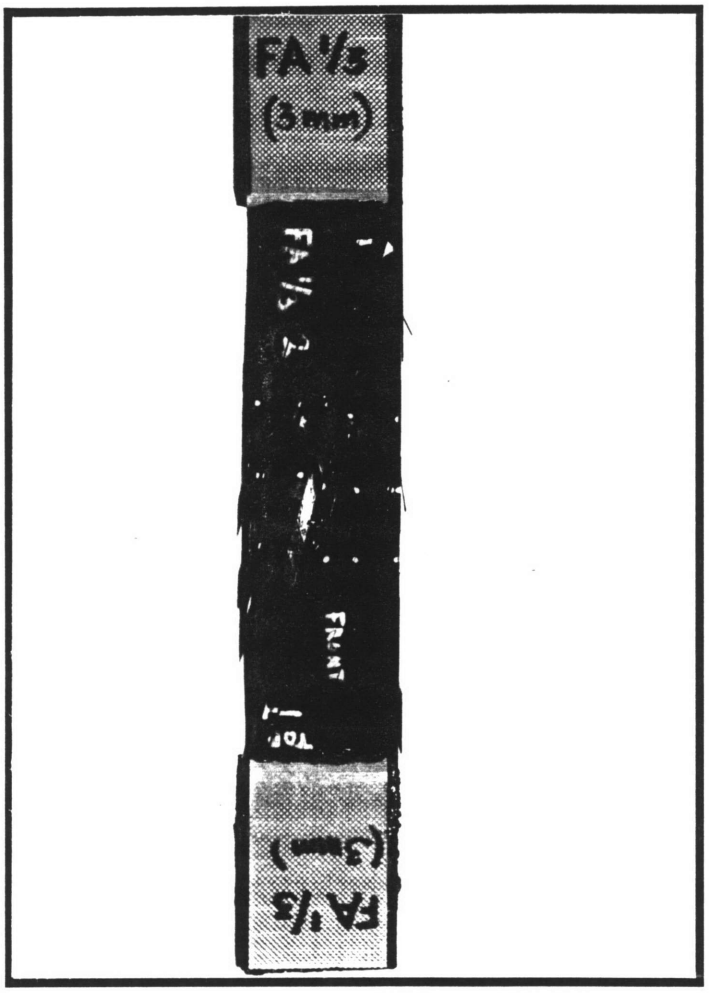

Figure 5.10 Photograph of a typical failure of a $[15_7/-15_7/0_7]_s$ specimen with 3 mm wide film adhesive strips.

the specimen with full plies of film adhesive and differed again from the control specimens only in terms of increase in the fiber breakage. No other significant difference was noted. The increased fiber breakage is associated with the higher fracture stress for these specimens.

5.1.3 Specimens with Delamination Implants

The results for the specimens listed in Table 3.3 are presented herein. The specimens in this case have entire plies of film adhesive at the ±15° interface and have implanted teflon strips to simulate the initiated delamination. The results of these tests are presented in Table 5.7.

Since these specimens had delaminations implanted in them, no edge replicas were taken during the testing of the specimen. Furthermore, no attempt was made to study the growth of the delamination through the specimen. The specimens were loaded to final failure and this load was noted and compared to the failure loads of the specimens with and without film adhesive. The average failure stresses of the specimens with teflon implants are given in Table 5.7 to be 458 MPa, 450 MPa, and 591 MPa, for the specimens with 9 mm, 6 mm, and 3 mm wide teflon implants, respectively. The specimens with 9 mm and 6 mm wide teflon implants show behavior similar to each other, but those with 3 mm wide teflon implants differ significantly from the other two in their final fracture stress.

A comparison of the average fracture stresses for the specimens with teflon implant strips, the specimens with film adhesive strips, and the control specimens is made. The behavior of the specimens with 6 mm and 9 mm implants is similar to the behavior of the control specimens, in the average fracture stresses for the latter being about 7% higher than those of the specimen with 6 mm and 9 mm wide teflon implants, which falls within the

Table 5.7 Test Results for $[+15_7/FA/-15_7/0_7]_s$ specimens with teflon strips placed adjacent to the free edge at the +15°/FA interface

Test Number	Width of Delamination Implant (mm)	Fracture Stress (MPa)
1	9	408
2	9	457
3	9	476
4	9	493
Average Fracture Stress		459 (8.0%)[a]
1	6	464
2	6	422
3	6	431
4	6	483
Average Fracture Stress		450 (6.3%)
1	3	573
2	3	640
3	3	557
4	3	595
Average Fracture Stress		591 (6.1%)

[a] numbers in parentheses are coefficients of variation

range of experimental error. The average fracture stress of specimens with 3 mm teflon strip, however, varied by about 20% from the average fracture stress of the control specimens. Their results seems to correlate better to the specimens with film adhesive, with fracture stress being about 13% lower than the specimens with full plies of film adhesive.

Typical stress-strain curves for the specimens are shown in Figures 5.11 through 5.13 for specimens with 9 mm, 6 mm, and 3 mm wide teflon implants respectively. Their average longitudinal moduli are seen to be 94 GPa, 98 GPa, and 105 GPa, respectively using a nominal thickness of 5.628 mm. The latter is once again similar in behavior to the specimen with full plies of film adhesive whereas the other two indicate a lower modulus caused by the delamination implanted in them. A theoretical calculation of the modulus to be expected can be made by assuming the specimen to be made up of seven different laminates which separate out when the teflon implant is placed at the +15°/FA interfaces. These seven laminates are as follows, four [+15°] laminates, two $[FA/-15_7/0_7]_s$ laminates and one $[+15_7/FA/-15_7/0_7]_s$ laminate. The formula for the longitudinal modulus of the resulting specimen is

$$E_L = \frac{\sum_{i=1}^{7} E_i A_i}{\sum_{i=1}^{7} A_i} \tag{5.2}$$

Using equation 5.2, the values of the 9 mm, 6 mm and 3 mm specimens are found to be 114 GPa, 118 GPa and 122 GPa respectively. The trend of increasing modulus with decreasing size of the teflon implant, exhibited by the measured values is the same as the predicted values. The difference in actual values between the two is again accounted for by the difference in thickness of the actual specimens and the nominal thickness. The modulus data for the

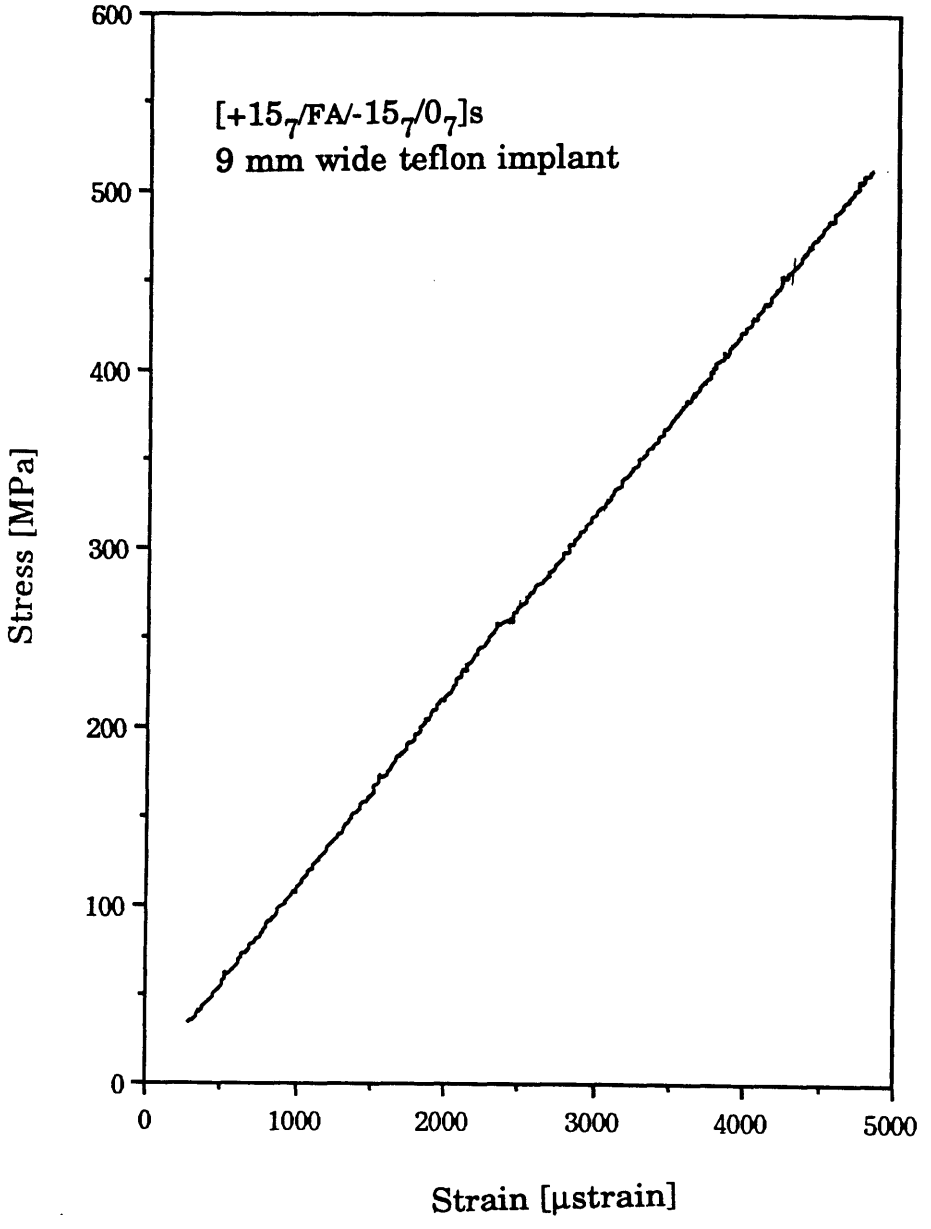

Figure 5.11 Typical stress-strain plot for $[15_7/FA/-15_7/0_7]_s$ specimens with 9 mm wide teflon implants at the +15°/FA interface.

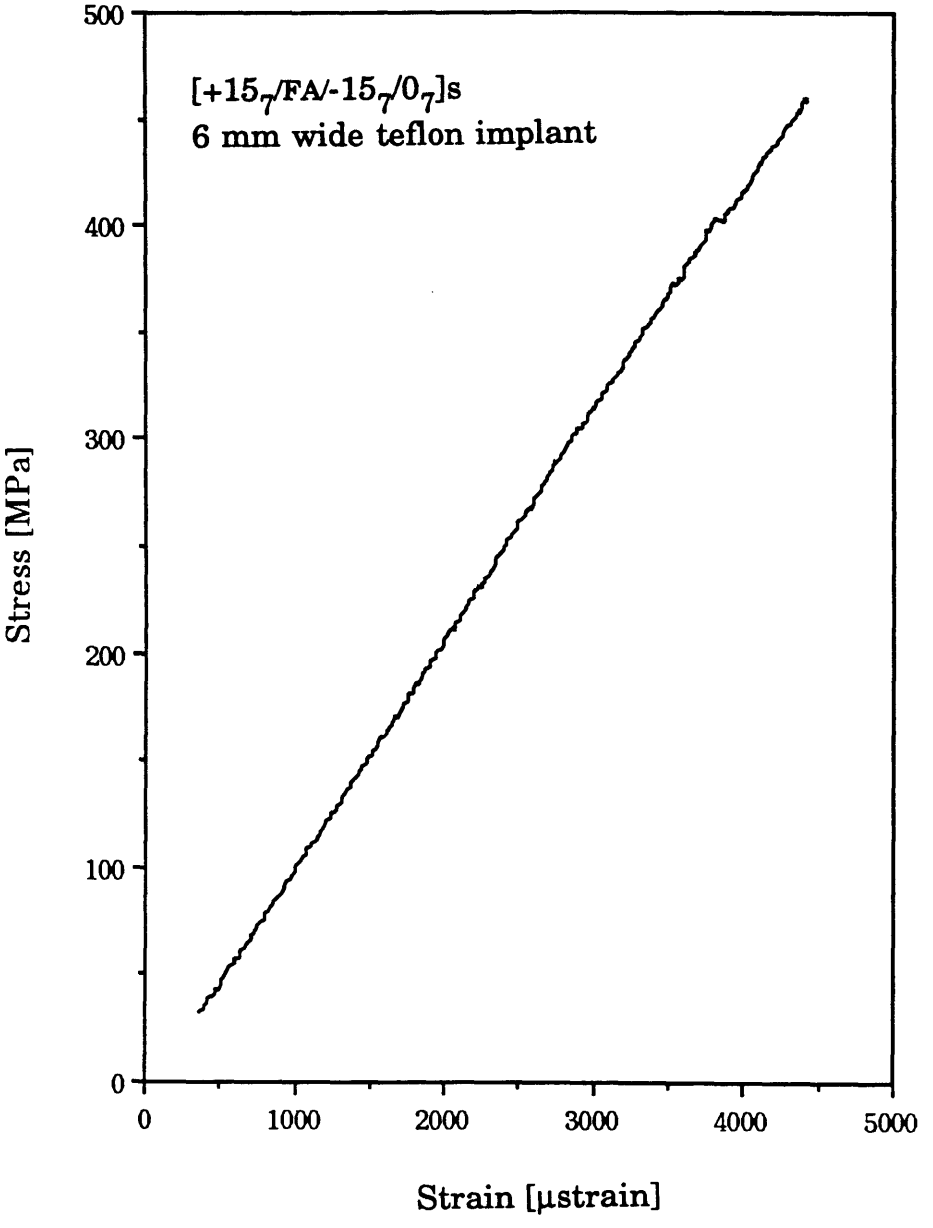

Figure 5.12 Typical stress-strain plot for $[15_7/FA/-15_7/0_7]_s$ specimens with 6 mm wide teflon implants at the +15°/FA interface.

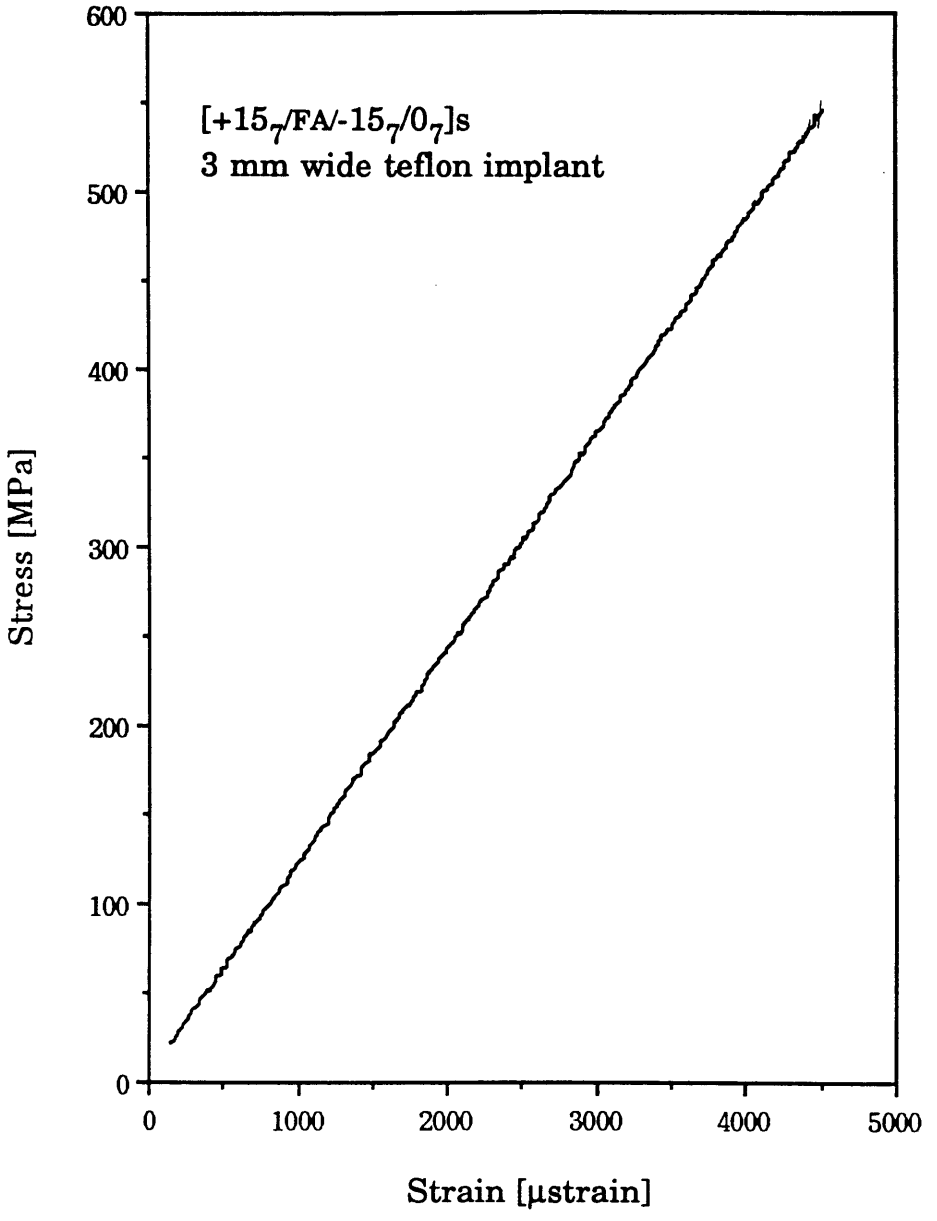

Figure 5.13 Typical stress-strain plot for $[15_7/FA/-15_7/0_7]_s$ specimens with 3 mm wide teflon implants at the +15°/FA interface.

3 mm specimens is close to that of the specimen with the full width of film adhesive.

The failed specimens, with teflon implants exhibit characteristics which are similar to each other except in the amount of fiber breakage. The specimens with 9 mm wide and 6 mm wide teflon implants did not exhibit much fiber breakage, as is shown in Figures 5.14 and 5.15. On the other hand, the specimens with 3 mm wide teflon implants behaved like the specimens without teflon implants and the increased fiber breakage in these specimens at failure is seen in the photograph in Figure 5.16.

If the failure of all the specimens tested are compared, then a similarity in behavior is observed in the form of prominent angle ply splits almost extending across the specimen width. All the specimens also show delamination separating the +15°/-15° interface. The only major difference seemed to be the increased fiber breakage seen in the specimens with film adhesive, as compared to the control specimens which is also evident from the photographs. This is to be expected as these specimens failed at loads which were on average 50% higher than the failure stress of the control specimens. This is also borne out by the specimen with 3 mm wide teflon implants which behaved like the specimens without implants and exhibited greater fiber breakage than the specimens with 9 mm and 6 mm wide teflon implants which were closer to the control specimens in their failure stresses.

5.2 Analytical Results

The software package, DOSE, was used to evaluate the interlaminar stress state at the position of the dropoff of the film adhesive in the $[+15_7/FA/-15_7/0_7]_s$ laminate. The interlaminar stresses were calculated for all

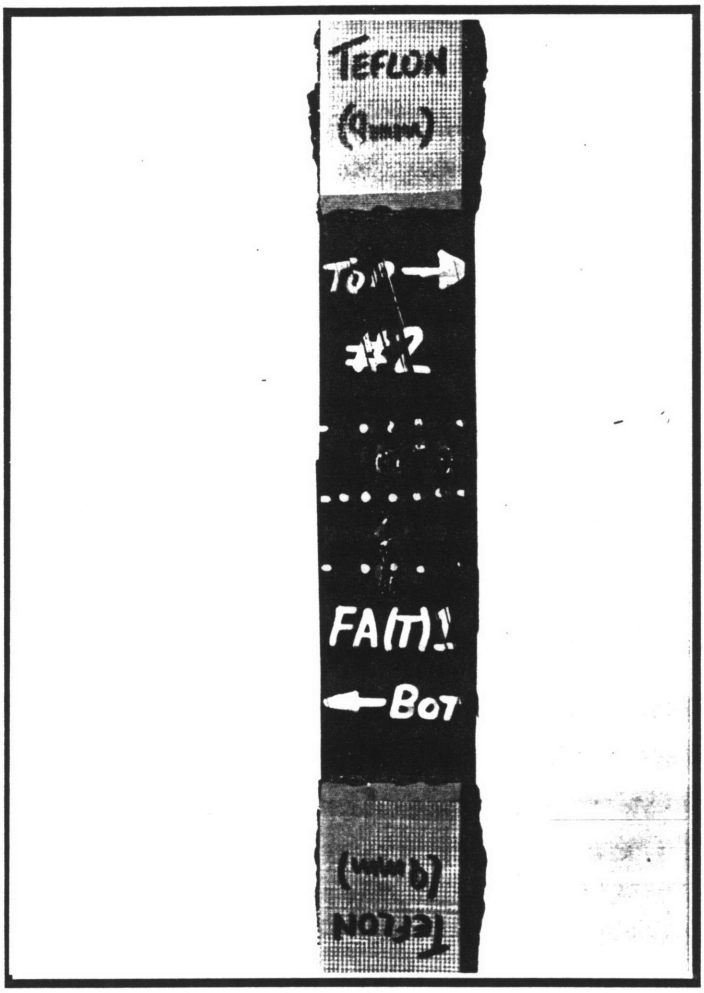

Figure 5.14 Photograph of a typical failure of a $[15_7/FA/-15_7/0_7]_s$ with 9 mm wide teflon strip implants.

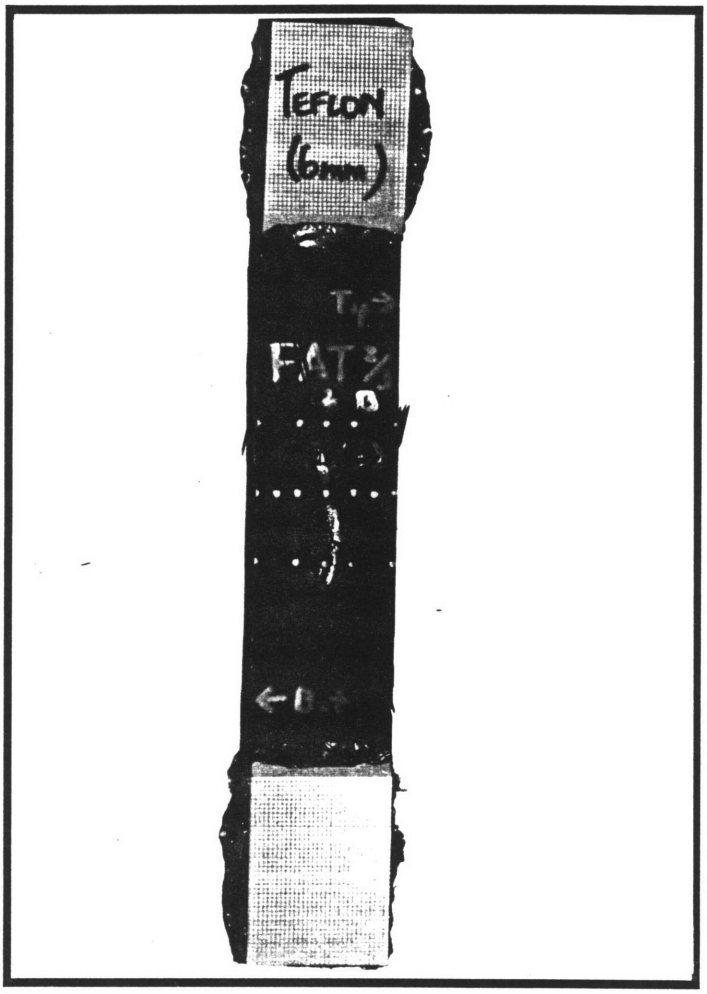

Figure 5.15 Photograph of a typical failure of a $[15_7/FA/-15_7/0_7]_s$ with 6 mm wide teflon strip implants.

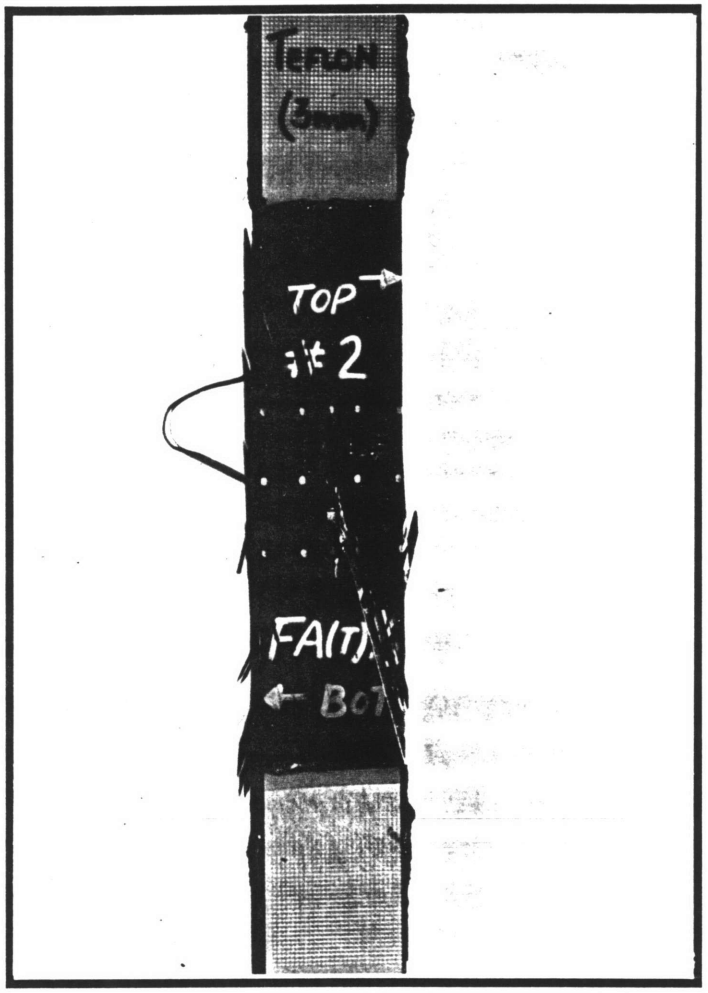

Figure 5.16 Photograph of a typical failure of a $[15_7/-15_7/0_7]_s$ with 3 mm wide teflon strip implants.

interfaces of the laminate. The Laminated Plate theory stresses were calculated for regions A and B such that the longitudinal strain, ε_{11}, in both the regions turned out to be the same. In the present case where the region A is the laminate $[+15_7/FA/-15_7/0_7]_s$ and the region B is a $[+15_7/-15_7/0_7]_s$ laminate, if a longitudinal stress σ_{11} of 100 MPa is applied to region A, then a σ_{11} of 106.9 MPa is to be applied to region B in order to obtain the same ε_{11} of 850 μstrain in both regions. The Laminated Plate Theory stresses predicted in the plies in both the regions of the laminate are presented in Tables 5.8 and 5.9. These stresses are along the laminate axes and were a set of input parameters required by the program DOSE.

The top right corner in Figures 5.17 through 5.20 illustrate the coordinate axes used in presenting the results of the free edge stresses and the dropoff stresses. The free edge stresses are given only for region A, since the dropoff is situated next to the free edge of this region and there is likely to be an interference between the dropoff and the free edge stresses in region A.

The axes system for the dropoff region presented in Figures 5.21 through 5.24 are such that the z-axis represents the interface of the dropoff, the negative region of the x-axis represents the region A and a movement down this axes implies moving closer towards the free edge. The positive direction of the x-axis leads into the region B with increasing values of x. The variation of the out-of-plane stresses in the dropoff region are shown in Figures 5.21 through 5.24 and the in-plane stresses are presented in Figures 5.25 through 5.28.

A comparison of the free edge stresses bears out the fact that the magnitude of the highest interlaminar stress is that of the σ_{1z} stress at the 15°/FA interface and the FA/-15° interface. It can be seen from Figure 5.17 that the magnitude of σ_{1z} at the free edge is about 17% of the far-field σ_{11A}, where

Table 5.8 Laminated Plate theory stresses for plies in region A for a laminate loading of σ_{11} equal to 100 MPa in region A

	Ply			
Stress[a]	$(15°)_7$	(FA)	$(-15°)_7$	$(0)_7$
σ_{11}	100.6	3.7	100.6	119.6
σ_{22}	2.1	-1.8	2.1	-3.7
σ_{12}	23.3	0.0	23.3	0.0

[a] all values in MPa

Table 5.9 Laminated Plate theory stresses for plies in region B for a laminate loading of σ_{11} equal to 106.9 MPa in region B

	Ply		
Stress[a]	$(15°)_7$	$(-15°)_7$	$(0°)_7$
σ_{11}	100.5	100.6	119.5
σ_{22}	1.9	1.9	-3.8
σ_{12}	23.3	-23.3	0.0

[a] all values in MPa

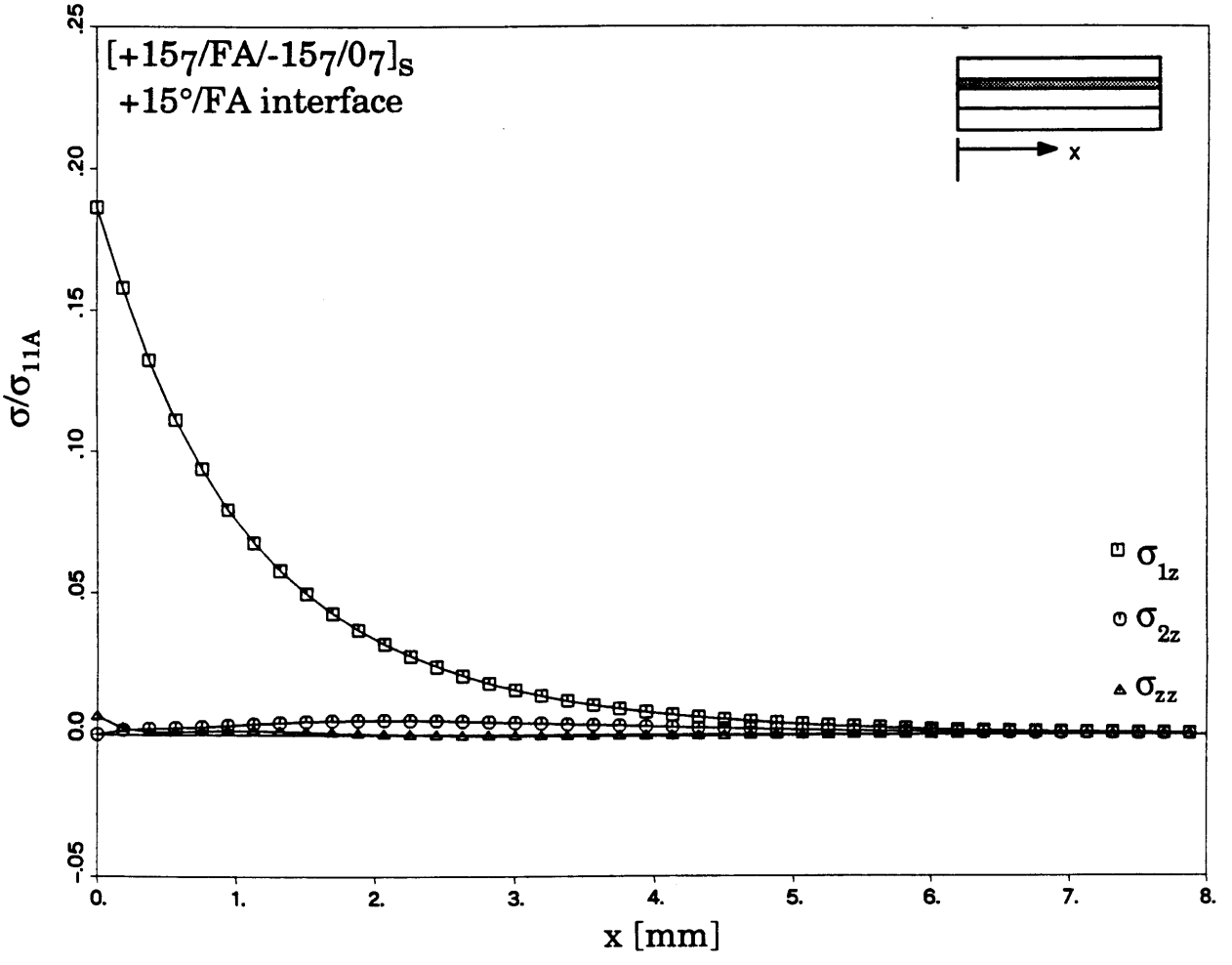

Figure 5.17 Interlaminar stresses at the free edge in region A of the model at the +15°/FA interface of a $[15_7/FA/-15_7/0_7]_s$ laminate.

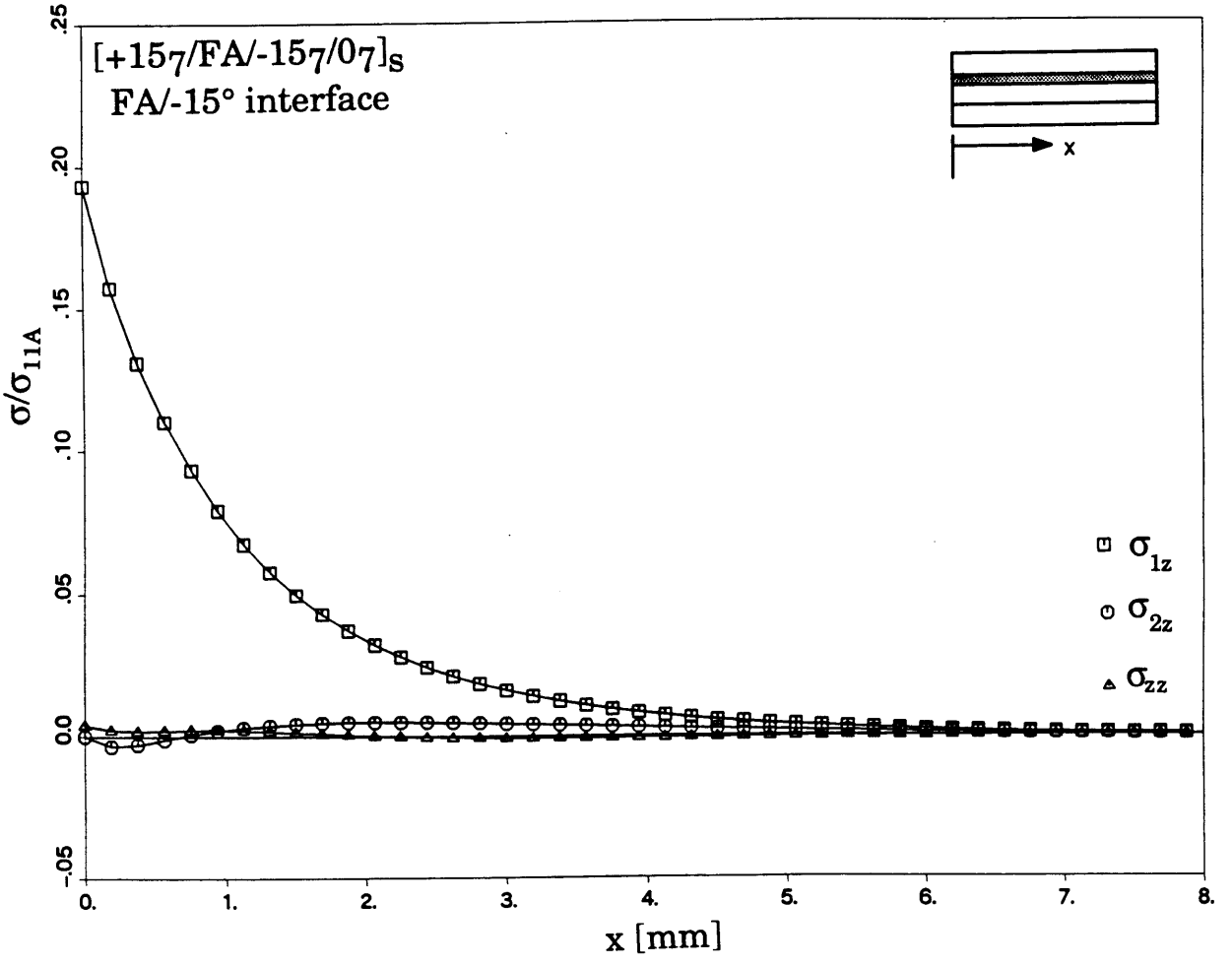

Figure 5.18 Interlaminar stresses at the free edge in region A of the model at the FA/-15° interface of a $[15_7/FA/-15_7/0_7]_s$ laminate.

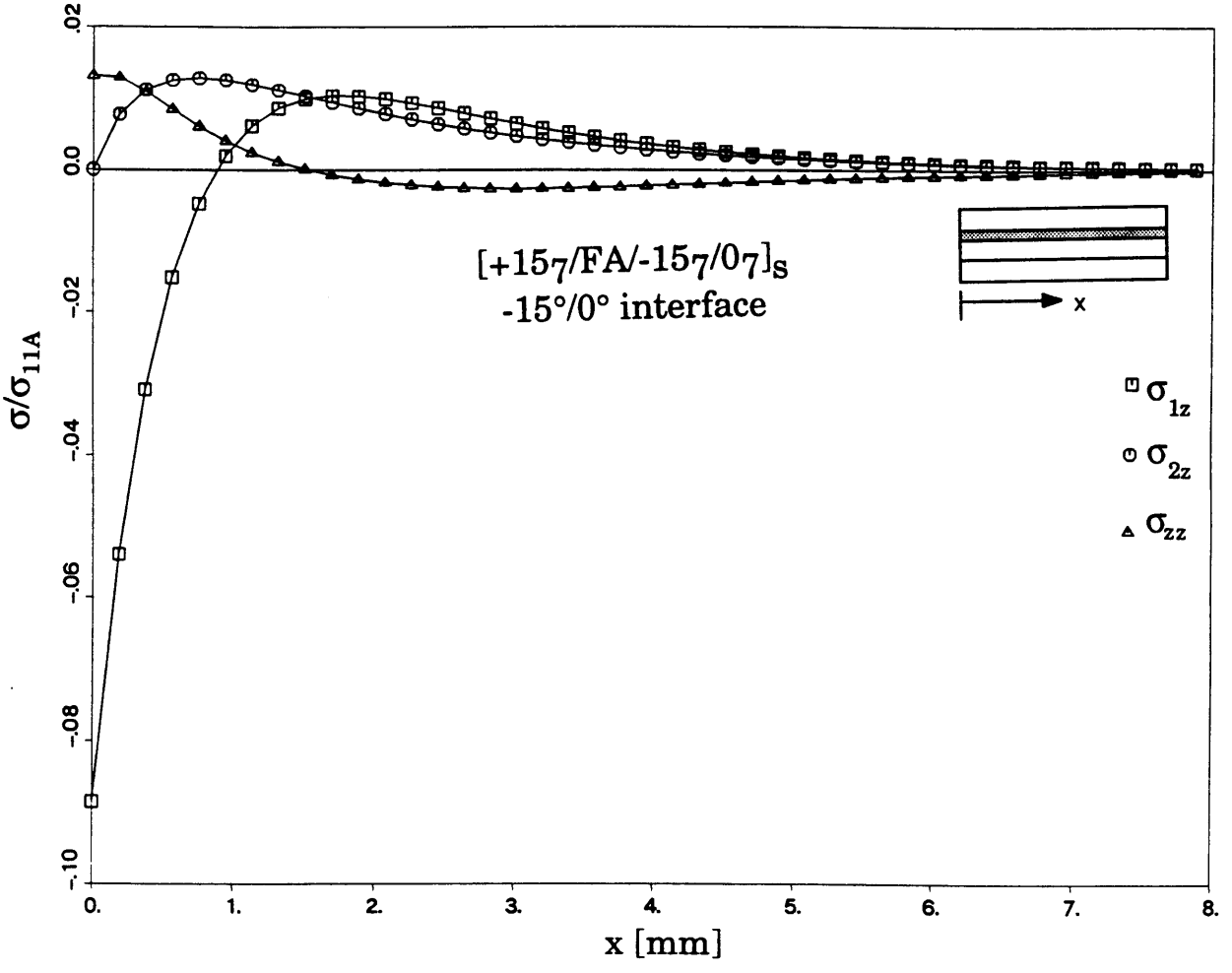

Figure 5.19 Interlaminar stresses at the free edge in region A of the model at the -15°/0° interface of a $[15_7/FA/-15_7/0_7]_s$ laminate.

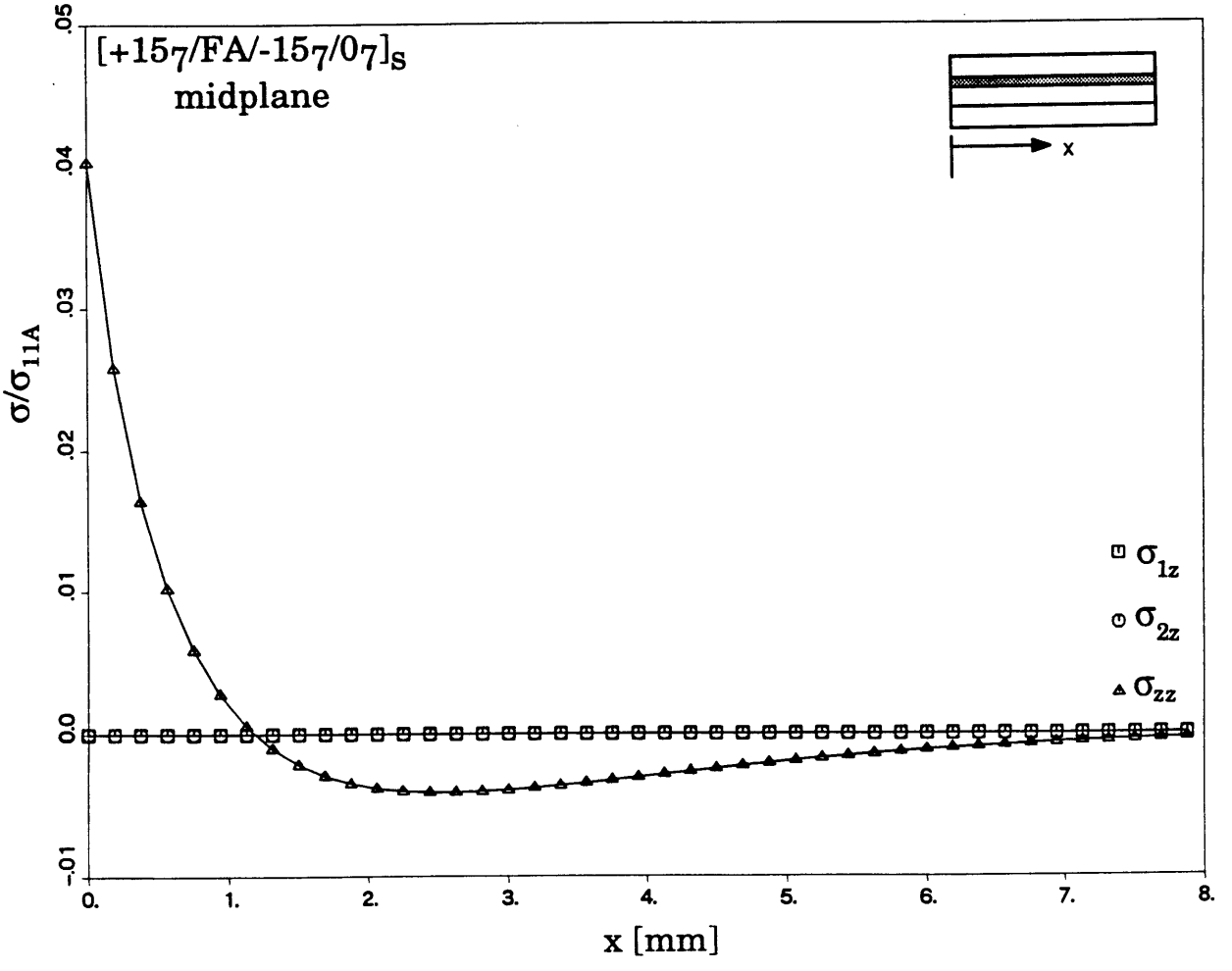

Figure 5.20 Interlaminar stresses at the free edge in region A of the model at the midplane of a $[15_7/FA/-15_7/0_7]_s$ laminate.

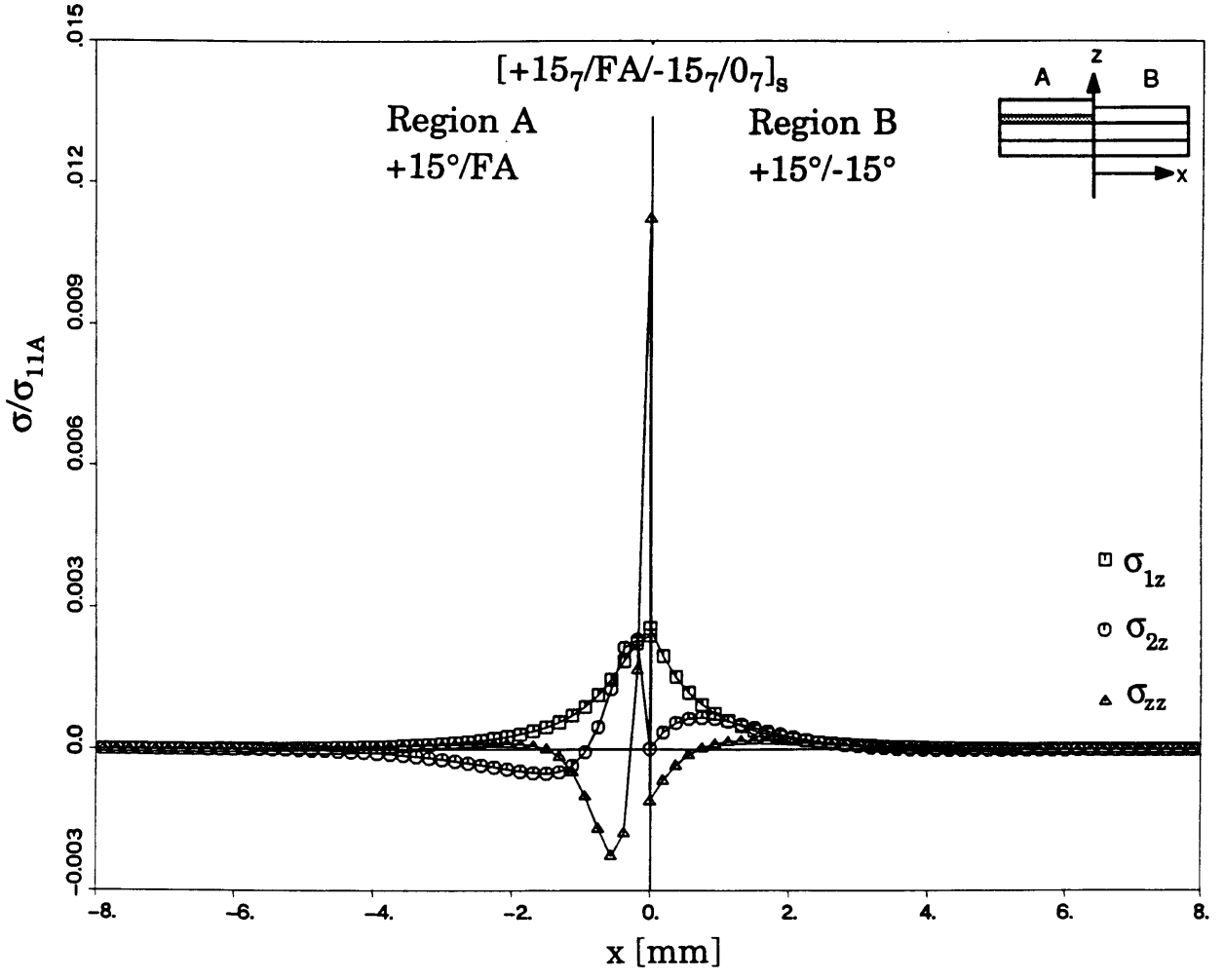

Figure 5.21 Interlaminar stresses at the dropoff in region A at the +15°/FA interface and in region B at the +15°/-15° interface of a $[15_7/FA/-15_7/0_7]_s$ laminate.

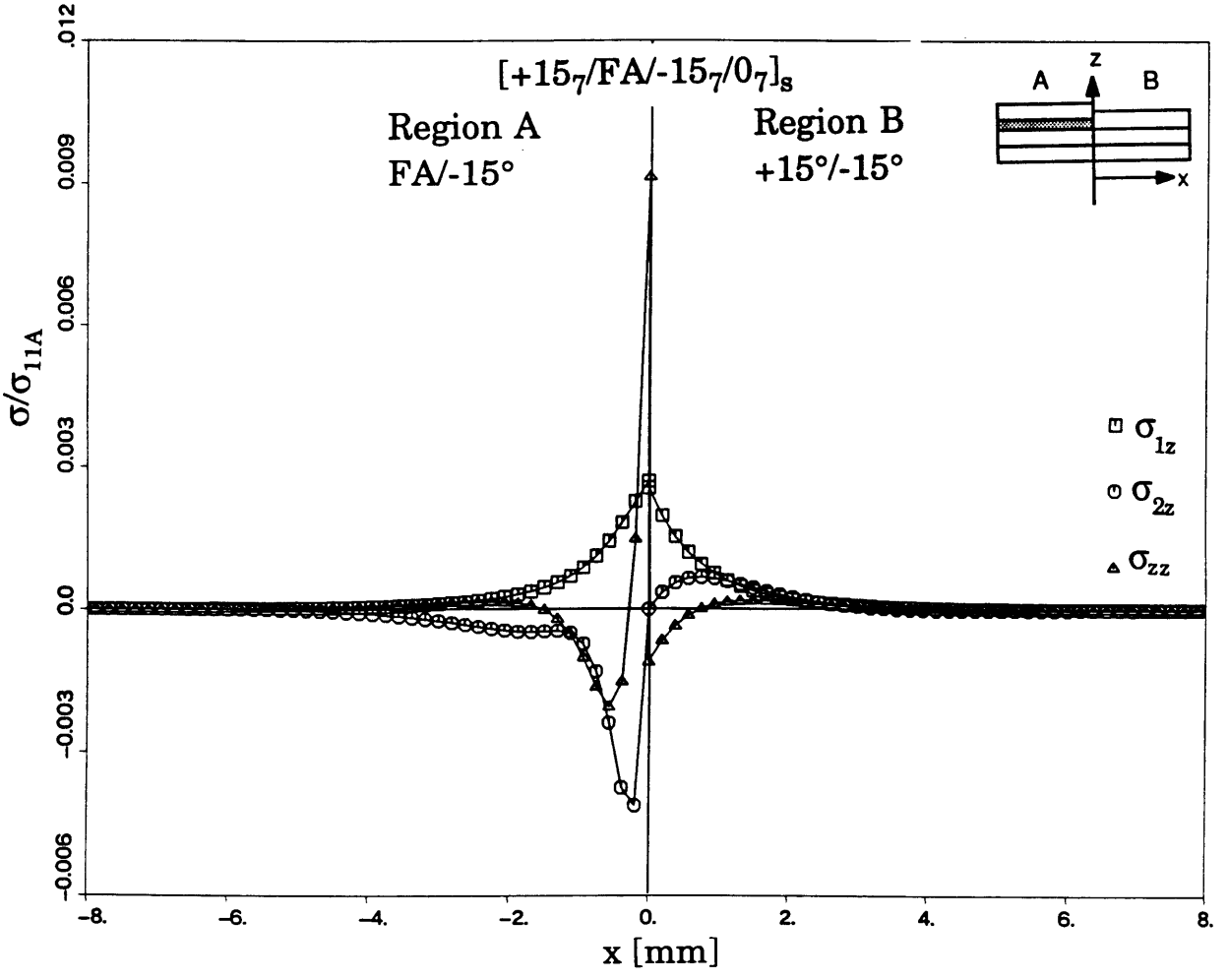

Figure 5.22 Interlaminar stresses at the dropoff in region A at the FA/-15° interface and in region B at the +15°/-15° interface of a $[15_7/FA/-15_7/0_7]_s$ laminate.

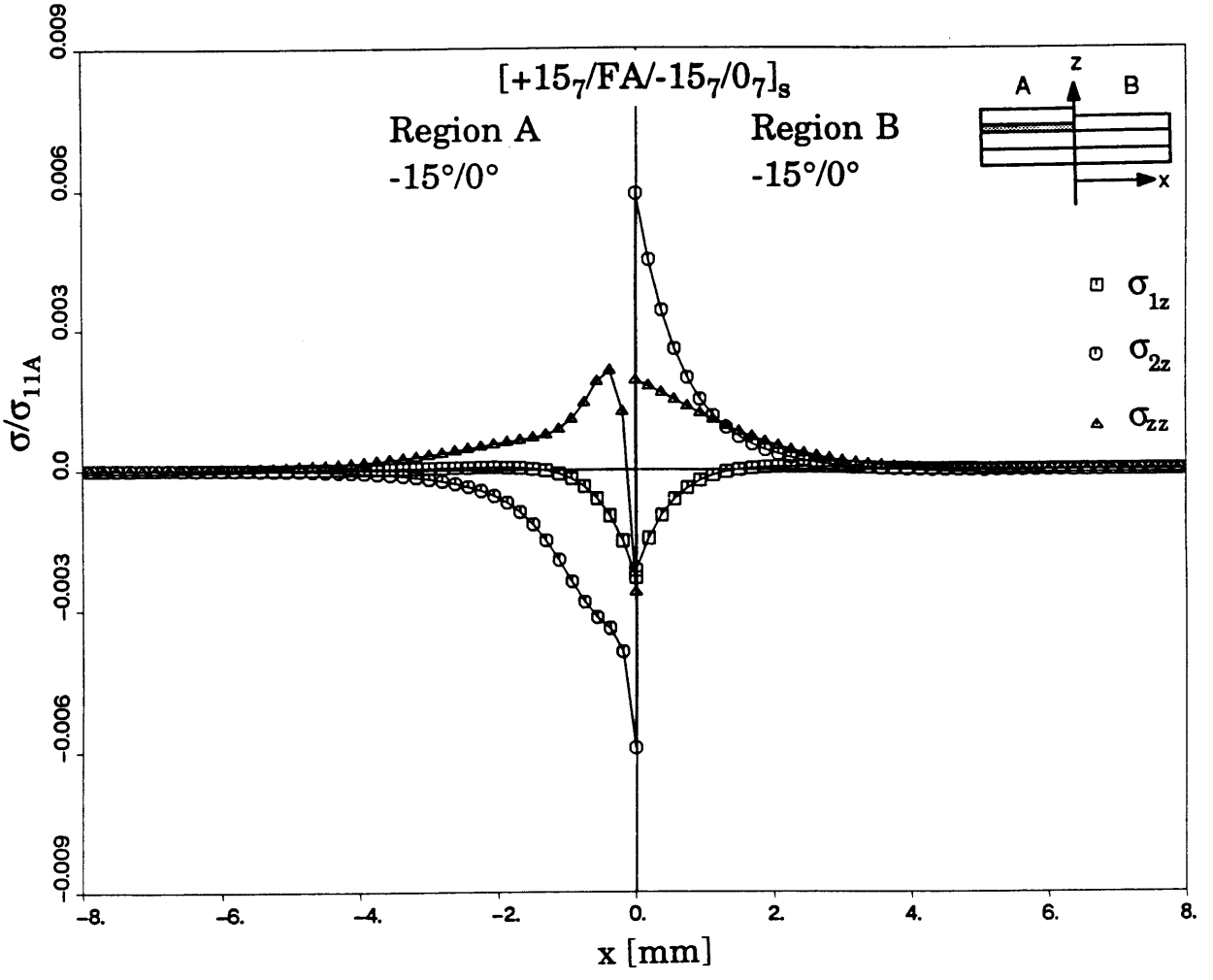

Figure 5.23 Interlaminar stresses at the dropoff in region A at the -15°/0° interface and in region B at the -15°/0° interface of a $[15_7/FA/-15_7/0_7]_s$ laminate.

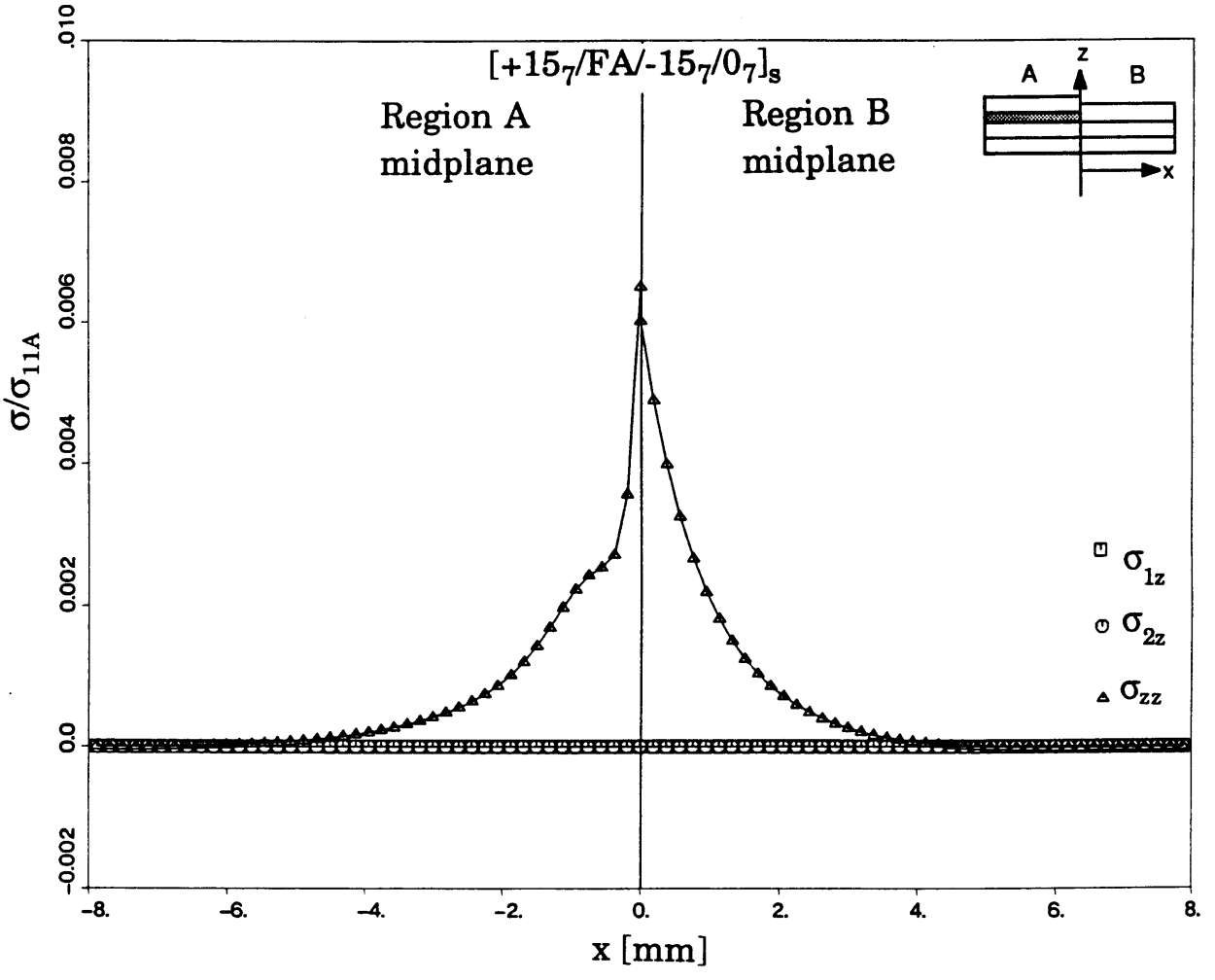

Figure 5.24 Interlaminar stresses at the dropoff in region A and region B at the midplane of a $[15_7/FA/-15_7/0_7]_s$ laminate.

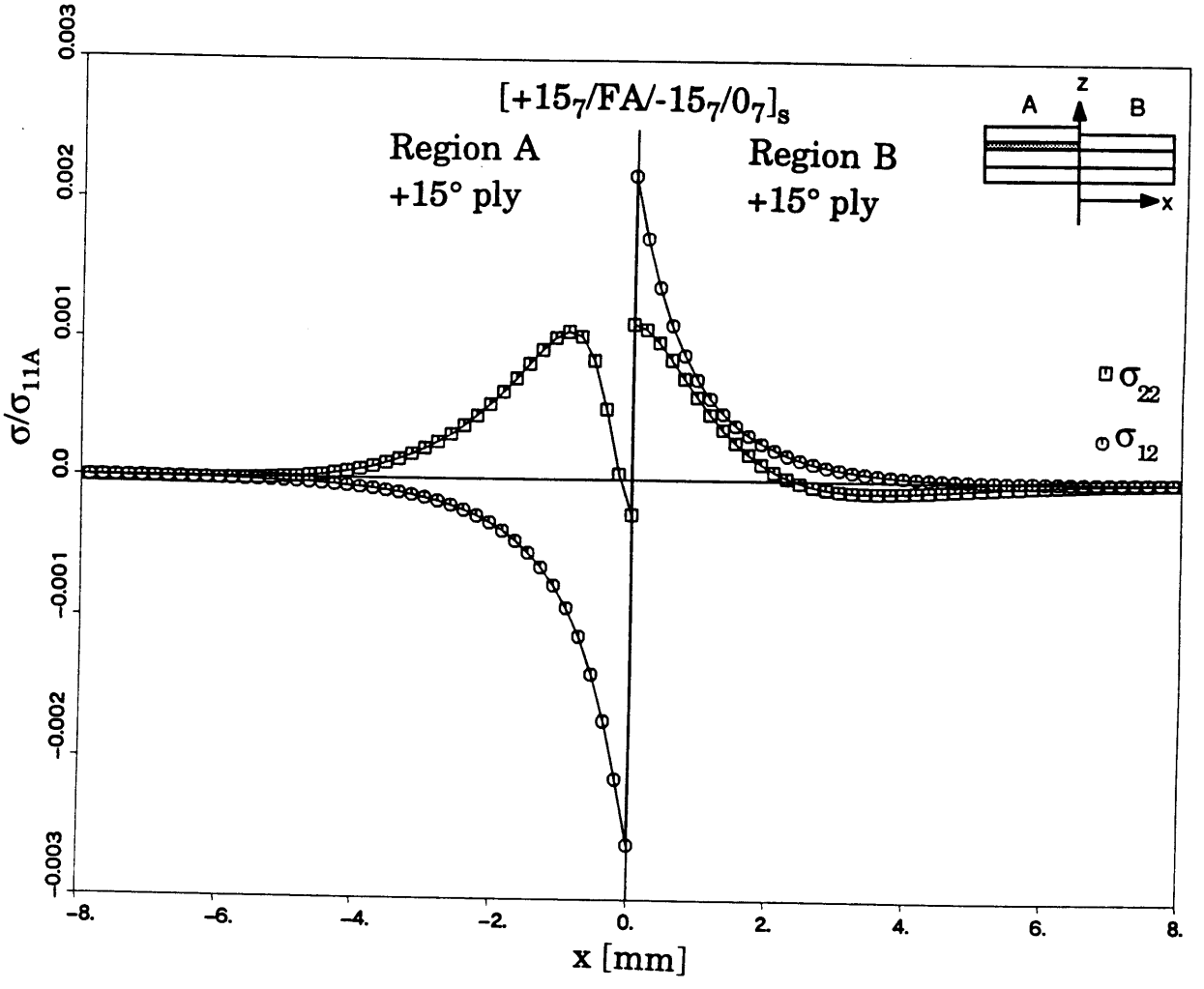

Figure 5.25 In-plane stresses at the dropoff in region A in the +15° ply and in region B in the +15° ply of a $[15_7/FA/-15_7/0_7]_s$ laminate.

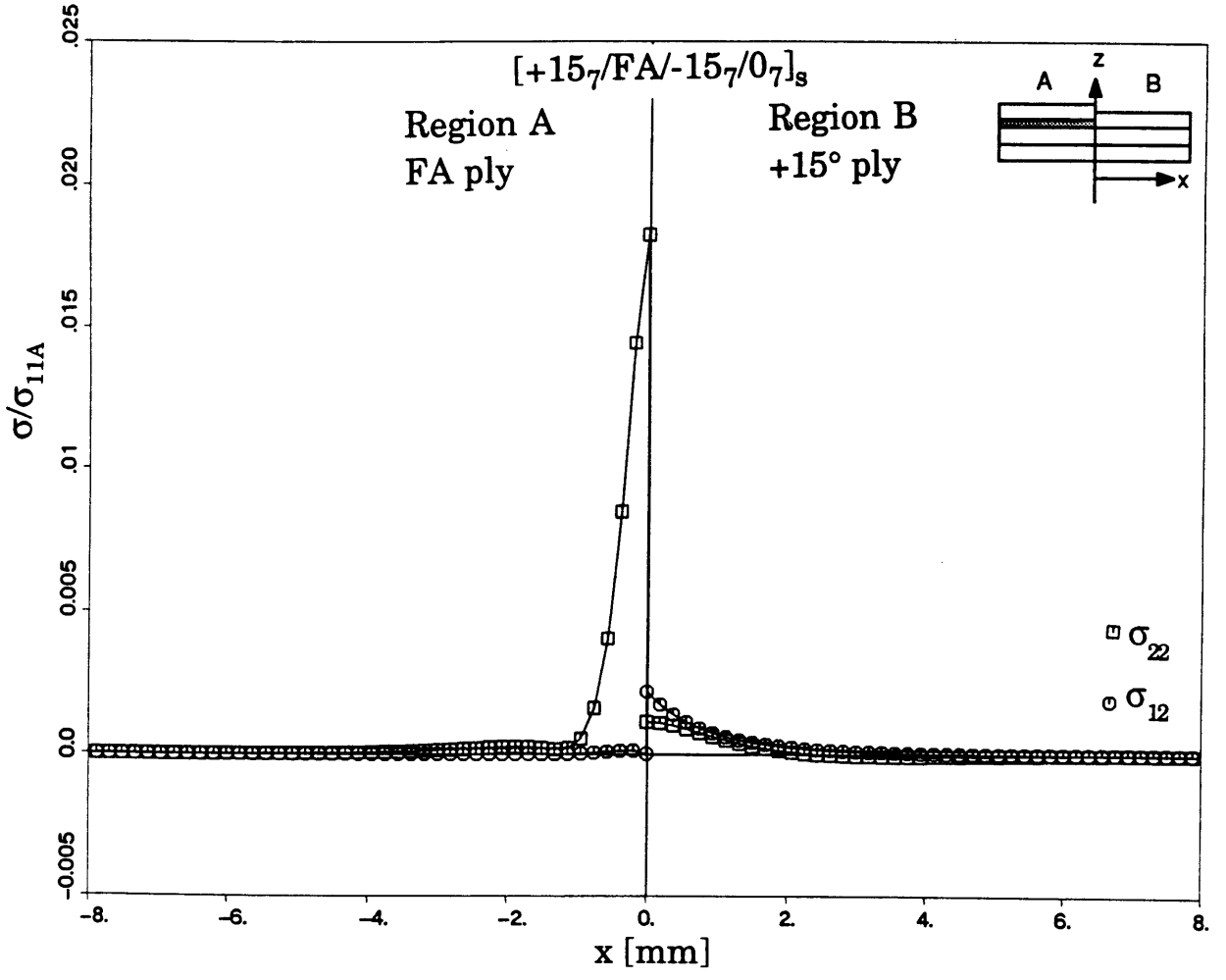

Figure 5.26 In-plane stresses at the dropoff in region A in the FA ply and in region B in the +15° ply of a $[15_7/FA/-15_7/0_7]_s$ laminate.

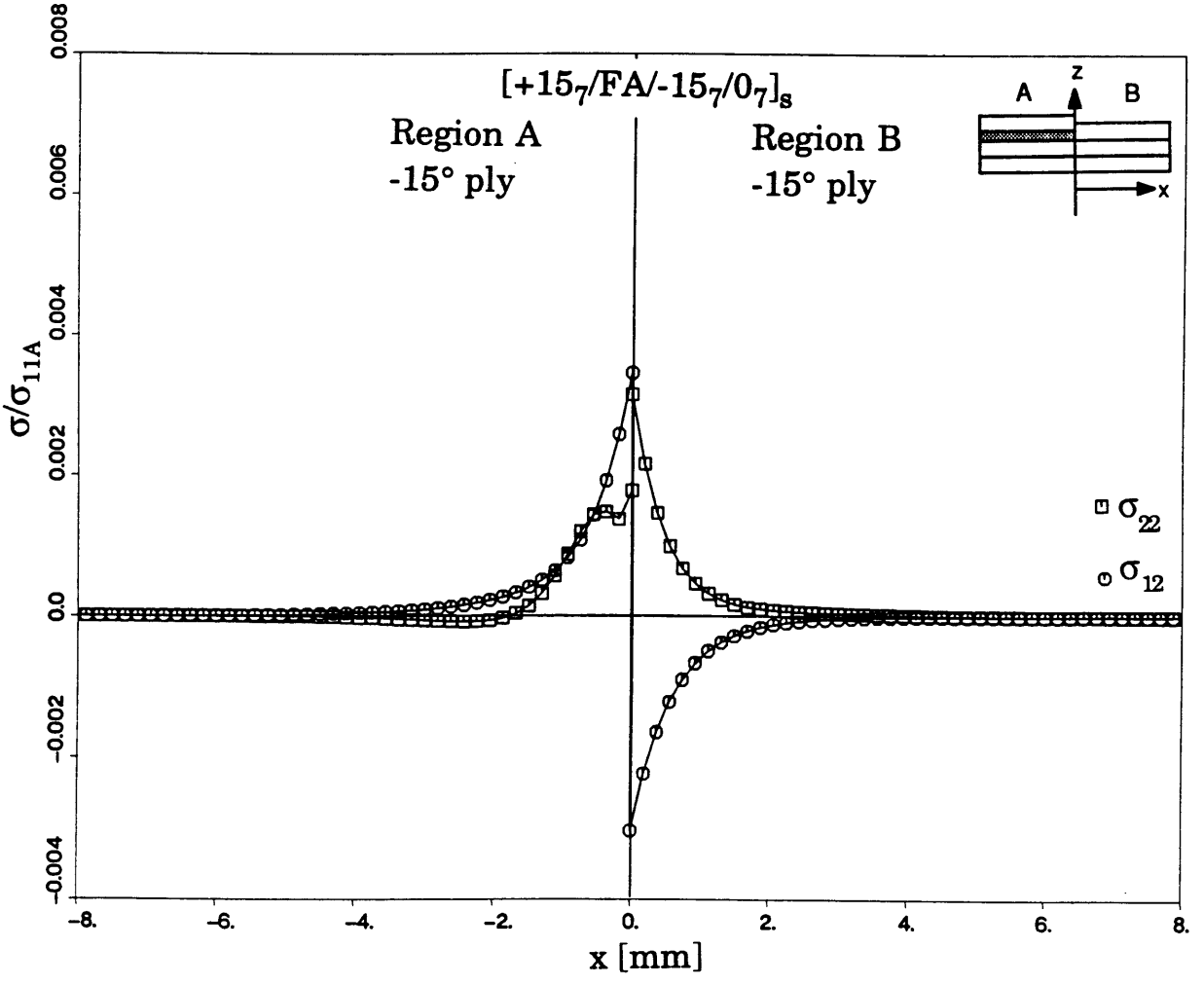

Figure 5.27 In-plane stresses at the dropoff in region A in the -15° ply and in region B in the -15° ply of a $[15_7/FA/-15_7/0_7]_s$ laminate.

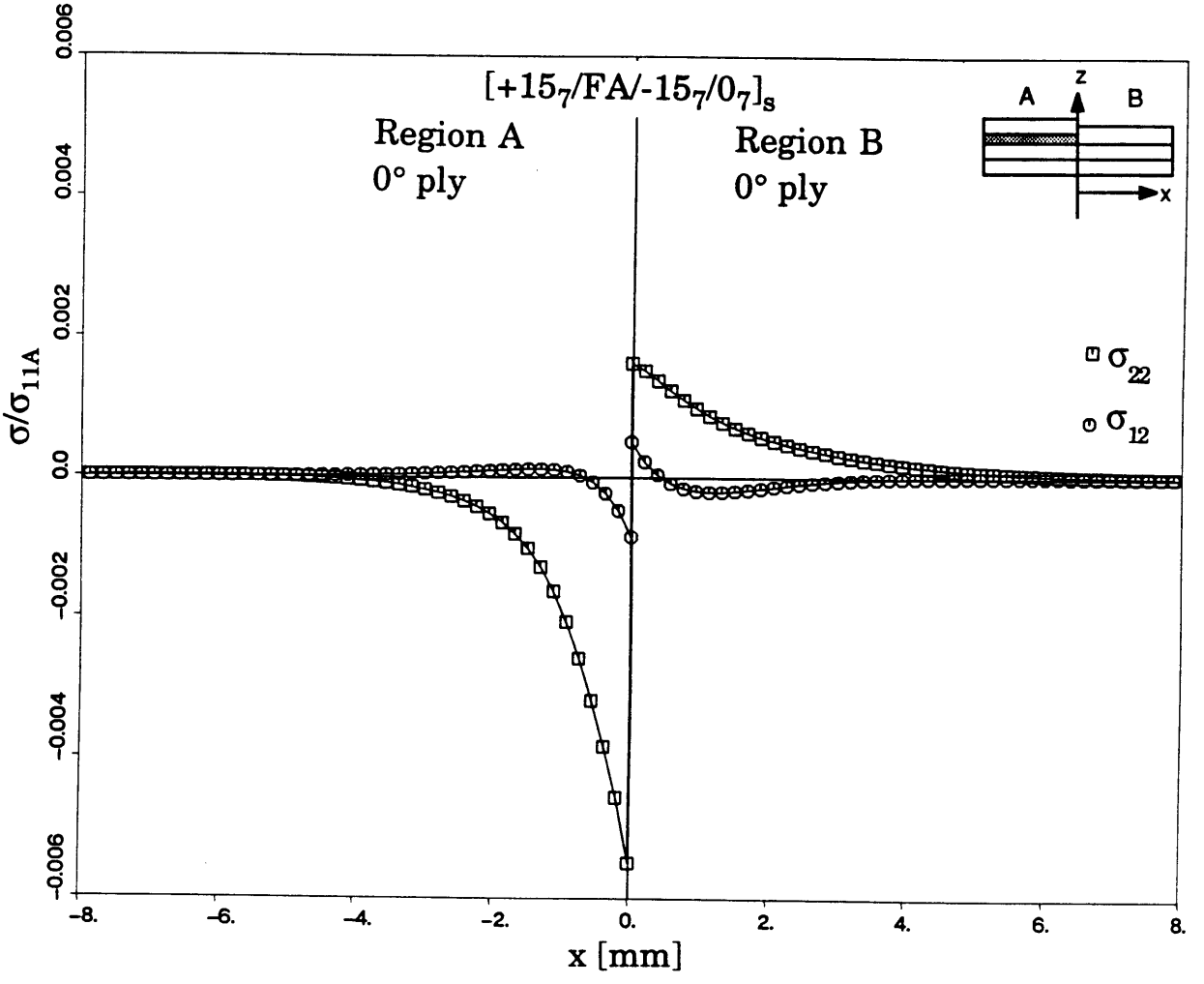

Figure 5.28 In-plane stresses at the dropoff in region A in the 0° ply and in region B in the 0° ply of a $[15_7/FA/-15_7/0_7]_s$ laminate.

σ_{11A} is the far-field applied longitudinal stress in region A. The stresses σ_{2z} and σ_{zz} at the free edge are less than 2% of the σ_{1z} and hence are negligibly small as compared to σ_{1z}. The stresses in the vicinity of the dropoff at the +15°/FA interface in region A and the +15°/-15° interface of region B are shown in Figure 5.21. These stresses are clearly seen to be extremely small, in almost all cases being about 10% or less of the σ_{1z} stress at the free edge.

It is seen that the free edge stresses at a distance of 3 mm from the free edge are greater than the interlaminar stresses due to the dropoff. Thus, even in the case where the dropoff is located at 3 mm from the free edge the interference between the dropoff and the free edge interlaminar stresses would probably not result in stresses as high as the stresses at the free edge itself . Therefore though there is likely to be an interference between the free edge interlaminar stresses and the dropoff interlaminar stresses, the magnitude of the interlaminar stresses at the dropoff are not large enough to cause any significant change in the interlaminar stresses in the region. Amongst the interlaminar stresses at the dropoff, the highest is seen to be the σ_{zz} in region A, with a magnitude of about 1% of the far-field σ_{11A}. The interlaminar stresses at the dropoff are seen to be less than 0.5 % of the far-field σ_{11A} in region B.

The next interfaces considered are the FA/-15° in region A and the +15°/-15° interface in region B. The dropoff stresses are shown in Figure 5.22, and the corresponding free edge stresses are shown in Figure 5.18. The argument made earlier regarding the interlaminar stresses at the dropoff still hold here, i.e., they are an order of magnitude smaller than the interlaminar stresses at the free edge. Although there will be an interaction of the free edge and dropoff stresses when the dropoff is located at x equal to 3 mm, there should not be a significant change in the magnitude of the stresses as

compared to the 17% of σ_{11A} at the free edge. It should be noted here that linear addition of the two interlaminar stresses is all that can be performed to indicate the interaction between them. In actuality, the stresses would interact in a more complicated fashion.

The results for the free edge at the -15°/0° interface in region A and B are shown in Figure 5.19. The highest interlaminar stresses at the dropoff shown in Figure 5.23 are again an order of magnitude smaller than the free edge stresses. The highest stress here is σ_{2z} as compared to the σ_{zz} at the previous interface, but the peak magnitude of this σ_{2z} is less than 10% of the peak free edge interlaminar stress. The interlaminar stress σ_{1z} is the highest at the free edge and is about 10% of the far-field σ_{11A}.

The midplane interlaminar stresses at the dropoff are shown in Figure 5.24. The interlaminar shear is zero and σ_{zz} is the highest at the free edge and the dropoff region due to the symmetry of the laminate. However, in terms of the magnitude, the free edge stress is around 4% of σ_{11A}, as seen from Figure 5.20, and the dropoff stress is around 0.7% of σ_{11A}. Interaction between the two types of the stresses would occur if the dropoff was at x equal to 3 mm. Again, the change in stresses should not be significant if this occurs.

The boundary layer region for the specimens with full plies of film adhesive was shown in Table 3.1 to be about 9 mm in width. On examining the interlaminar stresses at the dropoff region in Figures 5.21 through 5.24, qualitatively, it can be seen that the stresses die away to zero over a distance of 6 mm on both sides of the dropoff. This 6 mm is a distance by which the stresses drop down to less than a hundredth of the peak interlaminar stresses at the dropoff. No analytical formulae have been used in arriving at this number and this is just an order of magnitude of the distance over which the effect of the dropoff region is felt and could be termed as the "boundary layer"

due to the dropoff. It represents the region around the dropoff which has interlaminar stresses due to the dropoff.

The in-plane stresses within the various plies change as the dropoff region is approached, and the contribution of the companion problem to the in-plane stresses are presented in Figures 5.25 through 5.28. The peak stresses seen from these figures can be added on to the Classical Laminated Plate theory predicted stresses given in Tables 5.9 and 5.10 to provide the actual value of the in-plane stresses at the dropoff location. It is seen that the contribution of the companion problem to the in-plane stresses at the dropoff is about an order of magnitude smaller than the stresses obtained from Classical Laminated Plate theory and hence are not significant, except in the case of the dropped ply where the stresses are the exact opposite of each other as was imposed by the boundary condition in order that the in-plane stresses carried by the dropped ply go to zero at dropoff. The in-plane stresses in the companion problem are seen to die to zero within a distance of 4 mm in both regions A and B.

CHAPTER 6

DISCUSSION OF RESULTS

6.1 Specimens with film adhesive implants

Delamination suppression has been earlier achieved by the use of cocured film adhesive layers, as shown by Lagace et al. [26] where the film adhesive is placed at all interfaces of the laminate. The current study demonstrates that there exist efficient ways in which the film adhesive can be placed within a laminate susceptible to delamination initiation, again resulting in successful delamination suppression without the use of excessive amounts of film adhesive.

All the control specimens, without any film adhesive, exhibited delamination at the +15°/-15° interface and the fracture of the specimen occurred almost immediately following the delamination initiation. All the other specimens tested incorporated film adhesive in order to suppress this early occurrence of delamination and thus push the delamination initiation load and the fracture stress higher.

The first step towards efficient placement involved placement of the film adhesive only at the interface which was most susceptible to delamination as predicted by the Quadratic Delamination Criterion. This was an improvement over placing the film adhesive at all interfaces of the laminate as this still achieved the purpose of delaying the initiation. This was successfully shown to delay the delamination initiation load to a point 50% higher than in the case of the control specimens. The next step towards further optimizing the placement of the film adhesive was the restriction of the film adhesive to

regions in the laminate where interlaminar stresses are significant. This is the boundary layer near the free edge of the specimen. The results of these tests shows that the specimens with strips of film adhesive are as successful in suppressing delamination as entire plies of film adhesive. In the present case, film adhesive strips of thickness 0.203 mm and widths of 3 mm, 6 mm and 9 mm are used and the observed differences in the delamination initiation stress and the final fracture stress for these specimens with different widths of film adhesive, and as compared to specimens with full width plies of film adhesive, seem to be marginal as was shown in section 5.1.

A simple one-dimensional shear lag model was proposed by Weems [32] to explain the mechanism of operation of the film adhesive. Two specimens one without the film adhesive layer and another with the cocured layer, are illustrated in Figure 6.1. It is seen from this that the compliant film adhesive layer leads to the reduction in the shear strain (ν_2 is less than ν_1 in Figure 6.1) in the boundary layer region, and hence a reduction in the peak interlaminar shear stress within the laminate boundary layer region. This leads to the delay in the delamination initiation load. In the present case, however, where film adhesive strips are used instead of a full width of film adhesive, there will arise an in-plane stress gradient where the strip is terminated within the laminate. This leads to the presence of interlaminar stresses at the dropoff end of the film adhesive strip. Thus, the efficient usage of the film adhesive in the form of strips leads to the reduction of the peak interlaminar stresses at the free edge on one hand but causes interlaminar stresses at the dropoff on the other.

The magnitude of the interlaminar stresses that are caused at the free edge will depend on the amount of in-plane load being carried by the dropped ply. Since the ply is being dropped off, the in-plane stresses carried by the ply

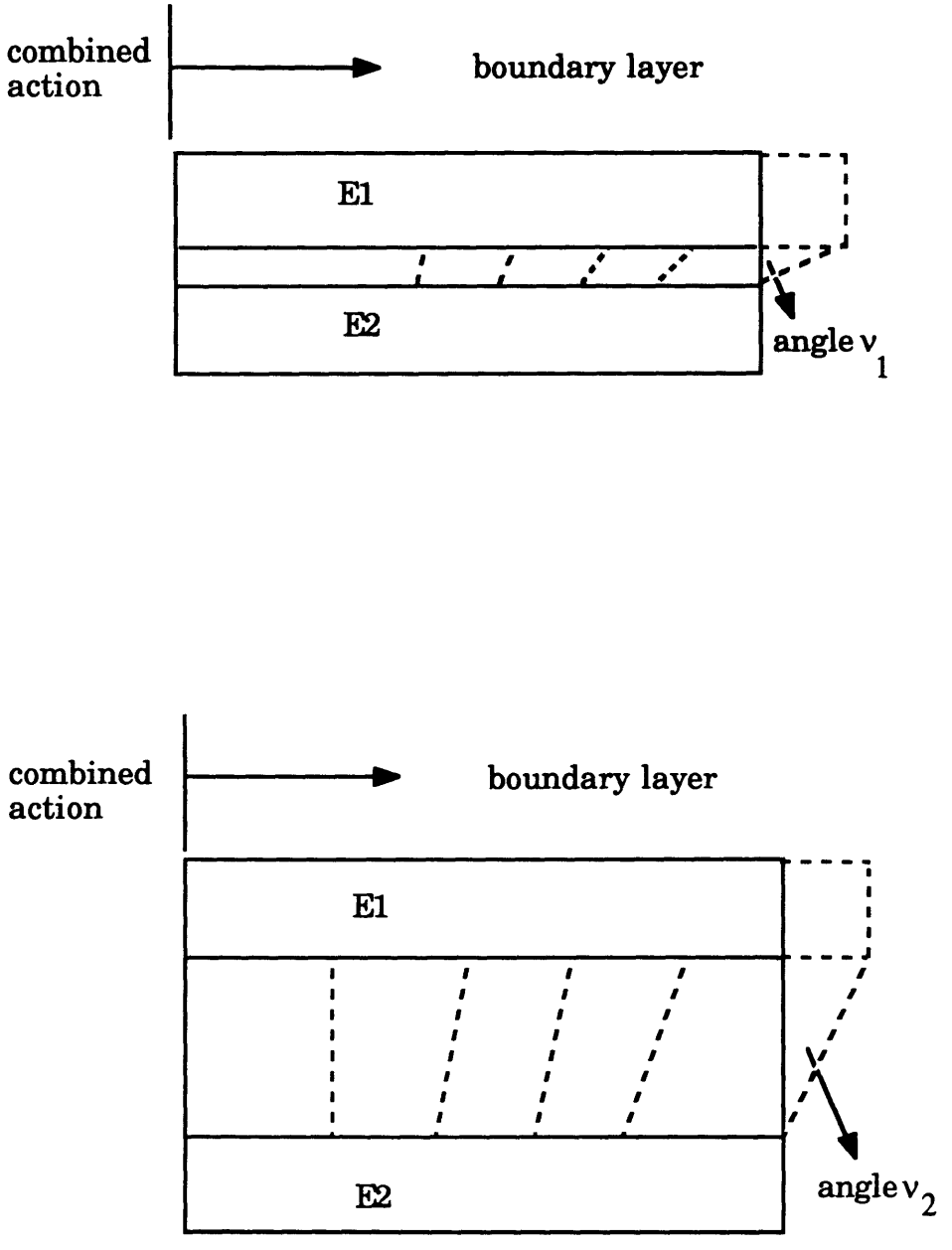

Figure 6.1 One dimensional shear lag model illustrating the effect of shear layer thickness on interlaminar stresses.

are gradually transferred to the adjacent plies by interlaminar shear stresses till the dropped ply eventually loses all its in-plane load at the dropoff. In the present case, the film adhesive is very thin and relatively compliant, and thus does not carry significant in-plane load. Hence, the transfer of in-plane stresses via the interlaminar stresses in the region near the dropoff, does not lead to significant interlaminar stresses. Thus, the interference of these dropoff interlaminar stresses with the free edge interlaminar stresses is not a critical factor in the behavior of these specimens in terms of the delamination occuring at the dropoff region. This is borne out by the fact that the specimens with 3 mm, 6 mm and 9 mm wide strips, which have varying degrees of interference between the free edge and dropoff interlaminar stresses, do not exhibit any experimentally-important difference in their delamination initiation stresses. Thus, the strip width, at least up to experimentally-manufacturable widths, is not a critical factor in the behavior of these specimens.

The analytical results for the interlaminar stresses at the dropoff using the software package DOSE seem to agree with the above arguments as the interlaminar stresses at the free edge are almost an order of magnitude higher than at the dropoff. Thus, taken by themselves, the interlaminar stresses at the dropoff in the present case are not significant. However, in the case of the specimens with 3 mm and 6 mm wide strips, the termination point of the film adhesive strips which fall well within the boundary layer region of the free edge. There could thus be an interaction of the two stresses leading to a more complicated stress state. The model does not explicitly account for such cases of interference. However, a general idea of the magnitude of such stresses can be obtained by using linear superposition of the free edge and dropoff interlaminar stresses to determine the final stress state. It can be seen

from Figures 5.17 through 5.28, discussed earlier in section 5.2, that in the case of 3 mm and 6 mm wide strips, even a linear addition of the free edge and dropoff interlaminar stresses results in stresses at the dropoff which are lower by about an order of magnitude than the stresses at the free edge. Thus, in the present specimens tested, the effects of the stresses at the dropoff can be concluded to be minimal and the delamination behavior of the specimen is still determined by the interlaminar stresses at the free edge.

If the fracture stresses of the various specimens are compared to the in-plane fracture stress as predicted by the Tsai-Wu criterion, it is seen that even in the case of the specimens with film adhesive, this stress is not achieved. Weems [32] has shown that the ability of the film adhesive to suppress delamination is dependent on the thickness of the film adhesive layer. It could be reasoned, therefore, that in the present case the film adhesive thickness used is capable of only delaying delamination, but a thicker film adhesive layer may lead to the delay of the delamination initiation load past the predicted in-plane failure load of the specimen, which would imply that the specimen would then exhibit in-plane failure alone. In the case where film adhesive strips are used however, the increase in the thickness of the strip has further ramifications. A thicker strip would imply higher interlaminar stresses at the dropoff and if these stresses tend to be comparable in magnitude to the free edge stresses, then there may result a difference in the behavior of the specimens with different strips of film adhesive due to their varying levels of interference between the free edge and dropoff interlaminar stresses. Even in cases where the dropoff occurs outside the boundary layer region of the free edge, there would arise the need to examine the possibility of the delamination initiating at the dropoff region.

Thus, delamination suppression is possible with the efficient use of film adhesive strips as shown by the results of the present investigation. If this study were to be considered from the practical manufacturing view point, then the advantages that can be obtained are the weight savings associated with the efficient use of the film adhesive. It, however, becomes labor intensive to manufacture strip widths of very small sizes and also locate them accurately on the specimen. Therefore, for manufacturing purposes, this study is to be used as a method of finding the minimum characteristics of the strip to be used, in terms of the thickness, the width of the strip, and the material to be used, in order that the delamination is suppressed up to the desired load. The analysis can also be used to ensure that with the size of the strip used, interference of the interlaminar stresses at the dropoff with the interlaminar stresses at the free edge does not occur. Once this case of the critical size is determined, it can be used as a lower limit, and film adhesive strips of sizes greater than this can be used as per the dictates of manufacturing cost minimization. This would ensure that the laminates being built are capable of suppressing delamination up to the desired load in as cost effective a manner as possible.

In the event that the strip size considered is thick as compared to nominal ply thickness, then there are other problems introduced into the manufacturing procedure. The laminate would now exhibit significant bumps, and hence a special cure set up with machined top plates would be required to accomodate the shape of the specimen. During the flow stage of the manufacture, special care may be required to prevent the film adhesive from flowing out of the laminate due to the external pressure applied, this would be a problem more to be encountered if the film adhesive is restricted to the form of strips at the free edge of the specimen.

6.2 Specimens with Delamination Implants

Specimens with film adhesive interlayers failed with delamination as one of the modes of final failure, along with fiber breakage. The average values of the delamination initiation load and fracture stresses for the various specimens shown earlier in Table 5.6 indicate that the specimens were intact in most cases almost up to the point of final failure. This seems to indicate that once delamination had initiated within the specimen, it would grow through the specimen almost immediately, thus indicating that the delamination initiation and final failure of the specimen occur close to each other. The film adhesive therefore seems to be capable of suppressing the initiation of delamination, but does not seem to be have much affect on the growth of the same.

The second set of experiments were performed to study the effect of film adhesive on the growth of pre-existing delaminations within specimens which have full plies of film adhesive at the +15°/-15° interface. These specimens had teflon implants in them at the free edge at the +15°/FA interface to simulate delamination.

The results from these specimens indicate that once delamination has initiated, the film adhesive is not capable of suppressing the growth of the specimen. The specimens with 6 mm and 9 mm wide delamination implants exhibit behavior similar to that of the control specimens, seemingly ignoring the presence of the full width of film adhesive layer within them. There is, however, the discrepency in the behavior of the specimens with 3 mm wide teflon implants, which exhibit behavior more similar to the specimens with

full plies of film adhesive. This indicates that these specimens do not appear to recognize the presence of the implanted delamination.

Brewer [42] has shown that the growth of the delamination, though energetically feasible, cannot occur without the presence of the delamination, initiation. It has been shown [42] that in the case of the $[+15_7/-15_7/0_7]_s$ laminate, the growth of the delamination is feasible at a certain stage in its loading spectrum, but does not occur because the delamination initiation has not occurred. The results in the present case can be looked at from the same view point, and the specimens with 6 mm and 9 mm wide teflon implants behave as pre-existing delamination initiations and so the growth and subsequent failure of the specimens occur when the specimen reaches a load which is energitically feasible for delamination growth.

In the case of the specimens with 3 mm wide teflon strip implants, however, the 3 mm wide implanted delamination is not regarded as a delamination initiation by the specimen. A possible explanation is that when any undamaged specimen is tested, it exhibits a delamination initiation of a certain critical size at the delamination initiation load. This is known as a "pop-in" delamination. Any preinitiated delamination of size smaller than this critical size is not considered as an initiation by the laminate, and hence the growth of such a preinitiated delamination will not occur, and the specimen will continue to get loaded until the "pop-in" delamination initiation actually occurs and only subsequently does the growth take place. Hence, the specimens with 3 mm wide teflon strips reach a higher load than the other specimens with wider teflon implants, and thus exhibit behavior closer to that of specimens with full plies of film adhesive without any delamination.

The presence of the film adhesive at a delamination critical interface thus seems to serve the purpose of suppressing the delamination initiation in

the specimen, irrespective of whether it is present in the form of strips at the edge of the specimen or as an entire ply. The film adhesive, however, is incapable of suppressing the growth of the delamination once the delamination has initiated within the specimen.

6.3 Evaluation and Limitations of the Analysis

The analysis is aimed at providing a quick estimate of the stresses arising in the dropoff region. It forms a useful preliminary design tool wherein laminates with dropoffs, can be quickly evaluated to examine the state of the interlaminar stresses at dropoffs. This should help evaluate several laminate layups, with different plies dropped off, in order to find the case with low interlaminar stresses at the dropoff. Since the material properties and the laminate layup are the only input requirements, the software can be used to evaluate several laminates rapidly.

The analysis is based on a simplified model assumed for the ply dropoff problem. This model ignores the 'dropoff region' itself and matches the stresses in the region before and after the dropoff, as shown in Figure 4.3. One of the limitations of this model is that the plies above the dropped region in reality curve down as shown in Figure 4.3. Thus, this curvature of the plies gives rise to interlaminar stresses. Since the current model for the dropoff stresses does not consider the dropoff region, it does not take into account these interlaminar stresses. Thus, the interlaminar stresses arising from the geometry of the dropoff region could interfere with the presently calculated interlaminar stresses to give a different stress state. Also, if the dropoff region is considered, then the dropped ply gradually tapers in the dropoff region during which also it transfers the in-plane stresses that it carries, into the

neighboring plies by interlaminar stresses. This however is extremely complicated to model and the present model is simplified in this respect.

Another limitation of the present problem model is that the model cannot take into consideration the interaction between the free edge interlaminar stresses and the dropoff interlaminar stresses and hence, in the case of the dropoff being within the free edge boundary layer, a linear superposition is all that can be effected to give the overall stress state at the dropoff. The actual interaction behavior would, on the other hand, be more complex in its behavior. In most cases, however, it is seen that the region of influence of the interlaminar stresses at the dropoff is extremely small and such interferences are unlikely to occur.

This analysis is a generalized analysis which allows the evaluation of a large number of laminates in a rapid manner in order to eliminate the configurations with high interlaminar stresses. This can be applied not only to the case of the film adhesive strips being dropped off, but also to cases where actual load-carrying plies of a laminate are dropped off.

The analysis can also be extended to cases wherein the dropoff of the ply occurs in a direction normal to the loading direction, unlike the present case of the film adhesive strip where the dropoff edge is parallel to the loading direction. Some of the alterations to be effected in the analysis would be that the stresses σ_{11}, σ_{12} and σ_{1z} would have to be matched between the regions A and B instead of the currently matched σ_{22}, σ_{12}, and σ_{1z}. In the present analysis the problem was essentially reduced to a two-dimensional problem in the x_2 and z direction. But in the case of the dropoff being normal to the loading direction (x_1), the problem will have to be reduced into a two-dimensional one in the x_1 and z direction.

CHAPTER 7

CONCLUSIONS AND RECOMMENDATIONS

Film adhesive layers were cocured at the delamination critical interface, +15°/-15°, of the $[\pm 15_7/0_7]_s$ laminate. Film adhesive strips were used to examine efficient usage of the film adhesive in suppressing delamination. An analysis was developed, on the basis of a simplified model, to determine the interlaminar stresses at the termination of the film adhesive strip. Furthermore, delamination implants were inserted in specimens with film adhesive to examine whether the film adhesive was capable of suppressing delamination growth, in the case of a preinitiated delamination. Based on the work presented herein, the following conclusions are drawn:

1. Placement of the film adhesive at a delamination critical interface is seen to delay delamination initiation in the laminate as effectively as film adhesive placed at all interfaces of the laminate.

2. Film adhesive strips placed at the free edge of the laminate are seen to be as successful in delaying delamination as entire plies of film adhesive.

3. The width of the film adhesive strips, at least up to manufacturable widths, did not have any effect on the delamination behavior of the specimens, with all the tested widths being equally successful in delaying delamination.

4. The presence of the film adhesive increases the fracture stress of the specimens considerably over that of the control specimens, however, the

fracture stress does not exhibit any marked difference between specimens with various widths of film adhesive.

5. The analysis of the interlaminar stresses at the film adhesive dropoff location indicates that these stresses are about an order of magnitude smaller than the interlaminar stresses at the free edge of the laminate.

6. The interaction between the dropoff interlaminar stresses and the free edge interlaminar stresses when the boundary layers of the two interfere, do not lead to any significant change and this is reflected by the similarity in the behavior of the specimens with various widths of film adhesive.

7. The change in the in-plane load carried by the plies at the dropoff is not significant enough to cause any difference in the in-plane failure load of the specimen.

8. The cocured film adhesive layer is not capable of delaying the growth of delamination in a specimen, once initiation has occurred.

9. There appears to be a critical delamination initiation size which must exist before any growth of the delamination can occur.

The present work thus indicates success in the efficient use of film adhesive in the form of strips to curtail delamination initiation at the free edge of a composite laminate. However, work needs to be done to further examine the ramifications of the various parameters such as the film adhesive thickness of the strips and various laminate types in determining the behavior

of the film adhesive strips more completely. Hence, the following recommendations are offered:

1. A study to examine the effects of film adhesive strips of various thicknesses should be carried out.

2. A study of the growth of the delamination crack should be made to compare the delamination growth behavior in specimens with and without film adhesives.

3. A study should be conducted to examine the possible existence of a "critical" delamination size as a prerequisite for growth of the delamination.

4. Since delamination is an important damage mode around holes, the effectiveness of film adhesive in delaying delamination and its effects on the final failure in laminates with holes should be studied.

5. The possiblity of the use of film adhesive for suppressing delamination initiation in composites under cyclic loading should be investigated.

6. The capability of the analysis in conjunction with the Quadratic Delamination Criterion to predict delamination initiation at a dropoff region should be studied.

7. The analysis should be extended to the case where the dropoff occurs perpendicular to the loading direction.

REFERENCES

1. Lagace, P.A., "Delamination Fracture Under Tensile Loading," *Proceedings of the Sixth Conference on Fibrous Composites in Structural Design*, AMMRC-MS-83-2, Army Materials and Mechanics Research Center, 1983.

2. Jackson, A.C., "Testing of the L-1011 Advanced Composite Vertical Fin," *Proceedings of the Sixth Conference on Fibrous Composites in Structural Design*, AMMRC-MS-83-2, Army Materials and Mechanics research Center, 1983.

3. Chan, W.S., Rogers, C., Cronkite, J.D., and Martin, J., "Delamination Control of Composite Rotor Hubs," presented at the 40th Annual Forum of the American Helicopter Society, Arlington, VA, 16-18 May, 1984.

4. Pipes, B.R., and Pagano, N.J., "Interlaminar Stresses in Composite Materials Under Uniform Axial Extension," *Journal of Composite Materials*, *4*, 1970.

5. Pagano, N.J., and Soni, S.R., "Global-Local Variational Model," *International Journal of Solids and Structures*, *19*, 1983.

6. Wang., A.S.D.,and Crossman, F.W., "Some New Results on Edge Effects in Symmetric Composite Laminates," *Journal of Composite Materials*, *11*, 1977.

7. Rybicki, E.F., "Approximate Three Dimensional Solutions for Symmetric Laminates Under In-Plane Loading," *Journal of Composite Materials*, *5*, 1971.

8. Stanton, E.L., Crain, M., and Neu, T.F., "A Parametric Cubic Modelling System for General Solids of Composite Material," *Int. J of Numerical Methods in Engineering, 11*, 1977.

9. Hsu, P.W., and Herakovich, C.T., "Edge Effects in Angle Ply Composite Laminates," *Journal of Composite Materials, 11*, 1977.

10. Whitcomb, J.D., Raju, I.S., and Goree, J.G., "Reliability of the Finite Element Method for Calculation of Free Edge Stresses in Composite Laminates," *Computers and Structures, 15*, 1982.

11. Wang, S.S., and Choi, I., "Boundary-Layer Effects in Composite Laminates: Part 1 - Free-Edge Stress Singularities," *Journal of Applied Mechanics, 49*, 1982.

12. Wang, S.S., and Choi, I., "Boundary-Layer Effects in Composite Laminates: Part 2 - Free-Edge Solutions and Basic Characteristics," *Journal of Applied Mechanics, 49*, 1982.

13. Kassapoglou, C., and Lagace, P.A., "An Efficient Method for the Calculation of Interlaminar Stresses in Composite Materials," *Journal of Applied Mechanics, 53,* 1986.

14. Saeger, K., and Lagace, P.A., "The Reduced Eigenfunction Solution Technique for the Solution of Interlaminar Stresses for a Straight Free Edges," TELAC Report No.88-8, Massachusetts Institute of Technology, June 1988

15. O'Brien, T.K., "Characteristics of Delamination Onset and Growth in a Composite Laminate," *Damage in Composite Materials, ASTM STP 775,* American Society for Testing and Materials, 1982.

16. O'Brien, T.K., "Analysis of Local delaminations and Their Influence on Composite Laminate Behavior," *Delamination and Debonding of Materials, ASTM STP 876*, American Society for Testing and Materials, 1985.

17. Wang, A.S., Crossman, F.W., and Law, G.E. Jr., "Interlaminar Failure in Epoxy Based Composite Laminates," *Proceedings of the the 29th MFPG Symposium on Advance Composite-Design and Applications*, National Bureau of Standards, Washington, DC, 1979

18. Rybicki, E.F., Schmueser, D.W., and Fox, J., "An Energy Release Rate Approach for Stable Crack Growth in the Free Edge Delamination Problem," *Journal of Composite Materials, 11*, 1977.

19. Kim, R.Y., and Soni, S.R., "Experimental and Analytical Studies on the Onset of Delamination in Laminated Composites", *Journal of Composite Materials, 18*, 1984.

20. Brewer, J.C., and Lagace, P.A., "Quadratic Stress Criterion for Initiation of Free Edge Delamination", *Journal of Composites, 22*, 1988.

21. Mignery, L.A., Tan, T.M., and Sun, C.T., " The Use of Stitching to Suppress Delamination in Laminated Composites", *Delamination and Debonding, ASTM STP 876,* American Society for Testing and Materials, 1985.

22. Kim, R.Y., " A Technique for Prevention of Delamination", *Proceedings of the Seventh Annual Mechanics of Composites Review*, AFWAL-TR-82-4007, Air Force Wright Aeronautical Laboratories, 1982.

23. Herakovich, C.T., "Influence of Layer Thickness on the Strength of Angle-Ply Laminates", *Journal of Composite Materials, 16*, 1982.

24. Lagace, P.A., Brewer, J.C., and Kassapoglou, C., "The Effect of Thickness on Interlaminar Stresses and Delamination", *Journal of Composite Technology and Research, 9*, 1987

25. Herakovich, C.T., "On the Relationship Between Engineering Properties and Delamination of Composite Materials", *Journal of Composite Materials, 15,* 1981.

26. Lagace, P.A., Weems, D.B., and Brewer, J.C., "Suppression of Delamination via an Interply Adhesive Layer", Presented at the 3rd Japan-U.S. Conference on Composite Materials, Tokyo, Japan, June 1986.

27. Chan, W.S., Rogers, C., and Aker, S., "Improvements of Edge Delamination Strength of Composite Laminates using Adhesive Layers", *Testing and Design, ASTM STP 893*, American Society for Testing and Materials, 1984.

28. Chan, W.S., "Delamination Arrester - An Adhesive Inner Layer in Laminated Composite Laminates", *Composite Materials: Fatigue and Fracture, ASTM STP 907*, American Society for Testing and Materials, 1984.

29. Vizzini, A.J., "Prevention of Free Edge Delamination via Edge Alteration", *Proceedings of 29th Structures, Structural Dynamics and Materials Conference*, Part 1, Williamsburg,Va., pp. 365-370.

30. Chan, W.S. and Ochoa, O.O., "Suppression of Edge Delamination in Composite Laminates by Terminating a Critical Ply Near the Edges," *Proceedings of 29th Structures, Structural Dynamics and Materials Conference*, Part 1, Williamsburg,Va., pp. 359-364.

31. Masters, J.E., Courter, J.L. and Evans R.B., "Impact Fracture and Failure Suppression using Interleafed Composites," *Material Science for the Future, 31st International SAMPE Symposium, April 8-10, 1986,* Society for the Advancement of Material and Process Engineering,

32. Weems, D.B., "The Effect of Thick Interlaminar Shear Layers on the Behavior of Graphite/Epoxy Laminates," TELAC Report 87-4, Department of Aeronautics and Astronautics, Massachusetts Institute of Technology, February 1987.

33. Kassapoglou, C., "Interlaminar Stresses at Straight Free Edges of Composite Laminates," TELAC Report 84-18, Department of Aeronautics and Astronautics, Massachusetts Institute of Technology, October 1984.

34. Lagace, P.A., and Brewer, J.C., "TELAC Manufacturing Course Notes," TELAC Report 81-14, Massachusetts Institute of Technology, September 1981.

35. Kemp, B.L., and Johnson, E.R., "Response and Failure Analysis of a Graphite Epoxy Laminate Containing Terminating Internal Plies", *Proceedings of the AIAA/ASME/ASCE/AHS 26th Structures, Structural Dynamics and Materials Conference*, Part 1, Orlando, Florida, April 15-17, 1985, pp. 13-24.

36. Adams, D.F., Ramkumar, R.L., and Walrath, D.E., "Analysis of Porous Laminates in the presence of Ply Dropoff's and Fastener Holes", Northrop Technical Report NOR 84-113, and University of Wyoming, Laramie, Wyoming, May '84.

37. Curry, J.M., Johnson, E.R., and Starnes, J.H., Jr., "Effect of Ply Dropoff's on the Strength of Graphite Epoxy Laminates",*Proceedings of the AIAA/ASME/ASCE/AHS 28th Structures, Structural Dynamics and Materials Conference*, Part 1, Monterey, California, April 6-8, 1987, pp. 737-747.

38. Fish, J.C., "Tensile Strength of Composite Structures with Internal Ply Drops and Free-Edge Effects," University of Maryland, College Park, Department of Aerospace Engineering, Ph.D. Thesis, April 1988.

39. Saeger, K.J., "An Efficient Semi-Analytic Method for the Calculation of Interlaminar Stress around Holes," TELAC Report 89-11, Department of Aeronautics and Astronautics, Massachusetts Institute of Technology, August 1989.

40. Lagace, P.A., and Weems, D.B., "A Through-the-thickness Strength Specimen for Composites", *Test Methods and Design Allowables for Fibrous Composites, second volume, ASTM STP 1003*, American Society for Testing and Materials, 1986.

41. Tsai, S.W., and Wu, E.M., "A Generalized Theory of Strength for Anisotropic Materials," *Journal of Composite Materials, 5*, 1971.

42. Brewer, J.C., "Failure of Graphite/Epoxy Induced by Delamination," TELAC Report 88-6, Department of Aeronautics and Astronautics, Massachusetts Institute of Technology, May 1988.

APPENDIX A

FORTRAN SOURCE CODES

The software package called the Dropoff Stress Evaluator (DOSE) was used to calculate the interlaminar stresses. It consists of two programs which are contained in this appendix. The first program is DROPOFF.FOR, which evaluates the eigenvalues and eigenvectors required in the calculation of the interlaminar stresses at the dropoff for any given laminate. The next stage is to run the program PPRO.FOR - a postprocessing program, which uses the results from DROPOFF.FOR to provide the interlaminar stresses at any given interface in the laminate. Certain routines from standard packages like LINPACK.FOR and EISPACK.FOR have been used in DROPOFF.FOR.

There are only two input files required for running the program DROPOFF.FOR. The first is the material data, which is to be input into the file MATDAT.DAT. The second is the data for the laminate being evaluated, which should include the angle of each ply, the material of each ply and the Classical Laminated Plate theory stresses, σ_{22} and σ_{12} in each ply. The exact format in which these are to be input has been described in the comment statements in program DROPOFF.FOR.

```
CCCCCCCCCCCCCCCCCCCCCCCCCCCCCCCCCCCCCCCCCCCCCCCCCCCCCCCCCCCCCCCCCCCCCCCCCCCC
                  DROPOFF STRESS EVALUATOR  [DOSE]
                                  by
                              Narendra V.Bhat
CCCCCCCCCCCCCCCCCCCCCCCCCCCCCCCCCCCCCCCCCCCCCCCCCCCCCCCCCCCCCCCCCCCCCCCCCCCC
```



```
CCCCCCCCCCCCCCCCCCCCCCCCCCCCCCCCCCCCCCCCCCCCCCCCCCCCCCCCCCCCCCCCCCCCCCCCCCCC
C               PROGRAM  :   DROPOFF.FOR
CCCCCCCCCCCCCCCCCCCCCCCCCCCCCCCCCCCCCCCCCCCCCCCCCCCCCCCCCCCCCCCCCCCCCCCCCCCC
c
CCCCCCCCCCCCCCCCCCCCCCCCCCCCCCCCCCCCCCCCCCCCCCCCCCCCCCCCCCCCCCCCCCCCCCCCCCCC
C       This program is a formulation to calculate the interlaminar
C       stresses at the ply dropoff regions.
C       This is based on a simplified analysis.
c_______________________________________________________________________
C       matrices:
C       ANGA: The angle of the plies of the laminate BEFORE DROPOFF
C       ANGB: The angle of the plies of the laminate AFTER DROPOFF
C       H   : The heights of the various plies of the laminate
C       E   : This matrix consists of the elastic modulii of the matl.
C       SPA : This represents the material properties S* BEFORE DROPOFF
C       SPB : This represents the material properties S* AFTER DROPOFF
C       UL  : This is an matrix of constants used in calculting
C             SM.........
C       SM  : The only submatrix making up the matrix A
C                                 SM | 0
C                        [A]  =  ------
C                                 0  | 0
C       SN,SO,SQ,ST : The submatrices making up the matrix B
C                                 SN | SO
c                        [B]  =  ------
C                                 SQ | ST
C       SR,SS,SU,SV : The submatrices making up the matrix C
C                                 SR | SS
C                        [C]  =  ------
C                                 SU | SV
C       A   : The co-effecient matrix of the variable {F''''}
C       B   : The co-effecient matrix of the variable {F''}
```

```
C       C   : The co-effecient matrix of the variable {F}
C       ALPHA : This is the matrix that  enters into
C               the eigen value problem (see EQUATIONS)
C                                B | A
C             [ ALPHA ]    =    -----
C                                A | 0
C       BETA  :  This is the matrix that enters into the eigen-
C                value problem (see EQUATIONS)
C                              -C | 0
C             [ BETA  ]    =    -----
C                                0 | A
C
C       WORK1,WORK2,IPVT : These are matrices reqd. by DGEDI &DGECO
C                          in LINPAK for inversion purposes.
c
C       THE EQUATIONS  :
C                        here {F} implies { F }
C                                         { G }
c
C               [ A ]{ F'''' } +[ B ]{ F'' }+[ C ]{ F } = {0} ----(1)
c
C               [ ALPHA ] {F''  }   =  [ BETA ] {F  }
C                         {F'''' }             {F'' }        ----(2)
c
c
CCCCCCCCCCCCCCCCCCCCCCCCCCCCCCCCCCCCCCCCCCCCCCCCCCCCCCCCCCCCCCCCCCCCCCCCCCCCCCC
c
        IMPLICIT DOUBLE PRECISION (A-H,O-Z)
        DIMENSION  E(2,6),SPA(20,20),SPB(20,20),ANGA(20),ANGB(20)
        DIMENSION  HA(20),HB(20),UL(20,20),MATA(20),MATB(20)
        DIMENSION  A(40,40),B(40,40),C(40,40),ALPHA(80,80)
        DIMENSION  BETA(80,80),DET(2)
        DIMENSION IPVTA(9),IPVTB(6),WORKA(9),WORKB(6)
        REAL*8     NU(2,3)
        DIMENSION VR(100,100),VI(100,100),WR(100),WI(100)
        DIMENSION FV1(20),FV2(20),FV3(20),IV1(20),Z(80,80)
        COMPLEX*8 ZTEMP,EA(100),EB(100)
        COMPLEX*8 VFA(0:100,0:100),VFB(0:100,0:100)
        COMPLEX*8 VGA(0:100,0:100),VGB(0:100,0:100)
        COMPLEX*8 CBCON(100,100),ZIE(100,100),SIG1(20,2),SIG2(20,2)
        COMPLEX*8 ZVA(50,50),ZVB(50,50)
c
CCCCCCCCCCCCCCCCCCCCCCCCCCCCCCCCCCCCCCCCCCCCCCCCCCCCCCCCCCCCCCCCCCCCCCCCCCCCCCC
C       CONTENTS OF THE VARIOUS FILES :
C
C       MATDAT.DAT : This contains the material data in the form of
C                    E's and NU 's
C       LAMDAT.DAT : This contains the data of the laminate used in
C                    the form of ANGLES and thicknesses(H) of
C                    the plies, and the CLPT stresses s22 and s12 in the
C                    following format:
C                    PLY ANGLE, MATERIAL#, THICKNESS, S22, S12
C                    The first line of LAMDAT.DAT should contain the
```

```
C                    number of plies in the laminate.
C       OUTPUT.DAT : This contains the eigenvalues and eigenvectors for
C                    region A and region B.
CCCCCCCCCCCCCCCCCCCCCCCCCCCCCCCCCCCCCCCCCCCCCCCCCCCCCCCCCCCCCCCCCCCCCCCCCC
        COMMON  E,NU,NPL
        OPEN (UNIT=1,FILE='MATDAT.DAT',STATUS='OLD')
        OPEN (UNIT=2,FILE='LAMDAT.DAT',STATUS='OLD')
        OPEN (UNIT=3,FILE='OUTPUT.DAT',STATUS='OLD')
        OPEN (UNIT=4,FILE='OUT2.DAT',STATUS='NEW')

        DTR=(ATAN(1.))*4./180.
CCCCCCCCCCCCCCCCCCCCCCCCCCCCCCCCCCCCCCCCCCCCCCCCCCCCCCCCCCCCCCCCCCCCCCCCCC
C       READING INPUT DATA FROM FILE MATDAT.DAT
CCCCCCCCCCCCCCCCCCCCCCCCCCCCCCCCCCCCCCCCCCCCCCCCCCCCCCCCCCCCCCCCCCCCCCCCCC
        do 10   i=1,2
        do 10   j=1,9
        if (j.le.6) then
        READ(1,*) E(I,J)
        else
        READ(1,*) NU(I,J-6)
        endif
 10     continue
        READ(2,*) NPLIES,IDRP
        DO 50 IREG=1,2
        DATA A,B,C,ALPHA,BETA,VFA,VFB,VGA,VGB/58404*0./
          IF(IREG.EQ.1) THEN
           NPL=NPLIES
          ELSE
           NPL=NPLIES-1
          ENDIF

CCCCCCCCCCCCCCCCCCCCCCCCCCCCCCCCCCCCCCCCCCCCCCCCCCCCCCCCCCCCCCCCCCCCCCCCCC
C       READING INPUT DATA FROM FILE LAMDAT.DAT
CCCCCCCCCCCCCCCCCCCCCCCCCCCCCCCCCCCCCCCCCCCCCCCCCCCCCCCCCCCCCCCCCCCCCCCCCC
C
        DO 200  J=1,NPL
C
        IF (IREG.EQ.1) THEN
        READ(2,*) ANGA(J),MATA(J),HA(J),SIG1(J,1),SIG1(J,2)
        ANGA(J)=ANGA(J)*DTR
        ELSE
        READ(2,*) ANGB(J),MATB(J),HB(J),SIG2(J,1),SIG2(J,2)
        ANGB(J)=ANGB(J)*DTR
        ENDIF
C
  200   CONTINUE

CCCCCCCCCCCCCCCCCCCCCCCCCCCCCCCCCCCCCCCCCCCCCCCCCCCCCCCCCCCCCCCCCCCCCCCCCC
C       CERTAIN CONSTANTS WHICH ARE TO BE USED REPEATEDLY ARE DEFINED
CCCCCCCCCCCCCCCCCCCCCCCCCCCCCCCCCCCCCCCCCCCCCCCCCCCCCCCCCCCCCCCCCCCCCCCCCC
C
        NPL2=2*NPL
        NPL3=3*NPL
```

```
      NM1=NPL-1
      NM12=NM1*2
      NM13=NM1*3
      I6N9=6*NPLIES-9
      I9N9=9*NPLIES-9

CCCCCCCCCCCCCCCCCCCCCCCCCCCCCCCCCCCCCCCCCCCCCCCCCCCCCCCCCCCCCCCCCCCCCCCCC
C     DESCRIPTIONS OF THE VARIOUS SUBROUTINES DEVELOPED FOR DOSE.FOR
CCCCCCCCCCCCCCCCCCCCCCCCCCCCCCCCCCCCCCCCCCCCCCCCCCCCCCCCCCCCCCCCCCCCCCCCC
C
C     CONMTL --> calculates the material properties SP
C     CONUL  --> calculates the intermediate constants UL
C     MAKABC --> creates the matrices [A],[B],[C],[ALPHA],[BETA]
C                & it makes use of the subroutine CONMNQ.
C     CONMNQ --> calculates the matrices SM,SN.....
C     BC -------> this subroutine uses the boundary conditions to obtain
C                 the constants associated with the solutions.  It is called
C                 on only after the eigenvectors and eigenvalues have been
C                 calculated.
CCCCCCCCCCCCCCCCCCCCCCCCCCCCCCCCCCCCCCCCCCCCCCCCCCCCCCCCCCCCCCCCCCCCCCCCC

      IF (IREG.EQ.1) THEN
      CALL CONMTL(ANGA,MATA,SPA)
      CALL CONUL(SPA,HA,UL,NPL)
      CALL MAKABC(UL,NPL,HA,ALPHA,BETA,A,B,C)
      ELSE
      CALL CONMTL(ANGB,MATB,SPB)
      CALL CONUL(SPB,HB,UL,NPL)
      CALL MAKABC(UL,NPL,HB,ALPHA,BETA,A,B,C)
      ENDIF

CCCCCCCCCCCCCCCCCCCCCCCCCCCCCCCCCCCCCCCCCCCCCCCCCCCCCCCCCCCCCCCCCCCCCCCCC
C     THE SUBROUTINES DGECO & DGEDI ARE OBTAINED BY LINKING THIS
C     PROGRAM, DOSE WITH THE SOFTWARE PACKAGE LINPAK.
CCCCCCCCCCCCCCCCCCCCCCCCCCCCCCCCCCCCCCCCCCCCCCCCCCCCCCCCCCCCCCCCCCCCCCCCC
      IF (IREG.EQ.1) THEN
      CALL DGECO(BETA,80,NM13,IPVTA,RCOND,WORKA)
      ELSE
      CALL DGECO(BETA,80,NM13,IPVTB,RCOND,WORKB)
      ENDIF

CCCCCCCCCCCCCCCCCCCCCCCCCCCCCCCCCCCCCCCCCCCCCCCCCCCCCCCCCCCCCCCCCCCCCCCCC
C     THIS WARNING IMPLIES THAT THE MATRIX BETA WHICH IS BEING INVERTED
C     IS SINGULAR
CCCCCCCCCCCCCCCCCCCCCCCCCCCCCCCCCCCCCCCCCCCCCCCCCCCCCCCCCCCCCCCCCCCCCCCCC
      IF ((1+RCOND).EQ.1.0) THEN
      WRITE(5,*)'*****SINGULAR MATRIX*****'
      GOTO 913
      ENDIF
      DO 232 J=1,NM13
      IF (IREG.EQ.1) THEN
      CALL DGESL(BETA,80,NM13,IPVTA,ALPHA(1,J),0)
      ELSE
```

```
      CALL DGESL(BETA,80,NM13,IPVTB,ALPHA(1,J),0)
      ENDIF
 232  CONTINUE

CCCCCCCCCCCCCCCCCCCCCCCCCCCCCCCCCCCCCCCCCCCCCCCCCCCCCCCCCCCCCCCCCCCCCCCCCCC
C     RG IS A SUBROUTINE OBTAINED BY LINKING THE PROGRAM DOSE WITH THE
C     SOFTWARE PACKAGE EISPAK.
CCCCCCCCCCCCCCCCCCCCCCCCCCCCCCCCCCCCCCCCCCCCCCCCCCCCCCCCCCCCCCCCCCCCCCCCCCC

      CALL RG(80,NM13,ALPHA,WR,WI,1,Z,IV1,FV1,IERR)
      WRITE(5,*)' ERROR CODE=',IERR
C
      DO 900  K=1,NM13
C
         IF (IREG.EQ.1) THEN
           EA(K)=CMPLX(WR(K),WI(K))
           EA(K)=1.D0/CSQRT(EA(K))
         ELSE
           EB(K)=CMPLX(WR(K),WI(K))
           EB(K)=1.D0/CSQRT(EB(K))
         ENDIF
C
             IF(WI(K).NE.0.0) GOTO 902
      DO 901  J=1,NM12
C
          IF(IREG.EQ.1) THEN
             IF(J.LE.NM1)THEN
                VFA(J,K)=CMPLX(Z(J,K))
             ELSE
                VGA(J-NM1,K)=CMPLX(Z(J,K))
             ENDIF
          ELSE
             IF(J.LE.NM1)THEN
                VFB(J,K)=CMPLX(Z(J,K))
             ELSE
                VGB(J-NM1,K)=CMPLX(Z(J,K))
             ENDIF
          ENDIF
C
 901  CONTINUE
      GOTO 900
 902          IF(WI(K).LT.0.0) GOTO 904
        DO 903  J=1,NM13
C
          IF(IREG.EQ.1) THEN
             IF(J.LE.NM1)THEN
                VFA(J,K)=CMPLX(Z(J,K),Z(J,K+1))
             ELSE
                VGA(J-NM1,K)=CMPLX(Z(J,K),Z(J,K+1))
             ENDIF
          ELSE
             IF(J.LE.NM1)THEN
                VFB(J,K)=CMPLX(Z(J,K),Z(J,K+1))
```

```
                ELSE
                   VGB(J-NM1,K)=CMPLX(Z(J,K),Z(J,K+1))
                ENDIF
              ENDIF
C
 903    CONTINUE
        GOTO 900
 904      DO 905  J=1,NM13
C
           IF(IREG.EQ.1) THEN
            IF(J.LE.NM1)THEN
             VFA(J,K)=CMPLX(REAL(VFA(J,K-1)),-AIMAG(VFA(J,K-1)))
            ELSE
             VGA(J-NM1,K)=CMPLX(REAL(VGA(J-NM1,K-1))
     1                                  ,-AIMAG(VGA(J-NM1,K-1)))
            ENDIF
           ELSE
            IF(J.LE.NM1)THEN
             VFB(J,K)=CMPLX(REAL(VFB(J,K-1)),-AIMAG(VFB(J,K-1)))
            ELSE
             VGB(J-NM1,K)=CMPLX(REAL(VGB(J-NM1,K-1))
     1                              ,-AIMAG(VGB(J-NM1,K-1)))
            ENDIF
           ENDIF
C
 905    CONTINUE
 900    CONTINUE

CCCCCCCCCCCCCCCCCCCCCCCCCCCCCCCCCCCCCCCCCCCCCCCCCCCCCCCCCCCCCCCCCCCCCCCCCCC
C       THE EIGENVALUES AND EIGENVECTORS ARE OUTPUT INTO THE FILE:
C                        OUTPUT.DAT
CCCCCCCCCCCCCCCCCCCCCCCCCCCCCCCCCCCCCCCCCCCCCCCCCCCCCCCCCCCCCCCCCCCCCCCCCCC
        WRITE(3,*) '    THE  EIGEN VALUES ARE  :-'
        WRITE(3,*)'                             '
C
        DO 910 J=1,NM13
        IF(IREG.EQ.1) THEN
        ZTEMP=EA(J)
        ELSE
        ZTEMP=EB(J)
        ENDIF
C
        WRITE(3,1100)J,WR(J),WI(J),REAL(ZTEMP),AIMAG(ZTEMP)
 1100   FORMAT(1X,I4,'  WR=',E12.6,'  WI=',E12.6,' SQRT =(',E12.6
     &  ,')+i(',E12.6,')')
 910    CONTINUE
C
        WRITE(3,*) '    THE  EIGEN VECTORS ARE  :-'
        WRITE(3,*)'                             '
        WRITE(3,*)'-------REAL PARTS-------'
        DO 920  I=1,NM12
        IF (IREG.EQ.1) THEN
         IF(I.LE.NM1) THEN
```

```
      WRITE(3,1101)I,(REAL(VFA(I,J)),J=1,NM13)
       ELSE
      WRITE(3,1101)I,(REAL(VGA(I-NM1,J)),J=1,NM13)
       ENDIF
      ELSE
       IF(I.LE.NM1) THEN
      WRITE(3,1101)I,(REAL(VFB(I,J)),J=1,NM13)
       ELSE
      WRITE(3,1101)I,(REAL(VGB(I-NM1,J)),J=1,NM13)
       ENDIF
      ENDIF
1101  FORMAT(1X,I4,') ',6(F8.4,' '))
920   CONTINUE
      WRITE(3,*)'                '
      WRITE(3,*)'-------IMAGINARY PARTS-------'
      DO 930  I=1,NM12
      IF (IREG.EQ.1) THEN
       IF(I.LE.NM1) THEN
      WRITE(3,1102)I,(AIMAG(VFA(I,J)),J=1,NM13)
       ELSE
      WRITE(3,1102)I,(AIMAG(VGA(I-NM1,J)),J=1,NM13)
       ENDIF
      ELSE
       IF(I.LE.NM1) THEN
      WRITE(3,1102)I,(AIMAG(VFB(I,J)),J=1,NM13)
       ELSE
      WRITE(3,1102)I,(AIMAG(VGB(I-NM1,J)),J=1,NM13)
       ENDIF
      ENDIF
1102  FORMAT(1X,I4,') ',6(F8.4,' '))
930   CONTINUE
C-----------------------------------------------------------------
50    CONTINUE

CCCCCCCCCCCCCCCCCCCCCCCCCCCCCCCCCCCCCCCCCCCCCCCCCCCCCCCCCCCCCCCCCCCCCCC
C     THE EIGENVALUES AND EIGENVECTORS BEING CALCULATED, NOW THE BOUNDARY
C     CONDITIONS ARE USE, BY CALLING SUBROUTINE BC TO EVALUATE THE CONSTANTS
C     ASSOCIATED WITH THE SOLUTION.
CCCCCCCCCCCCCCCCCCCCCCCCCCCCCCCCCCCCCCCCCCCCCCCCCCCCCCCCCCCCCCCCCCCCCCC
      CALL BC(EA,VFA,VGA,EB,VFB,VGB,SIG1,SIG2,
     1  ZIE,NPLIES,HA,HB,SPA,SPB,IDRP)
C
      WRITE(4,*) NPLIES,IDRP
C
      NM1=(NPLIES-1)
      NM12=2*(NPLIES-1)
      NM13=3*(NPLIES-1)
      itmp=nm13
      DO 1190 I=1,NM12
      DO 1190 J=1,NM13
      IF (I.LE.NM1) THEN
      ZVA(I,J)=VFA(I,J)*ZIE(J,1)
      ELSE
```

```
      ZVA(I,J)=VGA(I-nm1,J)*ZIE(J,1)
      ENDIF
 1190 CONTINUE
C
      DO 1200 I=1,NM13
      WRITE(4,*)I, REAL(EA(I)),AIMAG(EA(I))
 1200 CONTINUE
C
      DO 1205  I=1,NM12
      WRITE(4,*)I,(REAL(ZVA(I,J)),J=1,NM13)
 1205 CONTINUE
      DO 1206  I=1,NM12
      WRITE(4,*)I,(AIMAG(ZVA(I,J)),J=1,NM13)
 1206 CONTINUE
      do 1207 i=1,nplies
      write(4,*) ha(i)
 1207 continue
C
      NM1=(NPLIES-2)
      NM12=2*(NPLIES-2)
      NM13=3*(NPLIES-2)
      DO 1191 I=1,NM12
      DO 1191 J=1,NM13
      IF(I.LE.NM1) THEN
      ZVB(I,J)=VFB(I,J)*ZIE(J+itmp,1)
      ELSE
      ZVB(I,J)=VGB(I-nm1,J)*ZIE(J+itmp,1)
      ENDIF
 1191 CONTINUE
C
      DO 1210 I=1,NM13
      WRITE(4,*)I, REAL(EB(I)),AIMAG(EB(I))
 1210 CONTINUE
      DO 1215  I=1,NM12
      WRITE(4,*)I,(REAL(ZVB(I,J)),J=1,NM13)
 1215 CONTINUE
      DO 1216  I=1,NM12
      WRITE(4,*)I,(AIMAG(ZVB(I,J)),J=1,NM13)
 1216 CONTINUE
c 1103 FORMAT(1X,3I,e12.6,e12.6)
C
      do 1217 i=1,(nplies-1)
      write(4,*) hb(i)
 1217 continue
c
 913  END


CCCCCCCCCCCCCCCCCCCCCCCCCCCCCCCCCCCCCCCCCCCCCCCCCCCCCCCCCCCCCCCCCCCCCCCCCCC
C       THIS SUBROUTINE CALCULATES THE MATERIAL CONSTANTS S* WHICH ARE
C       INDICATED IN THIS PROGRAM BY 'SP'
CCCCCCCCCCCCCCCCCCCCCCCCCCCCCCCCCCCCCCCCCCCCCCCCCCCCCCCCCCCCCCCCCCCCCCCCCCC
```

```
C
      SUBROUTINE CONMTL(ANG,MAT,SP)
      IMPLICIT DOUBLE PRECISION (A-H,O-Z)
      DIMENSION  SP(20,9),ANG(20),MAT(20),S(9),E(2,6)
      REAL*8     NU(2,3)
      COMMON  E,NU,NPL
C
CCCCCCCCCCCCCCCCCCCCCCCCCCCCCCCCCCCCCCCCCCCCCCCCCCCCCCCCCCCCCCCCCCCCCCCCCCC
C     THE EQUIVALENCE BETWEEN THE CONSTANTS USED IN THE ANALYSIS USED
C     IN THE THESIS AND THOSE IN THE PROGRAM ARE AS FOLLOWS:
CCCCCCCCCCCCCCCCCCCCCCCCCCCCCCCCCCCCCCCCCCCCCCCCCCCCCCCCCCCCCCCCCCCCCCCCCCC
c
C     SP(1)=S*2222    S(1)=S1111
C     SP(2)=S*3333    S(2)=S1122
C     SP(3)=S*1212    S(3)=S1133
C     SP(4)=S*1313    S(4)=S2222
C     SP(5)=S*2323    S(5)=S2233
C     SP(6)=S*2233    S(6)=S3333
C     SP(7)=S*2212    S(7)=S4444=S2323
C     SP(8)=S*3312    S(8)=S5555=S1313
C     SP(9)=S*1323    S(9)=S6666=S1212
CCCCCCCCCCCCCCCCCCCCCCCCCCCCCCCCCCCCCCCCCCCCCCCCCCCCCCCCCCCCCCCCCCCCCCCCCCC
C
      DO 100 I=1,NPL
C
      K=MAT(I)
      S(1)=1.D0/E(K,1)
      S(2)=-NU(K,1)/E(K,1)
      S(3)=-NU(K,2)/E(K,1)
      S(4)=1.D0/E(K,2)
      S(5)=-NU(K,3)/E(K,2)
      S(6)=1.D0/E(K,3)
      S(7)=1.D0/E(K,4)
      S(8)=1.D0/E(K,5)
      S(9)=(1.D0/E(K,6))
C
      C1=COS(ANG(I))
      C2=C1*C1
      C3=C2*C1
      C4=C3*C1
      S1=SIN(ANG(I))
      S2=S1*S1
      S3=S2*S1
      S4=S3*S1
      S1111=C4*S(1)+S4*S(4)+2*C2*S2*S(2)+C2*S2*S(9)
      S2222=S4*S(1)+C4*S(4)+2*C2*S2*S(2)+C2*S2*S(9)
      S1122=C2*S2*(S(1)+S(4)-S(9))+(C4+S4)*S(2)
      S1212=C2*S2*(S(1)+S(4)-2*S(2))+
     1      (C4-2*C2*S2+S4)*S(9)/4.D0
      S1112=C3*S1*S(1)-C1*S3*S(4)+(C1*S3-C3*S1)*S(2)+
     1      (C1*S3-C3*S1)*S(9)/2.D0
      S2212=C1*S3*S(1)-C3*S1*S(4)+(C3*S1-C1*S3)*S(2)+
     1      (C3*S1-C1*S3)*S(9)/2.D0
```

```
      S3333=S(6)
      S1133=C2*S(3)+S2*S(5)
      S2233=S2*S(3)+C2*S(5)
      S3312=C1*S1*(S(3)-S(5))
      S1313=(C2*S(8)+S2*S(7))/4.D0
      S2323=(S2*S(8)+C2*S(7))/4.D0
      S1323=C1*S1*(S(8)-S(7))/4.D0
C-----------------------------------------------------------------
      SP(I,1)=S2222-S1122*S1122/S1111
      SP(I,2)=S3333-S1133*S1133/S1111
      SP(I,3)=S1212-S1112*S1112/S1111
      SP(I,4)=S1313
      SP(I,5)=S2323
      SP(I,6)=S2233-S1122*S1133/S1111
      SP(I,7)=S2212-S1122*S1112/S1111
      SP(I,8)=S3312-S1133*S1112/S1111
      SP(I,9)=S1323
C
 100  CONTINUE
C
      RETURN
      END

CCCCCCCCCCCCCCCCCCCCCCCCCCCCCCCCCCCCCCCCCCCCCCCCCCCCCCCCCCCCCCCCCCCCCCC
C     THIS SUBROUTINE CALCULATES THE INTERMEDIATE CONSTANTS AS INDICATED
C     BY 'L' IN THE THESIS
CCCCCCCCCCCCCCCCCCCCCCCCCCCCCCCCCCCCCCCCCCCCCCCCCCCCCCCCCCCCCCCCCCCCCCC
      SUBROUTINE  CONUL(SP,H,UL,NPL)
C
      IMPLICIT DOUBLE PRECISION(A-H,O-Z)
      DIMENSION  SP(20,9),H(20),UL(20,20)
C-----------------------
      DO 100  I=1,NPL
C-----------------------
      UL(I,1)=SP(I,2)*(H(I)**3)/10.D0
      UL(I,2)=SP(I,2)*(H(I)**3)/60.D0
      UL(I,3)=SP(I,2)*(H(I))/3.D0
      W23=2.D0/3.D0
      W43=4.D0/3.D0
      W83=8.D0/3.D0
      UL(I,4)=(SP(I,6)*((H(I))*W23))-(SP(I,5)*((H(I))*W83))
      UL(I,5)=-(SP(I,6)*((H(I))*W23))-(SP(I,5)*((H(I))*W43))
      UL(I,6)=(SP(I,8)*((H(I))*W23))-(SP(I,9)*((H(I))*W83))
      UL(I,7)=-(SP(I,8)*((H(I))*W23))-(SP(I,9)*((H(I))*W43))
      UL(I,8)=2.*SP(I,6)/H(I)
      UL(I,9)=2.*SP(I,1)/H(I)
      UL(I,10)=4.*SP(I,7)/H(I)
      UL(I,11)=SP(I,4)*((H(I))*W43)
      UL(I,12)=SP(I,8)*(4.)/H(I)
      UL(I,13)=SP(I,7)*(4.)/H(I)
      UL(I,14)=SP(I,3)*(8.)/H(I)
      UL(I,15)=SP(I,2)*(2.)/H(I)
C-----------------
```

```
 100    CONTINUE
C-----------------------
        RETURN
        END

CCCCCCCCCCCCCCCCCCCCCCCCCCCCCCCCCCCCCCCCCCCCCCCCCCCCCCCCCCCCCCCCCCCCCCCCCCC
C       THIS SUBROUTINE CALCULATES THE MATRICES SM,SN,.... ETC.
CCCCCCCCCCCCCCCCCCCCCCCCCCCCCCCCCCCCCCCCCCCCCCCCCCCCCCCCCCCCCCCCCCCCCCCCCCC
        SUBROUTINE CONMNQ(UL,NPL,H,SM,SN,SO,SR,SS,SQ,ST,SU,SV)
C
        IMPLICIT DOUBLE PRECISION (A-H,O-Z)
        DIMENSION  UL(20,15),UE(20),SM(20,20),SN(20,20),H(20)
        DIMENSION  ST(20,20),SV(20,20),SO(20,20),SR(20,20)
        DIMENSION  SQ(20,20),SS(20,20),UG(20),SU(20,20)
        DATA UG,UE/40*0.0/
C-----------------------------
        DO 444 IO=1,NPL
        DO 444 IP=1,NPL
C-----------------------------
        SM(IO,IP)=0.0
        SN(IO,IP)=0.0
        ST(IO,IP)=0.0
        SV(IO,IP)=0.0
        SO(IO,IP)=0.0
        SR(IO,IP)=0.0
        SQ(IO,IP)=0.0
        SS(IO,IP)=0.0
        SU(IO,IP)=0.0
C-----------------------------
 444    CONTINUE
C-----------------------------
        UE(NPL)=H(NPL)*0.5
        UG(NPL)=0.0
C
C-----------------------------
        DO 222  K=NPL ,2,-1
C-----------------------------
        K1=K-1
        UG(K1)=UG(K)+UL(K,15)*H(K)*H(K)
        UE(K1)=(H(K1)+H(K))*0.5
C-----------------------------
 222    CONTINUE
C-----------------------------
C-----------------------------
        DO 100 I=1,NPL
        DO 200 J=1,NPL
C-----------------------------
        IM1=I-1
        IP1=I+1
        JP1=J+1
C
        HI1=H(I)**2
        HI2=H(IP1)**2
```

```
      HJ1=H(J)**2
      HJ2=H(JP1)**2
C
      IF (J.LT.IM1) THEN
          SM(I,J)=UE(J)*(UE(I)*UG(I)+UL(I,3)*H(I)-UL(IP1,3)*H(IP1))
          SN(I,J)=UE(J)*(UL(I,8)*H(I)-UL(IP1,8)*H(IP1))
          SO(I,J)=0.
          SR(I,J)=0.
          SS(I,J)=0.
          SQ(I,J)=UE(J)*(UL(I,12)*H(I)-UL(IP1,12)*H(IP1))
          ST(I,J)=0.
          SU(I,J)=0.
          SV(I,J)=0.
      ELSE
           IF(J.EQ.IM1) THEN
               SM(I,J)=UE(J)*(UE(I)*UG(I)+UL(I,3)*H(I)
     1                -UL(IP1,3)*H(IP1))-UL(I,2)
               SN(I,J)=UE(J)*(UL(I,8)*H(I)-UL(IP1,8)*H(IP1))+UL(I,5)
               SO(I,J)=UL(I,7)
               SR(I,J)=-UL(I,9)
               SS(I,J)=-UL(I,10)
               SQ(I,J)=UE(J)*(UL(I,12)*H(I)-UL(IP1,12)*H(IP1))+UL(I,7)
               ST(I,J)=-UL(I,11)
               SU(I,J)=-UL(I,10)
               SV(I,J)=-UL(I,14)
           ELSE
               IF(J.EQ.I) THEN
                  SM(I,J)=UE(I)*(UE(I)*UG(I)
     &                -2*UL(IP1,3)*H(IP1))
     &                +(UL(I,1)+UL(IP1,1))
                  SN(I,J)=UE(J)*(-2*UL(IP1,8)*H(IP1))
     1                        +UL(I,4)+UL(IP1,4)
                  SO(I,J)=-UE(I)*(UL(IP1,12)*H(IP1))
     1                        +UL(I,6)+UL(IP1,6)
                  SR(I,J)=UL(I,9)+UL(IP1,9)
                  SS(I,J)=UL(I,10)+UL(IP1,10)
                  SQ(I,J)=(-UE(J)*UL(IP1,12)*H(IP1))+UL(I,6)+UL(IP1,6)
                  ST(I,J)=-2*(UL(I,11)+UL(IP1,11))
                  SU(I,J)=UL(I,10)+UL(IP1,10)
                  SV(I,J)=UL(I,14)+UL(IP1,14)
               ELSE
                    IF(J.EQ.IP1) THEN
                       SM(I,J)=UE(I)*(UE(J)*UG(J)+UL(J,3)*H(J)
     1                        -UL(JP1,3)*H(JP1))
     1                        -UL(IP1,2)
                       SN(I,J)=UE(I)*(UL(J,8)*H(J)-UL(JP1,8)*H(JP1))
     1                              +UL(IP1,5)
                       SO(I,J)=UE(I)*(UL(J,12)*H(J)-UL(JP1,12)*H(JP1))
     1                        +UL(J,7)
                       SR(I,J)=-UL(IP1,9)
                       SS(I,J)=-UL(IP1,10)
                       SQ(I,J)=UL(IP1,7)
                       ST(I,J)=-UL(IP1,11)
```

```
                        SU(I,J)=-UL(IP1,10)
                        SV(I,J)=-UL(IP1,14)
                      ELSE
                        SM(I,J)=UE(I)*(UE(J)*UG(J)
     1                         +UL(J,3)*H(J)-UL(JP1,3)*H(JP1))
                        SN(I,J)=UE(I)*(UL(J,8)*H(J)-UL(JP1,8)*H(JP1))
                        SO(I,J)=UE(I)*(UL(J,12)*H(J)-UL(JP1,12)*H(JP1))
                        SR(I,J)=0.
                        SS(I,J)=0.
                        SQ(I,J)=0.
                        ST(I,J)=0.
                        SU(I,J)=0.
                        SV(I,J)=0.
                      ENDIF
                   ENDIF
                ENDIF
             ENDIF
C-------------------------
 200    CONTINUE
 100    CONTINUE
C-------------------------
        RETURN
        END

CCCCCCCCCCCCCCCCCCCCCCCCCCCCCCCCCCCCCCCCCCCCCCCCCCCCCCCCCCCCCCCCCCCCCCCCCC
C       THIS SUBROUTINE WRITES THE MATRICES: [A], [B] AND [C]
C       AND THE MATRICES:  [ALPHA],[BETA]
C       THIS MAKES USE OF THE SUBROUTINE CONMNQ
CCCCCCCCCCCCCCCCCCCCCCCCCCCCCCCCCCCCCCCCCCCCCCCCCCCCCCCCCCCCCCCCCCCCCCCCCC
        SUBROUTINE MAKABC(UL,NPL,H,ALPHA,BETA,A,B,C)
c
        IMPLICIT DOUBLE PRECISION (A-H,O-Z)
        DIMENSION A(40,40),B(40,40),C(40,40),ALPHA(80,80),BETA(80,80)
        DIMENSION SM(20,20),SN(20,20),ST(20,20),SV(20,20),UL(20,20)
        DIMENSION SO(20,20),SR(20,20),SQ(20,20),SS(20,20),SU(20,20)
        DIMENSION H(20)
C-------------------------------------------------------------
        CALL CONMNQ(UL,NPL,H,SM,SN,SO,SR,SS,SQ,ST,SU,SV)
C-------------------------------------------------------------
        NPL2=2*NPL
        NPL3=3*NPL
        NM1=NPL-1
        NM12=NM1*2
        NM13=NM1*3
C-------------------------
        DO 300  I=1,NM12
        DO 350  J=1,NM12
C-------------------------
        IMNPL=I-NM1
        JMNPL=J-NM1
C
        IF ((I.LE. NM1).AND.(J.LE.NM1)) THEN
        A(I,J)=(1./(H(1))**5)*SM(I,J)
```

```
        ELSE
        A(I,J)=0.
        ENDIF
C
        IF ((I.LE. NM1).AND.(J.LE.NM1)) THEN
        B(I,J)=(1/(H(1))**3)*SN(I,J)
        ELSE
             IF((I.LE.NM1).AND.(J.GT.NM1)) THEN
             B(I,J)=(1/(H(1))**3)*SO(I,JMNPL)
             ELSE
                  IF((I.GT.NM1).AND.(J.LE.NM1)) THEN
                  B(I,J)=(1/(H(1))**3)*SQ(IMNPL,J)
                  ELSE
                       IF((I.GT.NM1).AND.(J.GT.NM1))THEN
                     B(I,J)=(1/(H(1))**3)*ST(IMNPL,JMNPL)
                       ENDIF
                  ENDIF
             ENDIF
        ENDIF
C
        IF ((I.LE. NM1).AND.(J.LE.NM1)) THEN
        C(I,J)=(1/H(1))*SR(I,J)
        ELSE
             IF((I.LE.NM1).AND.(J.GT.NM1)) THEN
             C(I,J)=(1/H(1))*SS(I,JMNPL)
             ELSE
                  IF((I.GT.NM1).AND.(J.LE.NM1))THEN
                  C(I,J)=(1/H(1))*SU(IMNPL,J)
                  ELSE
                       IF((I.GT.NM1).AND.(J.GT.NM1))THEN
                       C(I,J)=(1/H(1))*SV(IMNPL,JMNPL)
                       ENDIF
                  ENDIF
             ENDIF
        ENDIF
C-------------------------
 350    CONTINUE
 300    CONTINUE
C-------------------------

CCCCCCCCCCCCCCCCCCCCCCCCCCCCCCCCCCCCCCCCCCCCCCCCCCCCCCCCCCCCCCCCCCCCCCCCCCCCCCC
C       WRITING THE MATRICES [ ALPHA ] and [ BETA ] FOR THE CALCULATION
C       OF EIGENVALUES AND EIGENVECTORS
CCCCCCCCCCCCCCCCCCCCCCCCCCCCCCCCCCCCCCCCCCCCCCCCCCCCCCCCCCCCCCCCCCCCCCCCCCCCCCC
C
C-------------------------
        DO 700 IR=1,NM13
        DO 710 IC=1,NM13
C-------------------------
        ICMNP2=IC-NM12
        IRMNP2=IR-NM12
        IF ((IR.LE.NM12).AND.(IC.LE.NM12))THEN
        ALPHA(IR,IC)=B(IR,IC)
```

```
        ELSE
            IF ((IR.LE.NM12).AND.(IC.GT.NM12))THEN
            ALPHA(IR,IC)=A(IR,ICMNP2)
            ELSE
                IF ((IR.GT.NM12).AND.(IC.LE.NM12))THEN
                ALPHA(IR,IC)=A(IRMNP2,IC)
                ELSE
                ALPHA(IR,IC)=0
                ENDIF
            ENDIF
        ENDIF
c
        IF ((IR.LE.NM12).AND.(IC.LE.NM12))THEN
        BETA(IR,IC)=-C(IR,IC)
        ELSE
                IF ((IR.GT.NM12).AND.(IC.GT.NM12))THEN
                BETA(IR,IC)=A(IRMNP2,ICMNP2)
                ELSE
                BETA(IR,IC)=0
                ENDIF
        ENDIF
C-------------------------
  710   CONTINUE
  700   CONTINUE
C-------------------------
        RETURN
        END

CCCCCCCCCCCCCCCCCCCCCCCCCCCCCCCCCCCCCCCCCCCCCCCCCCCCCCCCCCCCCCCCCCCCCCCCCCC
C       THIS SUBROUTINE UTILIZES THE BOUNDARY CONDITIONS TO OBTAIN THE
C       CONSTANTS {a} & {b}.
CCCCCCCCCCCCCCCCCCCCCCCCCCCCCCCCCCCCCCCCCCCCCCCCCCCCCCCCCCCCCCCCCCCCCCCCCCC
        SUBROUTINE  BC(EA,VFA,VGA,EB,VFB,VGB,SIG1,SIG2,
     1  ZIE,NPLIES,HA,HB,SP1,SP2,IDRP)
c
        IMPLICIT DOUBLE PRECISION(A-H,O-Y),COMPLEX (Z)
        COMPLEX*8 VFA(0:100,0:100),EA(100),VFB(0:100,0:100),EB(100)
        COMPLEX*8 VGA(0:100,0:100),VGB(0:100,0:100),DELB(100)
        COMPLEX*8 OMGA(100,100),OMGB(100,100),DELA(100)
        COMPLEX*8 GAMMA(100,100),NETA(100),BCON(100,100)
        COMPLEX*8 cBCON(100,100),cZIE(100,100),ZIE(100,100)
        DIMENSION SIG1(20,2),SIG2(20,2),SP1(20,1),SP2(20,1)
        DIMENSION HA(20),HB(20)
        OPEN (UNIT=8,FILE='OMG.DAT',STATUS='NEW')
        OPEN (UNIT=4,FILE='JUNK.DAT',STATUS='NEW')

CCCCCCCCCCCCCCCCCCCCCCCCCCCCCCCCCCCCCCCCCCCCCCCCCCCCCCCCCCCCCCCCCCCCCCCCCCC
C       SUBROUTINE BC IS MADE UP OF TWO MORE SUBROUTINES viz. BCEQ12 AND
C       BCEQ3.  THE EQUATIONS OBTAINED FROM THESE TWO SUBROUTINES ARE PUT
C       TOGETHER AND SOLVED IN SUBROUTINE BC BY THE USE OF THE GAUSS ELIM-
C       INATION TECHNIQUE FOR SOLVING COMPLEX SIMULTANEOUS EQUATIONS
CCCCCCCCCCCCCCCCCCCCCCCCCCCCCCCCCCCCCCCCCCCCCCCCCCCCCCCCCCCCCCCCCCCCCCCCCCC
C
```

```
C       Subroutine BC :
C       INPUT :
C       EA,EB: The eigen value matrices of the regions A & B resptly.
C       VA,VB: The eigen vector matrices of the regions A & B resptly.
C       SIG1,SIG2 : The CLPT values for the regions A & B respectively
C                   The sigma22 is present in the column 1 and the
C                       sigma12 is present in the coloumn2 of the
C                       matrices SIG*(*,2)
C       HA,HB : These are matrices which contain the thicknesses of
C               the plies in the regions A & B respectively.
C       NPLIES : The number of plies in region A
C       IDRP : This refers to the ply that is dropped off from reg A
C       SP1,SP2 : The matrices which contain the S* values of each individual
C                 ply in the regions A & B respectively. SP*(I,*) is the
C                 general information accessed from these where the 'I' refers
C                 to the ply information.
c
C       OUTPUT :
C
C       BCON : This is the matrix which contains the equations to be solved
C              to obtain the matrix { a b lambda }T
C       ZIE : This is the coloumn vector which forms the RHS of the equation
C              to be solved.
c-------------------------------------------------------------------------
c
C       THEORY :
c
C       EQUATIONS FROM ENERGY MINIMIZATION WITH LAGRANGE MULTIPLIER:
C
C               [omgA]{a} ={delA}
c
C               [omgB]{b} ={delB}
c
C                                T
C               {a  b} [gamma]={0}
C                          __      __    __    __
C                         |    |    |  |      |
C        where            | AA | A  |  | a    |
C               (3n)     -|----|----|- | b    |  = { 0 }
C                         | B  | BB |  | lambda|
C                         |__  |  __|  |_    _|
C                          (3n-3) (3n-6)
C                            ||
C                            ||
C                            \/
C                          GAMMA [3n*(6n-9)]
c-------------------------------------------------------------------------
C          __                                                    __
C         |              |             |             |            |
C         | omgA(3n-3**) |      0      |      AA     |      B     |
C         |              |             |             |            |
C        -|--------------|-------------|-------------|------------|-
C         |              |             |             |            |
```

```
C          |      0       |omgA(3n-6**) |       A      |      BB      |
C          |              |             |              |              |
c [BCON]= -|--------------|-------------|--------------|--------------|-
C          |              |             |              |              |
C          |     AA       |     A       |       0      |      0       |
C          |              |             |              |              |
C         -|---[(3n-2)*(6n-9)]----------|--------------|--------------|-
C          |              |             |              |              |
C          |     B        |     BB      |       0      |      0       |
C          |              |             |              |              |
C          |__            |             |              |           __|
C
C                          BCON is (9n-11)*(9n-11)
c
C          __        __                                 __     __
C          |            |                               |        |
C          |   0 (3n-3) |                               | a(3n-3)|
C          |            |                               |        |
c [ZIE]=   <    0 (3n-6) >          [consts]=            <  b(3n-6) >
C          |            |                               |        |
C          | NETA(3n-2) |                               | lambda |
C          |__        __|                               | (3n)   |
C                                                       |__    __|
C         ZIE and consts are  (9n-11)*(1)
c
C       The equation to be solved is :
C
C                          [ BCON ]{consts} = {ZIE}
c
c-------------------------------------------------------------------------
        I6N9=6*NPLIES-9
        I9N9=9*NPLIES-12+1
        NM13=3*(NPLIES-1)
        NM23=3*(NPLIES-2)
C
        CALL BCEQ12(1,SP1,EA,VFA,VGA,HA,NPLIES,SIG1,100,
     1                  OMGA,DELA)
C
        CALL BCEQ12(2,SP2,EB,VFB,VGB,HB,NPLIES,SIG2,100,
     1                  OMGB,DELB)
C
        CALL BCEQ3(NPLIES,IDRP,VFA,VGA,VFB,VGB,EA,EB,GAMMA,
     1  NETA,SIG1,SIG2,HA,HB)
C
        DO 100 I=1,I9N9
        DO 100 J=1,I9N9
C
        IF (I.LE.NM13) THEN
C               ZIE(I,1)=DELA(I)
                ZIE(I,1)=0.0
           IF (J.LE.NM13) THEN
                BCON(I,J)=OMGA(I,J)
           ELSE
```

```
                IF(J.LE.I6N9) THEN
                 BCON(I,J)=0
                ELSE
                 BCON(I,J)=GAMMA(J-I6N9,I)
                ENDIF
           ENDIF
         ENDIF
C
         IF ((I.GT.NM13).AND.(I.LE.I6N9)) THEN
C               ZIE(I,1)=DELB(I-NM13)
                ZIE(I,1)=0.0
           IF (J.LE.NM13) THEN
             BCON(I,J)=0
           ELSE
             IF ((J.GT.NM13).AND.(J.LE.I6N9)) THEN
                BCON(I,J)=OMGB(I-NM13,J-NM13)
              ELSE
                BCON(I,J)=GAMMA(J-I6N9,I)
              ENDIF
           ENDIF
         ENDIF
C
         IF (I.GT.I6N9) THEN
                ZIE(I,1)=NETA(I-I6N9)
           IF (J.LE.I6N9) THEN
                BCON(I,J)=GAMMA(I-I6N9,J)
           ELSE
                BCON(I,J)=0
           ENDIF
         ENDIF
C
 100     CONTINUE

CCCCCCCCCCCCCCCCCCCCCCCCCCCCCCCCCCCCCCCCCCCCCCCCCCCCCCCCCCCCCCCCCCCCCCCCCCC
C        SUBROUTINE GAUSS IS USED TO SOLVE COMPLEX SIMULTANEOUS ALGEBRAIC
C        EQUATIONS
CCCCCCCCCCCCCCCCCCCCCCCCCCCCCCCCCCCCCCCCCCCCCCCCCCCCCCCCCCCCCCCCCCCCCCCCCCC
         CALL GAUSS(BCON,I9N9,100,ZIE,1,100)
c
         RETURN
         END

CCCCCCCCCCCCCCCCCCCCCCCCCCCCCCCCCCCCCCCCCCCCCCCCCCCCCCCCCCCCCCCCCCCCCCCCCCC
C                      SUBROUTINE:    BCEQ12
CCCCCCCCCCCCCCCCCCCCCCCCCCCCCCCCCCCCCCCCCCCCCCCCCCCCCCCCCCCCCCCCCCCCCCCCCCC
         SUBROUTINE BCEQ12(IREG,SP,E,VF,VG,H,NPLIES,SIG,NO
     1                    ,OMEGA,DEL)
C
         IMPLICIT DOUBLE PRECISION (A-H,O-Y), COMPLEX (Z)
         COMPLEX*8  KK,JJ,UU,TT,II,JK,KJ,UK,KU,UJ,JU
         COMPLEX*8  TI,IT,SK,SJ,SU
         COMPLEX*8  E(NO),VF(0:NO,0:NO),VG(0:NO,0:NO)
         COMPLEX*8  OMEGA(NO,NO),DEL(NO),ZC(20,20)
```

```
      DIMENSION       SIG(20,2),SP(20,1),H(20)
      real*4 temp
c-------------------------------------------------------------------
C     The subroutine BCEQ12 is used to calculate the matrices OMGA,OMGB
C     and DELA,DELB.  For this purpose it is called twice with the various
C     data of each region.
c
C     INPUT :
C     IREG : The region concerned (=1 or 2) this helps the subroutine to
C            determine whether there are 3n-3 or 3n-6 equations to be
C            determined for the given region.
C     E : Eigen value matrix fed in
C     V : Eigen vector matrix fed in
C     H : Thickness of the plies of the region concerned
C     SP : The S* matrix of the region
C     SIG : The CLPT values of sig22 & sig12 of the region.
c
C     OUTPUT :
C     OMEGA : The matrix which carries the equations obtained by the
C             minimization of energy for the region
C     DEL   : The RHS of the equations obtained for Omega above.
c
c-------------------------------------------------------------------
      do 10 i=1,NO
      do 20 j=1,NO
      omega(i,j)=cmplx(0.,0.)
 20   continue
      dEl(i)=CMPLX(0.,0.)
 10   continue
c
      NM2=NPLIES-2
      IF(IREG.EQ.1)THEN
         NPL=NPLIES
         NM1=NPL-1
         NM12=2*NM1
         IPL=3*(NM1)
      ELSE
         NPL=NPLIES-1
         NM1=NPL-1
         NM12=2*NM1
         IPL=3*(NM1)
      ENDIF
C
      DO 30  I=1,20
      DO 30  J=1,20
             ZC(I,J)=CMPLX(0.,0.)
 30   CONTINUE
C
      DO 40 I=1,NPL
      DO 40 J=1,IPL
      IJO=I-1
      DO 40 K=1,IJO,1
      IF(K.EQ.1) THEN
```

```
      ZC(I,J)=-VF(K,J)*(H(K))*0.5+ZC(I,J)
      ELSE
      ZC(I,J)=-VF(K,J)*(H(K-1)+H(K))*0.5+ZC(I,J)
      ENDIF
 40   CONTINUE
C
      DO 50  I=1,NPL
C
      H1=H(1)
      H12=H1**2
      H13=H1**3
      HI=H(I)
      HI2=HI**2
      HI3=HI**3
      HI4=HI2*HI2
      HI5=HI3*HI2
C
C
      do 80 M=1,IPL
      ILO=M
      do 70 N=1,ILO
c
      ZT=1.D0/(E(M)+E(N))
C
      ZTM=VF(I-1,M)-VF(I,M)
      ZTN=VF(I-1,N)-VF(I,N)
C
      KK=ZT*(HI*H1)*ZTM*ZTN
      JK=E(M)*E(M)*ZT*(1/H1)*ZTN*(HI3*(1.D0/6.D0)*(ZTM)
     1          +ZC(I,M)*HI)
      KJ=E(N)*E(N)*ZT*(1/H1)*ZTM*(HI3*(1.D0/6.D0)*(ZTN)
     1          +ZC(I,N)*HI)
      ZTN=VF(I-1,N)-VF(I,N)
      ZTM=VG(I-1,M)-VG(I,M)
C
      UK=ZT*(HI*H1)*ZTN*ZTM
C
      ZTN=VF(I-1,M)-VF(I,M)
      ZTM=VG(I-1,N)-VG(I,N)
c
      KU=ZT*(HI*H1)*ZTM*ZTN
      ZTM=(VF(I-1,M)*VF(I-1,N)+VF(I,M)*VF(I,N))*(1.D0/20.D0)-
     1     (VF(I-1,M)*VF(I,N)+VF(I,M)*VF(I-1,N))*(1.D0/120.D0)
      ZTN=(ZC(I,M)*(VF(I-1,N)-VF(I,N))+
     1     ZC(I,N)*(VF(I-1,M)-VF(I,M)))*(1.D0/6.D0)
C
      JJ=(E(M)*E(N)*E(M)*E(N))*ZT*(1.D0/H13)*(ZTM*HI5+
     1           ZTN*HI3+ZC(I,M)*ZC(I,N)*HI)

      ZTM=VG(I-1,M)-VG(I,M)
      ZTN=VF(I-1,N)-VF(I,N)
C
      UJ=E(N)*E(N)*(1.D0/H1)*ZT*ZTM*((HI3/6.D0)*ZTN
```

```
     1          +ZC(I,N)*HI)
C
        ZTN=VG(I-1,N)-VG(I,N)
        ZTM=VF(I-1,M)-VF(I,M)
C
        JU=E(M)*E(M)*(1.D0/H1)*ZT*ZTN*((HI3/6.D0)*ZTM
     1          +ZC(I,M)*HI)
        II=E(M)*E(N)*ZT*(HI3/H1)*(VF(I,M)*VF(I,N)*(1.D0/3.D0)
     1  +(VF(I-1,M)*VF(I,N)+VF(I-1,N)*VF(I,M))*(1.D0/6.D0)
     1  +VF(I-1,M)*VF(I-1,N)*(1.D0/3.D0))
C
        TI=E(M)*E(N)*ZT*(HI3/H1)*(
     1  VG(I,M)*VF(I,N)*(1.D0/3.D0)
     1  +(VG(I-1,M)*VF(I,N)+VF(I-1,N)*VG(I,M))*(1.D0/6.D0)
     1  +VG(I-1,M)*VF(I-1,N)*(1.D0/3.D0))
C
        IT=E(M)*E(N)*ZT*(HI3/H1)*(
     1  VG(I,N)*VF(I,M)*(1.D0/3.D0)
     1  +(VG(I-1,N)*VF(I,M)+VF(I-1,M)*VG(I,N))*(1.D0/6.D0)
     1  +VG(I-1,N)*VF(I-1,M)*(1.D0/3.D0))
C
        TT=E(M)*E(N)*ZT*(HI3/H1)*
     1  (VG(I,M)*VG(I,N)*(1.D0/3.D0)
     1  +(VG(I-1,M)*VG(I,N)+VG(I-1,N)*VG(I,M))*(1.D0/6.D0)
     1  +VG(I-1,M)*VG(I-1,N)*(1.0/3.0))
C
        ZTM=VG(I-1,M)-VG(I,M)
        ZTN=VG(I-1,N)-VG(I,N)
        UU=ZT*(HI*H1)*ZTM*ZTN
C
        ZK=HI*(1/E(M))*(VF(I-1,M)-VF(I,M))
        ZJ=(E(M)/(H12))*((VF(I-1,M)-VF(I,M))*HI3+ZC(I,M)*HI)
        ZU=(HI/E(M))*(VG(I-1,M)-VG(I,M))
c
        OMEGA(M,N)=(SP(I,1)*KK+SP(I,2)*JJ+SP(I,3)*(4.D0*UU)+
     1              SP(I,4)*(4.D0*TT)+SP(I,5)*(4.D0*II)+
     1              SP(I,6)*(KJ+JK)+SP(I,7)*2.D0*(UK+KU)+
     1              SP(I,8)*2.D0*(UJ+JU)+SP(I,9)*4.D0*(TI+IT))
     1                   *(1./h(i)**2)+ OMEGA(M,N)
c
        OMEGA(N,M)=OMEGA(M,N)
C
  70    CONTINUE
  80    CONTINUE
  50    CONTINUE
C
        RETURN
        END

CCCCCCCCCCCCCCCCCCCCCCCCCCCCCCCCCCCCCCCCCCCCCCCCCCCCCCCCCCCCCCCCCCCCCCCCC
C                     SUBROUTINE:    BCEQ3
CCCCCCCCCCCCCCCCCCCCCCCCCCCCCCCCCCCCCCCCCCCCCCCCCCCCCCCCCCCCCCCCCCCCCCCCC
        SUBROUTINE BCEQ3(NPLIES,IDRP,VF1,VG1,VF2,VG2,E1,E2,GAMMA
```

```
     1  ,NETA,SIG1,SIG2,HA,HB)
C
       IMPLICIT DOUBLE PRECISION (A-H,O-Y),COMPLEX (Z)
       COMPLEX*8 VF1(0:100,0:100),VG1(0:100,0:100),E1(100),E2(100)
       COMPLEX*8 VF2(0:100,0:100),VG2(0:100,0:100)
       COMPLEX*8 GAMMA(100,100),NETA(100)
       DIMENSION  SIG1(20,2),SIG2(20,2),HA(20),HB(20)
C
c-------------------------------------------------------------------
C      The subroutine BCEQ3 is used to calculate the matrices GAMMA
C      and NETA For this purpose it is called once only with the various
C      data of regions A & B.
c
C      INPUT :
C      NPLIES : The # of plies in the region A
C      IDRP   : The dropped ply
C      E1,E2 : Eigen value matrix fed in
C      V1,V2 : Eigen vector matrix fed in
C      SIG1,SIG2 : The CLPT values of sig22 & sig12 of the regions A & B.
C                      1-->reg A    2--> reg B
c
C      OUTPUT :
C      GAMMA : The matrix which carries the equations obtained by the
C              matching the three stresses sig22,sig12,sig2z at the face
C              x=0 for the regions A & B
C      NETA   : The RHS of the equations obtained for GAMMA above.
c
c-------------------------------------------------------------------
       N1=NPLIES-1
       N2=2*N1
       N3=3*N1
       NM1=N1-1
       NM2=N1-2
       NM3=N1-3
       NM13=3*(nplies-1)
       NM23=3*(nplies-2)
       I6N9=6*NPLIES-9

C
       DO 100 I=1,N1
       DO 100 M=1,I6N9
C
       IF (M.LE.NM13) THEN
C
          IF (I.LT.IDRP) THEN
               GAMMA(I,M)=(VF1(I-1,M)-VF1(I,M))*(1/ha(i))
               NETA(I)=SIG2(I,1)-SIG1(I,1)
          ENDIF
C
          IF(I.EQ.IDRP)  THEN
               GAMMA(I,M)=(VF1(I-1,M)-VF1(I,M))*(1/ha(i))
               NETA(I)=-SIG1(I,1)
          ENDIF
```

```
C
          IF (I.GT.IDRP) THEN
               GAMMA(I,M)=(VF1(I-1,M)-VF1(I,M))*(1/ha(i))
               NETA(I)=SIG2(I-1,1)-SIG1(I,1)
          ENDIF
C
        ELSE
C
          IF (I.LT.IDRP) THEN
c
               GAMMA(I,M)=-(VF2(I-1,M-NM13)-VF2(I,M-NM13))
     1                          *(1/hb(i))
          ENDIF
C
          IF(I.EQ.IDRP)  THEN
               GAMMA(I,M)=0
          ENDIF
C
          IF (I.GT.IDRP) THEN
               GAMMA(I,M)=-(VF2(I-2,M-NM13)-VF2(I-1,M-NM13))
     1                          *(1/hb(i))
          ENDIF
C
        ENDIF
C
 100    CONTINUE
C
        DO 200 I=1,N1
        DO 200 M=1,I6N9
C
        IF (M.Le.NM13) THEN
C
          IF (I.LT.IDRP) THEN
               GAMMA(I+N1,M)=(VG1(I-1,M)-VG1(I,M))*(1/ha(i))
               NETA(I+N1)=SIG2(I,2)-SIG1(I,2)
          ENDIF
C
          IF(I.EQ.IDRP)  THEN
               GAMMA(I+N1,M)=(VG1(I-1,M)-VG1(I,M))*(1/ha(i))
               NETA(I+N1)=-SIG1(I,2)
          ENDIF
C
          IF (I.GT.IDRP) THEN
               GAMMA(I+N1,M)=(VG1(I-1,M)-VG1(I,M))*(1/ha(i))
               NETA(I+N1)=SIG2(I-1,2)-SIG1(I,2)
          ENDIF
C
        ELSE
C
          IF (I.LT.IDRP) THEN
               GAMMA(I+N1,M)=(VG2(I-1,M-NM13)-VG2(I,M-NM13))
     1                          *(1/hb(i))
          ENDIF
```

```
C
          IF(I.EQ.IDRP)  THEN
               GAMMA(I+N1,M)=0
          ENDIF
C
          IF (I.GT.IDRP) THEN
               GAMMA(I+N1,M)=(VG2(I-2,M-NM13)-VG2(I-1,M-NM13))
     1                         *(1/hb(i))
          ENDIF
C
        ENDIF
C
        J=I+N1
 200    CONTINUE
C
        DO 300 I=1,(N1+1)
        DO 300 M=1,I6N9
C
        IF (M.LE.NM13) THEN
C
          IF (I.LT.(IDRP-1)) THEN
               GAMMA(I+N2,M)=VF1(I,M)*(-E1(M))
               NETA(I+N2)=0
          ENDIF
C
          IF(I.EQ.(IDRP-1))  THEN
               GAMMA(I+N2,M)=VF1(I,M)*(-E1(M))
               NETA(I+N2)=0
          ENDIF
C
          IF (I.EQ.IDRP) THEN
               GAMMA(I+N2,M)=VF1(I,M)*(-E1(M))
               NETA(I+N2)=0
          ENDIF
C
          IF (I.GT.IDRP) THEN
               GAMMA(I+N2,M)=VF1(I,M)*(-E1(M))
               NETA(I+N2)=0
          ENDIF
C
          IF(I.EQ.(N1+1)) THEN
               GAMMA(I+N2,M)=0
               NETA(I+N2)=0
          ENDIF
C
C
        ELSE
C
C
          IF (I.LT.(IDRP-1)) THEN
               GAMMA(I+N2,M)=-VF2(I,M-NM13)*(-E2(M-NM13))
          ENDIF
C
```

```
            IF(I.EQ.(IDRP-1))  THEN
                 GAMMA(I+N2,M)=0
            ENDIF
C
            IF (I.EQ.IDRP) THEN
                 GAMMA(I+N2,M)=0
            ENDIF
C
            IF (I.GT.IDRP) THEN
                 GAMMA(I+N2,M)=-VF2(I-1,M-NM13)*(-E2(M-NM13))
            ENDIF
C
C
            IF(I.EQ.(N1+1)) THEN
                 GAMMA(I+N2,M)=-VF2(IDRP-1,M-NM13)*(-E2(M-NM13))
            ENDIF
C
         ENDIF
C
         J=I+N2
C
 300     CONTINUE
C
         RETURN
         END

CCCCCCCCCCCCCCCCCCCCCCCCCCCCCCCCCCCCCCCCCCCCCCCCCCCCCCCCCCCCCCCCCCCCCCCCCC
C        THIS SUBROUTINE 'GAUSS', SOLVES COMPLEX, SIMULTANEOUS, ALGEBRAIC
C        EQUATIONS
CCCCCCCCCCCCCCCCCCCCCCCCCCCCCCCCCCCCCCCCCCCCCCCCCCCCCCCCCCCCCCCCCCCCCCCCCC
         SUBROUTINE  GAUSS(A,N,NP,B,M,MP)

         IMPLICIT DOUBLE PRECISION (A-H,O-Y),COMPLEX(Z)
         PARAMETER (NMAX=100)
         COMPLEX*16 A(NP,NP),B(NP,MP),DUM,PIVNV
         DIMENSION IPIV(NMAX),INDXR(NMAX),INDXC(NMAX)
C-------------------------------------------------------------------
C        Input :
c
c        A   : (N*N) matrix to be inverted stored in (NP*NP) dimension
c        B   : (N*M) RHS to be solved for in (NP*MP)  dimension
c
c        OUTPUT :
C
C        A   : The matrix INV[ A ]
c        B   : The solution vector for each RHS contributed by the coloumns
c                      of [B]
c-------------------------------------------------------------------
         DO 11 J=1,N
               IPIV(J)=0
 11      CONTINUE
C
         DO 22 I=1,N
```

```
            BIG=0
      DO 13 J=1,N
            IF(IPIV(J).NE.1) THEN
               DO 12 K=1,N
                  IF(IPIV(K).EQ.0) THEN
                    IF(CDABS(A(J,K)).GE.BIG) THEN
                       BIG=CDABS(A(J,K))
                       IROW=J
                       ICOL=K
                    ENDIF
                  ELSE
                       IF(IPIV(K).GT.1) THEN
                       WRITE(5,*) 'SINGULAR MATRIX'
                       GOTO 30
                       ENDIF
                  ENDIF
   12             CONTINUE
               ENDIF
   13    CONTINUE
         IPIV(ICOL)=IPIV(ICOL)+1
C
         IF(IROW.NE.ICOL) THEN
               DO 14   L=1,N
                  DUM=A(IROW,L)
                  A(IROW,L)=A(ICOL,L)
                  A(ICOL,L)=DUM
   14          CONTINUE
C
               DO 15   L=1,M
                  DUM=B(IROW,L)
                  B(IROW,L)=B(ICOL,L)
                  B(ICOL,L)=DUM
   15          CONTINUE
         ENDIF
C
         INDXR(I)=IROW
         INDXC(I)=ICOL
C
         IF(A(ICOL,ICOL).EQ.CMPLX(0.)) THEN
         WRITE(5,*) 'SIGULAR MATRIX'
         GOTO 30
         ENDIF
         PIVNV=1.D0/A(ICOL,ICOL)
         A(ICOL,ICOL)=DCMPLX(1.)
C
         DO 16   L=1,N
               A(ICOL,L)=A(ICOL,L)*PIVNV
   16    CONTINUE
         DO 17   L=1,M
               B(ICOL,L)=B(ICOL,L)*PIVNV
   17    CONTINUE
C
         DO 21   LL=1,N
```

```
          IF (LL.NE.ICOL) THEN
                DUM=A(LL,ICOL)
                A(LL,ICOL)=0.
C
                DO 18 L=1,N
                   A(LL,L)=A(LL,L)-A(ICOL,L)*DUM
 18             CONTINUE
C
                DO 19 L=1,M
                   B(LL,L)=B(LL,L)-B(ICOL,L)*DUM
 19             CONTINUE
C
          ENDIF
 21     CONTINUE
 22     CONTINUE
C
               DO 24   L=N,1,-1
                  IF(INDXR(L).NE.INDXC(L)) THEN
                       DO 23   K=1,N
                        DUM=A(K,INDXR(L))
                        A(K,INDXR(L))=A(K,INDXC(L))
                        A(K,INDXC(L))=DUM
 23                     CONTINUE
                  ENDIF
 24            CONTINUE
        RETURN
 30     END
```

```
CCCCCCCCCCCCCCCCCCCCCCCCCCCCCCCCCCCCCCCCCCCCCCCCCCCCCCCCCCCCCCCCCCCCCCCCCCCCCCC
C                                PROGRAM: PPRO.FOR
CCCCCCCCCCCCCCCCCCCCCCCCCCCCCCCCCCCCCCCCCCCCCCCCCCCCCCCCCCCCCCCCCCCCCCCCCCCCCCC
C
C       THIS IS THE POSTPROCESSOR PROGRAM WHICH PROVIDES THE VALUE OF THE
C       INTERLAMINAR STRESSES AT ANY DESIRED INTERFACE
C       THIS PROGRAM USES THE EIGENVALUES AND EIGEN VECTORS IN THE OUT2.DAT
C
C       INPUT:  interfaces in region A and region B where the s2z,s1z and szz
C               are required.  The interfaces are numbered from the bottom of
C               the laminate.
C       OUTPUT: The expressions for the interlaminar stresses can be obtained
C               from the file ANS.DAT
C-------------------------------------------------------------------------------

        IMPLICIT DOUBLE PRECISION (A-H,O-Y), COMPLEX(Z)
        COMPLEX*8 ZFP(20,100),ZGP(20,100),ZFPP(20,100)
        COMPLEX*8 ZF(20,100),ZG(20,100)
        COMPLEX*8 E(20),V(20,20),zz(10,10)
        COMPLEX*8 F(20,20)
        DIMENSION RV(20,20),SV(20,20),A(10,10),B(10,10),C(10,10)
        DIMENSION  H(20)
        OPEN(UNIT=1,FILE='OUT2.DAT',STATUS='OLD')
        OPEN(UNIT=2,FILE='ANS.DAT',STATUS='NEW')
        OPEN(UNIT=7,FILE='PIC.DAT',STATUS='NEW')
C
C-------------------------------------------------------------------------------
C       THE FILES USED ARE:
C       OUT2.DAT: THIS IS GENERATED BY DROPOFF.FOR AND CONTAINS ALL ITS
C                 RESULTS
C       ANS.DAT : THIS IS GENERATED BY PPRO.FOR AND CONTAINS ALL THE FINAL
C                 EXPRESSIONS FOR THE INTERLAMINAR STRESSES.
C-------------------------------------------------------------------------------
        READ(1,*)NPLIES,IDRP
        DO 111 IREG=1,2
C
        IF(IREG.EQ.1) THEN
                NPL=NPLIES
        ELSE
                NPL=NPLIES-1
        ENDIF
C
        NM13=3*(NPL-1)
        NM12=2*(NPL-1)
C

        DO 123 I=1,NPL
        DO 123 J=1,NM13
        ZFP(I,J)=0.0
        ZFPP(I,J)=0.0
        ZGP(I,J)=0.0
 123    CONTINUE
```

```
CCCCCCCCCCCCCCCCCCCCCCCCCCCCCCCCCCCCCCCCCCCCCCCCCCCCCCCCCCCCCCCCCCCCCCCCCCCCCCC
C       READING THE EIGENVALUES FROM THE FILE OUT2.DAT
CCCCCCCCCCCCCCCCCCCCCCCCCCCCCCCCCCCCCCCCCCCCCCCCCCCCCCCCCCCCCCCCCCCCCCCCCCCCCCC
        DO 10 I=1,NM13
        READ(1,*)K,ER,EI
        E(I)=CMPLX(ER,EI)
 10     CONTINUE

CCCCCCCCCCCCCCCCCCCCCCCCCCCCCCCCCCCCCCCCCCCCCCCCCCCCCCCCCCCCCCCCCCCCCCCCCCCCCCC
C       READING THE EIGENVECTORS FROM THE FILE OUT2.DAT
CCCCCCCCCCCCCCCCCCCCCCCCCCCCCCCCCCCCCCCCCCCCCCCCCCCCCCCCCCCCCCCCCCCCCCCCCCCCCCC
        DO 20   I=1,NM12
        READ(1,*)K,(RV(I,J),J=1,NM13)
 20     CONTINUE
        DO 30   I=1,NM12
        READ(1,*)K,(SV(I,J),J=1,NM13)
 30     CONTINUE
C
        DO 35   I=1,NPL
        READ(1,*)H(I)
 35     CONTINUE
C
        DO 40   I=1,NM13
        DO 40   J=1,NM13
                ZZ(I,J)=CMPLX(RV(I,J),SV(I,J))
 40     continue
c
        write(2,*)'*****************************************'
        write(2,*)'  LAMINATE :                  INTERFACE:'
        write(2,*)'*****************************************'
        WRITE(2,*)'# of plies =',NPL
c
        write(2,*)'*****************************************'
        write(2,*) 'Fi=exp(-B1*x'')*[A1*cos(W1*x'')+A2*sin(W1*x'')]+'
        write(2,*) '   exp(-B2*x'')*[A1*cos(W2*x'')+A2*sin(W2*x'')]+'
        write(2,*) '   exp(-B3*x'')*[A1*cos(W3*x'').........'
        write(2,*)'     '
        write(2,*)'*****************************************'
        write(2,*)'  '
        j=0
        DO 11 I=1,NM13
           j=j+1
        if(real(e(i)).EQ.real(e(i+1))) then
           j=j-1
        endif
 11     CONTINUE
        NACT=J
        j=1
        WRITE(7,*)NACT
        DO 93 I=1,NM13
        if(real(e(i)).ne.real(e(i+1))) then
           write(2,131)j,REAL(E(I)),j,-AIMAG(E(I))
           WRITE(7,*)j,REAL(E(I)),-AIMAG(E(I))
```

```
      else
         j=j-1
      endif
         j=j+1
 93   CONTINUE
      write(2,*)'****************************************'
 131  FORMAT(1X,'   B',I2,'= ',F10.6,'   W',I2,'= ',F10.6)

C---------------------
      do 91 ij=1,NM12
C---------------------
      i=1
      j=1
CCCCCCCCCCCCCCCCCCCCCCCCCCCCCCCCCCCCCCCCCCCCCCCCCCCCCCCCCCCCCCCCCCCCCCCC
C     SORTING OUT THE COMPLEX CONJUGATE EIGENVALUES AND EIGENVECTORS
CCCCCCCCCCCCCCCCCCCCCCCCCCCCCCCCCCCCCCCCCCCCCCCCCCCCCCCCCCCCCCCCCCCCCCCC
 90   if (real(e(i)).eq.real(e(i+1)))then
              t1=2*real(zz(ij,i))
              t2=2*aimag(zz(ij,i))
              IF(IJ.LE.(NPL-1)) THEN
              ZF(IJ,J)=CMPLX(T1,T2)
              ELSE
              ZG((IJ-NPL+1),J)=CMPLX(T1,T2)
              ENDIF
              i=i+1
      else
              t1=real(zz(ij,i))
              t2=0.
              IF(IJ.LE.(NPL-1)) THEN
              ZF(IJ,J)=CMPLX(T1,T2)
              ELSE
              ZG((IJ-NPL+1),J)=CMPLX(T1,T2)
              ENDIF

      endif
      i=i+1
      j=j+1
      if (i.le.nM13) goto 90
C---------------------
 91   continue
C---------------------

C---------------------
      do 191 ij=1,NM12
C---------------------
      i=1
      j=1
C
CCCCCCCCCCCCCCCCCCCCCCCCCCCCCCCCCCCCCCCCCCCCCCCCCCCCCCCCCCCCCCCCCCCCCCCCC
C     COMPUTING THE FIRST AND SECOND DERIVATIVE OF FUNCTIONS F & G.
CCCCCCCCCCCCCCCCCCCCCCCCCCCCCCCCCCCCCCCCCCCCCCCCCCCCCCCCCCCCCCCCCCCCCCCCC
 190  if (real(e(i)).eq.real(e(i+1)))then
              t1=2*real(zz(ij,i)*e(i))
```

```
                t2=2*aimag(zz(ij,i)*e(i))
                IF(IJ.LE.(NPL-1)) THEN
                ZFP(IJ,J)=CMPLX(T1,T2)
                ELSE
                ZGP((IJ-NPL+1),J)=CMPLX(T1,T2)
                ENDIF
                i=i+1
        else
                t1=real(zz(ij,i)*e(i))
                t2=0.
                IF(IJ.LE.(NPL-1)) THEN
                ZFP(IJ,J)=CMPLX(T1,T2)
                ELSE
                ZGP((IJ-NPL+1),J)=CMPLX(T1,T2)
                ENDIF
        endif
        i=i+1
        j=j+1
        if (i.le.nM13) goto 190
C-----------------------
 191    continue
C-----------------------

C-----------------------
        do 291 ij=1,(npl-1)
C-----------------------
        i=1
        j=1

CCCCCCCCCCCCCCCCCCCCCCCCCCCCCCCCCCCCCCCCCCCCCCCCCCCCCCCCCCCCCCCCCCCCCCCCCCCCCCCCCCCCCCC
C       COMPUTING  THE SECOND DERIVATIVES OF THE FUNCTION F.
CCCCCCCCCCCCCCCCCCCCCCCCCCCCCCCCCCCCCCCCCCCCCCCCCCCCCCCCCCCCCCCCCCCCCCCCCCCCCCCCCCCCCCC
 290    if (real(e(i)).eq.real(e(i+1)))then
                t1=2*real(zz(ij,i)*e(i)*e(i))
                t2=2*aimag(zz(ij,i)*e(i)*e(i))
                ZFPP(IJ,J)=CMPLX(T1,T2)
                i=i+1
        else
                t1=real(zz(ij,i)*e(i)*e(i))
                t2=0.
                ZFPP(IJ,J)=CMPLX(T1,T2)
        endif
        i=i+1
        j=j+1
        if (i.le.nM13) goto 290
 291    continue

CCCCCCCCCCCCCCCCCCCCCCCCCCCCCCCCCCCCCCCCCCCCCCCCCCCCCCCCCCCCCCCCCCCCCCCCCCCCCCCCCCCCCCC
C       DETERMINING THE sig2z  sigzz  sig1z  AT THE REQUIRED INTERFACE
CCCCCCCCCCCCCCCCCCCCCCCCCCCCCCCCCCCCCCCCCCCCCCCCCCCCCCCCCCCCCCCCCCCCCCCCCCCCCCCCCCCCCCC

        WRITE(5,*) '  THE INTERFACE OF INTEREST :'
        READ(5,*) INT
```

```
CCCCCCCCCCCCCCCCCCCCCCCCCCCCCCCCCCCCCCCCCCCCCCCCCCCCCCCCCCCCCCCCCCCCCCCC
C       COMPUTING THE CONSTANTS FOR S2Z.
CCCCCCCCCCCCCCCCCCCCCCCCCCCCCCCCCCCCCCCCCCCCCCCCCCCCCCCCCCCCCCCCCCCCCCCC
        WRITE(2,*) '  THE  SIG2Z :'
        WRITE(2,*) '-------------'
        DO 161 I=1,NACT
        T1=REAL(ZFP(INT,I))/H(1)
        T2=AIMAG(ZFP(INT,I))/H(1)
        WRITE(2,140) I,-T1,-T2
        WRITE(7,*) I,-T1,-T2
 161    CONTINUE
C
CCCCCCCCCCCCCCCCCCCCCCCCCCCCCCCCCCCCCCCCCCCCCCCCCCCCCCCCCCCCCCCCCCCCCCCC
C       COMPUTING THE CONSTANTS FOR S1Z.
CCCCCCCCCCCCCCCCCCCCCCCCCCCCCCCCCCCCCCCCCCCCCCCCCCCCCCCCCCCCCCCCCCCCCCCC
        WRITE(2,*) '  THE  SIG1Z :'
        WRITE(2,*) '-------------'
        DO 151 I=1,NACT
        T1=REAL(ZGP(INT,I))/H(1)
        T2=AIMAG(ZGP(INT,I))/H(1)
        WRITE(2,140) I,-T1,-T2
        WRITE(7,*) I,-T1,-T2
 151    CONTINUE
C
CCCCCCCCCCCCCCCCCCCCCCCCCCCCCCCCCCCCCCCCCCCCCCCCCCCCCCCCCCCCCCCCCCCCCCCC
C       COMPUTING THE CONSTANTS FOR SZZ.
CCCCCCCCCCCCCCCCCCCCCCCCCCCCCCCCCCCCCCCCCCCCCCCCCCCCCCCCCCCCCCCCCCCCCCCC
        WRITE(2,*) '  THE  SIGZZ :'
        WRITE(2,*) '-------------'
        DO 251 I=1,NACT
        T1=0.
        T2=0.
        DO 253 J=1,INT
        IF (J.LT.INT) THEN
        T1=-REAL(ZFPP(j,I))*0.5*(H(J)+H(J+1))/(H(1)**2)+T1
        T2=-AIMAG(ZFPP(j,I))*0.5*(H(J)+H(J+1))/(H(1)**2)+T2
        ELSE
        T1=-REAL(ZFPP(j,I))*0.5*H(J)/(H(1)**2)+T1
        T2=-AIMAG(ZFPP(j,I))*0.5*H(J)/(H(1)**2)+T2
        ENDIF
C
 253    CONTINUE
        WRITE(2,140) I,T1,T2
        WRITE(7,*) I,T1,T2
 251    CONTINUE
C
 140    FORMAT(1X,'COEFF OF B',I2,':  A1=',F12.6,'  A2=',F12.6)
c
CCCCCCCCCCCCCCCCCCCCCCCCCCCCCCCCCCCCCCCCCCCCCCCCCCCCCCCCCCCCCCCCCCCCCCCC
C       THE IN-PLANE STRESSES S22 AND S12 ARE COMPUTED NEXT
C       COMPUTING THE CONSTANTS FOR S22.
CCCCCCCCCCCCCCCCCCCCCCCCCCCCCCCCCCCCCCCCCCCCCCCCCCCCCCCCCCCCCCCCCCCCCCCC
        WRITE(2,*)'  THE SIG22:'
```

```
      WRITE(2,*) '----------'
      DO 351 I=1,NACT
      IF(INT.NE.1) THEN
      T1=REAL(ZF(INT-1,I)-ZF(INT,I))/H(INT)
      T2=AIMAG(ZF(INT-1,I)-ZF(INT,I))/H(INT)
      ELSE
      T1=REAL(-ZF(INT,I))/H(INT)
      T2=AIMAG(-ZF(INT,I))/H(INT)
      ENDIF
C
      WRITE(2,140) I,T1,T2
      WRITE(7,*) I,T1,T2
 351  CONTINUE
C
CCCCCCCCCCCCCCCCCCCCCCCCCCCCCCCCCCCCCCCCCCCCCCCCCCCCCCCCCCCCCCCCCCCCCCCCCCCCCCCCCC
C     COMPUTING THE CONSTANTS FOR S12
CCCCCCCCCCCCCCCCCCCCCCCCCCCCCCCCCCCCCCCCCCCCCCCCCCCCCCCCCCCCCCCCCCCCCCCCCCCCCCCCCC
      WRITE(2,*)'  THE SIG12:'
      WRITE(2,*) '----------'
      DO 451 I=1,NACT
      IF(INT.NE.1) THEN
      T1=REAL(ZG(INT-1,I)-ZG(INT,I))/H(INT)
      T2=AIMAG(ZG(INT-1,I)-ZG(INT,I))/H(INT)
      ELSE
      T1=REAL(-ZG(INT,I))/H(INT)
      T2=AIMAG(-ZG(INT,I))/H(INT)
      ENDIF
C
      WRITE(2,140) I,T1,T2
      WRITE(7,*) I,T1,T2
 451  CONTINUE

 111  CONTINUE
      close(2)
      CLOSE(1)
      END
```